EVOLUTION OF THE VACUOLAR H^+-ATPASE ENZYME COMPLEX

by

GREGORY CHARLES FINNIGAN

A DISSERTATION

Presented to the Department of Biology
and the Graduate School of the University of Oregon
in partial fulfillment of the requirements
for the degree of
Doctor of Philosophy

June 2011

DISSERTATION APPROVAL PAGE

Student: Gregory Charles Finnigan

Title: Evolution of the Vacuolar H^+-ATPase Enzyme Complex

This thesis has been accepted and approved in partial fulfillment of the requirements for the Doctor of Philosophy degree in the Department of Biology by:

George Sprague	Chairperson
Tom H. Stevens	Advisor
Victoria Herman	Member
Bruce Bowerman	Member
Ken Prehoda	Outside Member

and

Richard Linton	Vice President for Research and Graduate Studies/Dean of the Graduate School

Original approval signatures are on file with the University of Oregon Graduate School.

Degree awarded June 2011

DISSERTATION ABSTRACT

Gregory Charles Finnigan

Doctor of Philosophy

Department of Biology

June 2011

Title: Evolution of the Vacuolar H^+-ATPase Enzyme Complex

Approved: _____
Dr. George Sprague

The vacuolar proton-translocating ATPase (V-ATPase) is a multisubunit enzyme complex responsible for acidification of cellular organelles. The V-ATPase hydrolyzes ATP to pump protons across membranes to create an electrochemical gradient. Acidification of vesicular compartments is critical in numerous biological processes including protein trafficking, endocytosis, and ion homeostasis; defects in V-ATPase function can also lead to human diseases. While the function of the V-ATPase enzyme is highly conserved across eukaryotes, the molecular architecture of this protein complex has undergone unique structural changes through evolutionary time. The goal of this work is to investigate the assembly, transport, and evolution of this critical molecular machine in the model organism *Saccharomyces cerevisiae.*

A series of genetic screens was performed in budding yeast to identify factors and pathways that are involved in promoting full V-ATPase function. I utilized several "assembly factor" alleles to serve as sensitized genetic backgrounds to partially reduce enzyme function; this work implicated sphingolipid composition in promoting full vacuolar ATPase enzyme function.

I also used ancestral gene reconstruction to analyze the two isoforms of subunit a

of the V_0 subdomain (Vph1p and Stv1p) by recreating the most recent common ancestral subunit (Anc.a). Characterization of Anc.a demonstrated that this ancient subunit was able to properly assemble and function within a hybrid V-ATPase complex. While the Vph1p-containing complex localized to the vacuole membrane and the Stv1p-containing complex was present on the Golgi/endosome, incorporation of Anc.a caused the V-ATPase to localize to both types of cellular compartments.

Finally, I used ancestral reconstruction to investigate the lineage-specific gene duplication of one of the proteolipid subunits of the V_0 subcomplex that occurred within the fungal clade. I demonstrate that inclusion of a third proteolipid subunit within fungi (as compared to two subunits within metazoans) could have occurred via neutral processes by asymmetric degeneration of subunit-subunit interfaces that "ratcheted" the duplicated subunit with the V_0 ring. These results present a model that describes how macromolecular machines can increase in complexity through evolutionary time.

This dissertation includes previously published co-authored material and unpublished co-authored material.

CURRICULUM VITAE

NAME OF AUTHOR: Gregory Charles Finnigan

GRADUATE AND UNDERGRADUATE SCHOOLS ATTENDED:

University of Oregon, Eugene, OR
Gonzaga University, Spokane, WA

DEGREES AWARDED:

Doctor of Philosophy, Biology, 2011, University of Oregon
Bachelor of Science, Biology, 2005, Gonzaga University

AREAS OF SPECIAL INTEREST:

Molecular biology
Biochemistry
Genetics
Cellular biology
Molecular evolution

PROFESSIONAL EXPERIENCE:

Teaching assistant, Department of Biology, University of Oregon, Eugene, 2005-2007

GRANTS, AWARDS, AND HONORS:

Graduate Teaching Fellowship, Biology, 2005-2007

National Institute of Health, Genetics Training Grant, S T32 GM007257, 2006-2007, 2008-2010

William R. Sistrom Memorial Scholarship Award, University of Oregon, Department of Biology, 2009

Magna cum Laude, Gonzaga University, 2005

PUBLICATIONS:

FINNIGAN, G. C., HANSON-SMITH, V., HOUSER, B. D., PARK, H. J., and T. H. STEVENS, 2011 The reconstructed ancestral subunit a functions as both V-ATPase isoforms Vph1p and Stv1p in extant *S. cerevisiae*. Mol. Biol. Cell. (1st revision, refereed).

FINNIGAN, G. C., RYAN, M., and T. H. STEVENS, 2011 A genome-wide enhancer screen implicates sphingolipid composition in vacuolar ATPase function in *Saccharomyces cerevisiae*. Genetics **187:** 771-783.

ACKNOWLEDGMENTS

I thank Dr. Tom H. Stevens for assistance in preparation of this manuscript and valuable professional and personal advice over my graduate career. I am very privileged to have worked in his laboratory. Special thanks are also due to Dr. Patrick Phillips and Dr. Joe Thornton for inspiring an evolutionary approach in my graduate projects. I also want to thank Dr. Emily Coonrod and Dr. Laurie Graham for continued support and assistance with writing, experimental design, and professional development. Finally, I want to expression my appreciation to undergraduate researchers Gail Butler, Eric Black-Maier, Ben Houser, Harry Park, and Ben Vermillion who have assisted me in many experiments and projects. This research was supported by (i) Graduate Teaching Fellowship at the University of Oregon, (ii) the pre-doctoral Genetics Training Grant from the National Institute of Health (S T32 GM007257), and (iii) a grant from the National Institute of Health to Dr. Tom H. Stevens at the University of Oregon (GM38006).

To teachers Amy Lawson, Beth Crissy, and Joan Beardsley for igniting my passion for science.

TABLE OF CONTENTS

Chapter Page

I. INTRODUCTION TO THE V-ATPASE ENZYME 1

1. Structure and Function of the V-ATPase Enzyme Complex 1

2. Assembly of the Yeast V_0 Subcomplex 2

3. Regulation of the V-ATPase Complex 4

4. Additional Cellular Functions of the V-ATPase and Roles in Human Disease 5

5. An Evolutionary Approach to Study the V-ATPase Across Eukaryotes 7

6. Experimental Design to Address the Evolution of the V-ATPase Complex 10

II. GENOME WIDE ENHANCER SCREEN IMPLICATES SPHINGOLIPID COMPOSITION IN VACUOLAR ATPASE FUNCTION IN *SACCHAROMYCES CEREVISIAE* 12

1. Introduction 12

2. Materials and Methods 17

Plasmids and Yeast Strains 17

Culture Conditions 20

Synthetic Genetic Array Screen 21

Whole Cell Extract Preparation and Immunoblotting 21

Fluorescence Microscopy 22

V-ATPase Activity Assay 22

3. Results 23

Genome-Wide Synthetic Genetic Array (SGA) Screen for V-ATPase Effectors 23

HPH1/*HPH2* or *ORM1/ORM2* Null Mutants Cause Synthetic Growth Defects in *vma21QQ* Yeast 27

Chapter Page

Vacuolar Acidification, V_0 Assembly, and V-ATPase Localization are Normal in *HPH* and *ORM* Mutants 31

Loss of the *ORM* Genes (But Not the *HPH* Genes) Results in Reduced V-ATPase Enzyme Activity 34

The Orm Proteins Function in Sphingolipid Regulation 35

4. Discussion 37

III. THE RECONSTRUCTED ANCESTRAL SUBUNIT A FUNCTIONS AS BOTH V-ATPASE ISOFORMS VPH1P AND STV1P IN EXTANT *S. CEREVISIAE* 44

1. Introduction 45

2. Materials and Methods 48

In Silico Reconstruction of Ancestral Protein Sequences 48

Plasmids and Yeast Strains 50

Culture Conditions 53

Whole Cell Extract Preparation and Immunoblotting 54

Fluorescence Microscopy 55

3. Results 56

Anc.a Functions in Extant *S. cerevisiae* as Part of a Hybrid V-ATPase Complex 56

Anc.a Functionally Replaces Yeast Stv1p and Vph1p 62

Anc.a Localizes to Both the Golgi/Endosome and Vacuole in Yeast 63

The Anc.a V-ATPase Complex Utilizes Slowed Anterograde Trafficking to the Vacuole Membrane 66

4. Discussion 69

Chapter Page

IV. THE EVOLUTION OF MULTI-PARALOG PROTEIN COMPLEXITY IN THE VACUOLAR H^+-ATPASE V_0 PROTEOLIPID RING 76

1. Introduction 76

2. Methods Summary 79

3. Expanded Methods 81

In Silico Reconstruction of Ancestral Protein Sequences 81

Robustness to Alignment Uncertainty 82

Plasmids and Yeast Strains 83

Yeast Growth Assays 87

Whole Cell Extract Preparation and Immunoblotting 87

Fluorescence Microscopy 87

4. Results 88

The Reconstructed Ancestor Functions as Subunit c, c' or Both c and c' in Extant Budding Yeast 88

Intermediate Ancestors Anc.c and Anc.c' Function as Subunit c and c', Respectively 90

Single Amino Acid Substitutions Affect the Evolutionary Trajectory of the c and c' Subunits 91

5. Discussion 95

V. DISCUSSION AND SUMMARY 103

1. Genetic Screens and the V-ATPase 103

2. The Evolutionary History of the Two Subunit a Isoforms in Budding Yeast 108

3. The Evolution of Complexity 113

APPENDICES 120

Chapter Page

A. SUPPLEMENTARY INFORMATION FOR CHAPTER II 120

B. SUPPLEMENTARY INFORMATION FOR CHAPTER III 140

REFERENCES CITED 144

1. References Cited for Chapter I 144

2. References Cited for Chapter II 147

3. References Cited for Chapter III 153

4. References Cited for Chapter IV 160

5. References Cited for Chapter V 164

LIST OF FIGURES

Figure Page

Chapter I

1. Model of the Yeast V-ATPase Complex 2

Chapter II

1. Molecular Function of 144 Genes Identified in at Least 2 of 3 SGA Screens for an Enhanced Vma^- Phenotype 25

2. *HPH1* and *HPH2* Display Synthetic Growth Defects with V_0 Assembly Mutants 28

3. *ORM1* and *ORM2* Display Synthetic Growth Effects in Cells Expressing *Vma21QQ* 30

4. Loss of *HPH1/HPH2* or *ORM1/ORM2* Does Not Result in a Loss of Vacuolar Acidification 32

5. Vph1p Levels are Not Reduced in Strains Lacking Either *HPH1/HPH2* or *ORM1/ORM2* 33

6. V_1 and V_0 are Localized to the Vacuole Membrane in *Orm* Mutant Yeast 34

7. Orm Sensitivity to Buffered Calcium Media Can Be Suppressed by Inhibition of Sphingolipid Biogenesis 36

Chapter III

1. The Maximum Likelihood Phylogeny of Fungal V-ATPase Subunit a 57

2. Alignment of *S. cerevisiae* Stv1p, Vph1p, and Anc.a Amino Acid Sequences 58

3. Ancestral Subunit a Complements a Loss of Both *VPH1* and *STV1* 60

4. Expression of Anc.a Results in Acidification of the Yeast Vacuole 62

5. Expression of Anc.a Complements the Low Iron Growth Defect of *stv1*Δ Yeast 64

6. Anc.a Localizes to the Vacuole Membrane and Golgi/Endosomal Network..... 65

Figure Page

7. Anc.a Localization Shifts to the Vacuole Membrane After Treatment with Cycloheximide 68

8. Anc.a Does Not Perturb Stv1p Sorting in Budding Yeast 69

Chapter IV

1. Evolution of the V-ATPase Proteolipid Ring 78

2. Maximum Likelihood Phylogeny of V-ATPase Subunits c, c', and c" Protein Sequences 79

3. Protein Sequence Alignment of the *S. cerevisiae* Proteolipids Vma3, Vma11, and Vma16 to the Anc.c-c' and Anc.c" Subunits 80

4. Ancestral Sequence Reconstruction (ASR) Error as a Function of Insertion-Deletion Rate 83

5. Functional Growth Assays of Ancestral V-ATPase Subunits Expressed in Contemporary *S. cerevisiae* Mutants 89

6. Functional Growth Assays of Anc.c-c' and Anc.c" Lacking Critical Glutamic Acid Residues in Contemporary *S. cerevisiae* 90

7. Protein Sequence Alignment of Anc.c-c', Anc.c, Anc.c' and Yeast Vma3 and Vma11 Subunits Using CLUSTAL 92

8. Functional Growth Assays of Intermediate Ancestors Anc.c and Anc.c' 93

9. Two Single Amino Acid Changes Contribute Towards Subunit c and c' Identity 95

10. A Model of Subfunctionalization in the Fungal V_0 Proteolipid Ring 97

11. Translation Fusions Between Contemporary Yeast c" and Anc.c' Demonstrate the Positioning of These Two Subunits Within the V-ATPase Proteolipid Ring . 98

12. V-ATPase Complexes Containing Ancestral Proteolipids Display V_0 Assembly Defects 101

Appendix B

S1. Support for the Anc.a Reconstruction 141

Figure Page

S2. Stability of Anc.a Protein is Dependent on the Presence of the V-ATPase Assembly Factor, Vma21p 143

LIST OF TABLES

Table Page

Chapter II

1. Plasmids Used in This Study 17

2. Yeast Strains Used in This Study 19

3. Genes Found in Our Screens That are Involved in Either Protein Trafficking or are ER-Localized are Listed 26

4. V-ATPase Activity and Quinacrine Staining of Mutants 35

Chapter III

1. Plasmids Used in This Study 51

2. Yeast Strains Used in This Study 54

Chapter IV

1. Yeast Strains and Plasmids in This Study 85

2. Robustness to Uncertainty for Anc.c-c' and Anc.c" Sequences 91

3. All Single Amino Acid Changes Made to Anc.c-c' 94

Appendix A

S1. Genes Identified by Genome-Wide SGA Screens for V-ATPase Effectors 120

S2. Gene Ontology (GO) Analysis was Performed Using the *Saccharomyces* Genome Database (SGD) "Gene Ontology Term Finder" 133

Appendix B

S1. Protein Sequences Used to Generate the Maximum Likelihood Phylogeny of Anc.a 140

S2. Testing the Robustness to Uncertainty for the Anc.a Sequence 142

CHAPTER I

INTRODUCTION TO THE V-ATPASE ENZYME

1. *Structure and function of the V-ATPase enzyme complex*

The multi-subunit v-type, proton-translocating ATPase enzyme (V-ATPase) is a highly conserved molecular machine that serves to acidify eukaryotic organelles (Figure 1) (FORGAC 2007). The V-ATPase enzyme is highly conserved within all eukaryotes. Three types of ion translocating ATPase enzymes are thought to originate from a shared ancestor; the F_1F_0 (ATP-synthase), A_1A_0 (archeal ATP synthase), and V_1V_0 (vacuolar ATPase) share common structural motifs yet differ in their specific molecular functions (GRÜBER *et al*. 2001). The V-ATPase is composed of two subdomains: the V_1 portion (subunits A, B, C, D, E, F, G, and H) is responsible for hydrolysis of ATP whereas the V_0 portion (subunits a, d, e, c, c', and c") is responsible for transporting protons across a lipid bilayer (KANE 2006; FORGAC 2007). Whereas the V-ATPase is essential in most eukaryotes, disruption of V-ATPase function is not lethal within the budding yeast, *Saccharomyces cerevisiae* (KANE 2006). In this way, yeast serves as an excellent model system for studying the V-ATPase enzyme. There are fourteen different protein subunits that are required for full V-ATPase enzyme function and some are found in multiple copies per complex (GRAHAM *et al*. 2003).

Seen in Figure 1, the central core of the V_1 subdomain is composed of alternating A and B subunits. The two domains are connected through a grouping of additional subunits that serve as the "stalk." Following ATP hydrolysis, energy from the conformation change within V_1 is translated into rotation motion through this region to the "proteolipid ring" within the V_0 subdomain (FORGAC 2007). In yeast, this ring is

composed of three different membrane-bound subunits that shuttle protons across the lipid bilayer (WANG *et al.* 2007). The proteolipid ring rotates relative to the largest V-ATPase subunit, subunit a. This subunit serves as both a stationary "stator" as well as aids in proton translocation (FORGAC 2007). In *S. cerevisiae* there are two isoforms of subunit a, Stv1p or Vph1p, and only one is incorporated into the final enzyme complex (MANOLSON *et al*. 1992, 1994). Subunit a is significant as it dictates both the subcellular localization and regulation of the V-ATPase complex (KAWASAKI-NISHI *et al*. 2001a; KAWASAKI-NISHI *et al.* 2001b).

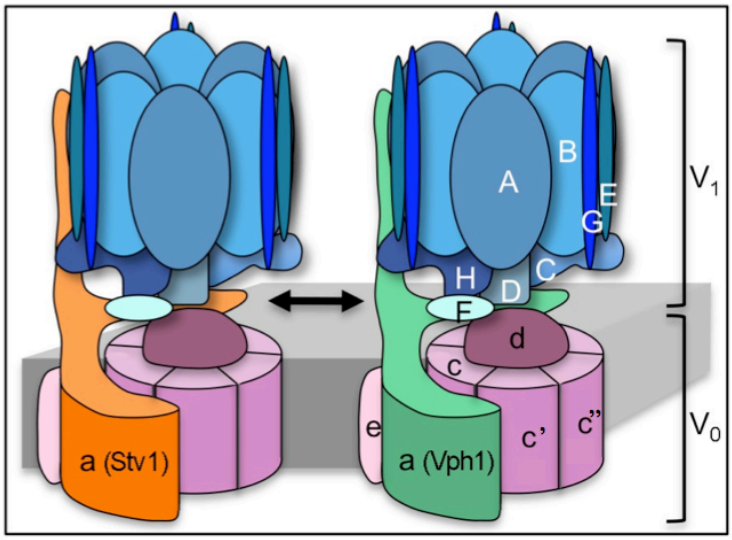

Figure 1. Model of the yeast V-ATPase complex. The 14 subunit complex is composed of two subdomains: the V_1 portion is responsible for ATP hydrolysis and the membrane-bound V_0 domain functions to translocate protons across the lipid bilayer. In yeast, there are two isoforms of subunit a; this subunit isoform determines the subcellular localization of the V-ATPase in *S. cerevisiae.*

2. *Assembly of the yeast V_0 subcomplex*

Within budding yeast, assembly of the V_0 and V_1 subdomains occurs within the endoplasmic reticulum (ER) and cytoplasm, respectively (KANE 2006). Studies have focused on assembly of the V-ATPase V_0 subdomain to understand how large, multi-subunit complexes can be properly built within the ER. Both proteomic and genetic

approaches have lead to the identification of additional proteins (Vma21p, Vma12p, Vma22p, Pkr1p, and Voa1p) that are required for proper assembly of a functional V-ATPase complex (HIRATA *et al*. 1993; HILL and STEVENS 1995; MALKUS *et al*. 2004; DAVIS-KAPLAN *et al*. 2006; RYAN *et al*. 2008). While none of these factors are components of the final enzyme complex, they associate with different groups of subunits and are proposed to act as chaperones for particular stages of V_0 assembly. For instance, the Vma12p-Vma22p complex has been shown to physically associate with subunit a (Vph1p or Stv1p) while Vma21p and Voa1p associate with the proteolipid ring early in assembly (HIRATA *et al*. 1993; HILL and STEVENS, 1995; MALKUS *et al*. 2004; RYAN *et al*. 2008). Interestingly, Vma21p remains associated with the complete V_0 subcomplex and is transported out of the ER to the Golgi (MALKUS *et al*. 2004). This assembly factor is then retrieved back to the ER to participate in multiple rounds of assembly. It is possible that Vma21p may also act in regulating exit of the completed V-ATPase subdomain out of the ER.

Recent studies have identified homologs of Vma21p within other organisms including *C. elegans*, *A. thaliana*, and *H. sapiens* (unpublished results; NEUBERT *et al*. 2008). This confirms that assembly factors are required for full V-ATPase function in organisms outside of budding yeast. More surprisingly was that expression of these homologs within *S. cerevisiae* resulted in functioning V-ATPase enzyme complexes (unpublished results; NEUBERT *et al*. 2008). The conservation of Vma21p function across species has prompted searches for additional factors in higher eukaryotes that might assist in early V_0 assembly. However, while the overall molecular function (acidification of organelles) of the V-ATPase has been tightly conserved across the tree

of life, the molecular architecture of the V-ATPase has continued to evolve and increase in complexity. One of the many questions that remain involves comparing the molecular differences between the metazoan and fungal proteolipid rings and their association with the assembly factor, Vma21p.

3. *Regulation of the V-ATPase complex*

Studies have also focused on the different ways the cells are able to modulate the activity of the V-ATPase (KAWASAKI-NISHI *et al*. 2001b; KANE 2006). Since acidification of the endo-membrane system is critical to numerous cellular functions, it is essential that V-ATPase activity can be accurately and efficiently regulated. While many enzymes are regulated through transcript expression (either temporal or spatial control), this seems unreasonably slow for an enzyme complex that is approximately 1 MDa, has fourteen essential peptides, and requires the assistance of at least five accessory proteins.

Instead, the V-ATPase can undergo rapid, reversible dissociation of the V_1 and V_0 subdomains (KANE 2006; FORGAC 2007). Dissociation of these two components completely eliminates enzyme activity and does not allow for disruption of the vesicular pH gradient through potential leakage of protons back across the membrane bound V_0 subdomain (ZHANG *et al*. 1992; KAWASAKI-NISHI *et al*. 2001a). In yeast, this controlled dissociation occurs in the absence of glucose and might be conserved in higher eukaryotes as well (KANE 2006).

Secondly, the local lipid environment has been shown to differentially affect the two V-ATPase isoforms in yeast (QI and FORGAC 2007). Vph1p and Stv1p control the transport of the V-ATPase to either the vacuolar membrane or Golgi/endosome,

respectively (MANOLSON *et al.* 1992, 1994). Interestingly, the subcellular location of the V-ATPase also influences *in vivo* dissociation: complexes residing on the Golgi/endosome are unable to undergo glucose-induced dissociation whereas either isoform can be regulated when located on the vacuolar membrane (KAWASAKI-NISHI *et al*. 2001b). Understanding how the local lipid composition influences V-ATPase function is also a relatively unexplored field. The effects of the lipidome have been described for the transport and activity of other protein cargo such as Pma1p and Gap1p (WANG and CHANG 2002; GAIGG *et al.* 2006; LAUWERS *et al.* 2007).

Finally, it has been proposed that cells are also able to subtly modulate the efficiency by which the V-ATPase couples ATP hydrolysis with proton translocation instead of completely abolishing enzyme activity through *in vivo* dissociation. There is a small difference in this enzyme efficiency between the Golgi and vacuolar isoforms and mutations have also been described (in subunit d and subunit A) that actually increase this coupling efficiency (FORGAC 2007).

4. *Additional cellular functions of the V-ATPase and roles in human disease*

While the primary role of the V-ATPase is to acidify membrane-bound compartments, additional functions have been attributed to this unique molecular machine. Many of these cellular processes are a consequence of the pH gradient generated by the V-ATPase such as endocytosis, vesicular transport, development, and ion homeostasis (FORGAC 2007). However, recent work has implicated the V-ATPase in both membrane fusion and pH sensing (FORGAC 2007). Interactions between the V-ATPase and SNARE (Soluble NSF Attachment Protein Receptor) proteins have been

described in recent reports (HIESINGER *et al.* 2005). Also, one model of vacuole fusion/fission, albeit controversial, proposes that the V-ATPase is necessary for membrane fusion (BAARS *et al.* 2007). Other physical interactions of V-ATPase subunits with vesicle formation regulators (such as the small GTPase Arf6p) have been shown to be pH dependent (HURTADO-LORENZO *et al*. 2006).

The V-ATPase has also been implicated in a number of human diseases. Entry of viruses and toxins (including influenza virus, Semliki forest virus, and vesicular stomatitus virus) into the cell has been shown to occur via an acidified compartment (GRUENBERG and VAN DER GOOT 2006). A similar mechanism is responsible for allowing entry of bacterial agents (such as diphteria toxin and anthrax toxin). Targeting of specific V-ATPase complexes and selective inhibition of enzyme function might allow for protection from viruses and toxins (FORGAC 2007).

While yeast are restricted to only two isoforms of the V-ATPase (containing either Stv1p or Vph1p), mammals have evolved a number of additional forms. Different isoforms of some of the subunits (include four different genes for subunit a) as well as differential splice variants create a more complex pool of V-ATPase complexes (QI and FORGAC 2008). Mammals have acquired a V-ATPase complex that functions on the plasma membrane and is involved in acidification of the extracellular space (OKA *et al.* 2001a; TOYOMURA *et al.* 2003). This process is critical in specific cell types such as those found in the distal tubule of the kidney. Similarly, plasma membrane-localized V-ATPases are responsible for bone resorption in osteoclasts. Defects in the V-ATPase in these specialized cells can lead to distal renal tubular acidosis and osteopetrosis, respectively (KARET *et al.* 1999; FRATTINI *et al.* 2000). Finally, connections have

been made between the V-ATPase and tumor metastasis and also tumor cell survival (MARTINEZ-ZAGUILÁN *et al.* 1999). Selective inhibition of the V-ATPase complex is currently an attractive field for combating these conditions.

5. *An evolutionary approach to study the V-ATPase across eukaryotes*

As recent work highlights the central role of the V-ATPase in numerous cellular processes and even human disease states, the importance of characterizing the many isoforms of the V-ATPase in mammalian systems has become evident. However, much of the basic biology and biochemistry that has been performed on the V-ATPase has been done in the model organism *S. cerevisiae* (see reviews GRAHAM *et al.* 2003; KANE 2006; FORGAC 2007). Work within budding yeast has many advantages as very tractable and efficient genetic and biochemical systems have been developed over the years to rapidly generate tens of thousands of interactions between mutants of interest (TONG and BOONE 2006). For this reason, work in yeast has been able to uncover many of the essential components, regulatory processes, and accessory proteins that are involved in the assembly, transport, and function of the yeast V-ATPase. Much of the work within budding yeast has been applicable to the same molecular machine in other species. In fact, many of the subunits from higher eukaryotes from both the fungal, plant, and animal clades are functional when expressed in *S. cerevisiae* in place of the yeast subunit (HARRISON *et al.* 1994; FINBOW *et al.* 1994; AVIEZER-HAGAI *et al.* 2000; IKEDA *et al.* 2001; NISHI *et al.* 2003; unpublished results).

However, this approach is not sufficient to address particular questions about the structural architecture, transport, or assembly of the V-ATPase enzyme. It is necessary to

properly address the relationship between the information obtained in yeast and the homologous enzyme complexes in other eukaryotes. For example, while the overall function of the enzyme is essentially identical in all eukaryotes--proton translocation across a membrane--the stoichiometry of the subunits, the number of enzyme isoforms, and the subcellular localization of the V-ATPase has dramatically changed through evolutionary time (see Chapter III and IV). Some of the most significant differences involve components of the V_0 subcomplex.

Firstly, within the metazoan clade the V_0 proteolipid ring only contains two subunits, subunit c and subunit c" whereas fungi contain three subunits c, c', and c" (unpublished results). Second, the number of separate genes encoding subunit a varies greatly within the eukaryotic tree of life; some fungi such as *S. cerevisiae* contain two isforms (*VPH1* and *STV1*) while other fungi such as *N. crassa* and *S. pombe* contain only a single isoform (CHAVEZ *et al.* 2006). Other species contain three or more isoforms of subunit a (OKA *et al.* 2001a; OKA *et al.* 2001b; TOYOMURA *et al.* 2003; WASSMER *et al.* 2006).

Comparison of the fungal V_0 subdomain to that of other species has been difficult; this type of *horizontal* evolutionary approach (HARMS and THORNTON 2010) that involves transfer of a subunit from one modern species to another modern species has been successful for some of the subunits of the V-ATPase that are extremely well conserved but remains problematic for comparison of (i) the proteolipid ring and (ii) the stator subunit. Investigation of the proteolipid ring is crucial; studies in yeast have demonstrated that this portion of the V_0 is closely chaperoned by dedicated assembly factors (unpublished results; MALKUS *et al.* 2004; RYAN *et al.* 2008). In yeast,

Vma21p binds directly to subunit c' (unpublished results; MALKUS *et al.* 2004) but it is unclear how *H. sapiens* Vma21p would function since humans do not contain subunit c'.

Furthermore, this raises a number of interesting questions regarding the evolution of protein complexity. How did the two and three-proteolipid rings evolve in metazoans and fungi, respectively? It is unclear if there is a selective advantage to having two versus three different proteolipid subunits. One possibility is that the increase in subunit composition can be attributed to neutral evolution and subsequent accumulation of an additional subunit through degeneration of existing subunit-subunit interfaces.

Subunit a of the V_0 subdomain is a second, interesting case study within the V-ATPase enzyme as it has a plethora of functional roles both internal to the complex itself as well as interacting with additional cellular partners (reviewed in FORGAC 2007). Understanding how each of the many subunit a isoforms contribute to assembly, localization, coupling efficiency, *in vivo* dissociation, and other functions such as membrane fusion or pH sensing is of great interest. Attempts to characterize subunit a isoforms from other species within budding yeast have not been successful (unpublished results). There is a large degree of sequence divergence among subunit a isoforms between eukaryotic clades (see Chapter III). However, prior to comparing subunit a proteins across different species, it will become necessary to address the mechanistic differences between V-ATPase complexes that evolved within each organism. Biochemical and genetic characterization of subunit a will be critical in uncovering the specialized roles of this protein within the complex. One of the most significant molecular functions of subunit a is localization of the V-ATPase enzyme to different subcellular compartments. This will aid in identifying mechanisms for differentially

targeting the V-ATPase to specific organelles; it is currently unknown how isoforms of the V-ATPase are separately targeted within eukaryotes.

6. *Experimental design to address the evolution of the V-ATPase complex*

The work presented here addresses a number of different questions regarding the function, transport, and evolution of the V-ATPase complex. The goal of characterizing the mechanistic details of V_0 assembly within budding yeast is to (i) inspire further study of similar (if not identical) processes within other eukaryotic systems including mammals and (ii) contribute to our knowledge of assembly of complex macromoleular machines. The work in Chapter II presents a series of genetic screens to search for additional factors, proteins, and/or genetic pathways that affect V-ATPase assembly, transport, or function. Characterizing novel (or previously overlooked) genetic pathways that are involved in V-ATPase activity and/or regulation can assist in understanding the evolution of this critical machine. This work has been done in collaboration with two additional co-authors (M. Ryan and T. H. Stevens) and is now published in the journal *Genetics*.

The aim of the third chapter is to investigate the evolution of one subunit within the V-ATPase complex. As previously mentioned, subunit a within the V_0 subdomain plays numerous critical roles in assembly, function, and trafficking of the V-ATPase enzyme. To address questions regarding the origins of subunit a within the fungal clade, I have used an evolutionary technique called ancestral gene reconstruction. This work has been done in collaboration with several co-authors. V. Hanson-Smith, B. D. Houser, H. J. Park, and T. H. Stevens have all contributed to this work. The creation and

subsequent characterization of the ancestral subunit a (Anc.a) has provided a model for the evolution of the two subunit a isoforms in budding yeast, Vph1p and Stv1p.

Finally, in Chapter IV, I use the V-ATPase as a model macromolecular machine to address the question of increasing [protein] complexity within biological systems. For these experiments, I used reconstructed ancestors of the subunits of the yeast proteolipid ring. This work was done in collaboration with co-authors V. Hanson-Smith, J. W. Thornton, and T. H. Stevens. The aim of this work was to understand how the proteolipid ring within the fungal clade could increase in complexity (whereas the metazoan ring did not). Together, these three studies have greatly increased our knowledge of both the elements governing V-ATPase function, but also the evolutionary history of this critical protein complex.

CHAPTER II

GENOME WIDE ENHANCER SCREEN IMPLICATES SPHINGOLIPID COMPOSITION IN VACUOLAR ATPASE FUNCTION IN *SACCHAROMYCES CEREVISIAE*

This work was published in volume 187 of the journal *Genetics* in March, 2011. G. C. Finnigan performed the synthetic genetic array screens and subsequent characterization of *HPH1*/*HPH2* and *ORM1*/*ORM2* gene pairs; M. Ryan assisted in performing the V-ATPase enzyme activity assays. G. C. Finnigan wrote the manuscript with editorial help from M. Ryan and T. H. Stevens. T. H. Stevens was the principle investigator for this work. All three co-authors are affiliated with the University of Oregon Institute of Molecular Biology (Eugene, OR, 97403).

1. *Introduction*

The vacuolar H^+-ATPase (V-ATPase) is a multisubunit complex that is highly conserved across eukaryotes (GRAHAM *et al.* 2003). It functions to actively acidify cellular compartments by coupling the hydrolysis of ATP to the translocation of protons across membranes through a conserved rotary mechanism (HIRATA et al., 2003; YOKOYAMA *et al.* 2003; IMAMURA *et al.* 2005). Organelle acidification plays a crucial role in various cellular functions such as vesicular trafficking, endocytosis, neurotransmitter uptake, membrane fusion, and ion homeostasis (KANE 2006; FORGAC 2007). Specialized isoforms of the V-ATPase complex can be found on different cellular membranes including the plasma membrane (FORGAC 2007). A number of human diseases have been associated with or directly linked to defects in the V-ATPase complex

osteopetrosis (FRATTINI *et al.* 2000), renal tubular acidosis (KARET *et al.* 1999), and cancer cell migration (MARTINEZ-ZAGUILÁN *et al.* 1999). The V-ATPase is an essential complex for all eukaryotes with the exception of some fungi.

The budding yeast *Saccharomyces cerevisiae* requires the V-ATPase to survive under specific environmental conditions including alkaline conditions or otherwise toxic levels of metals (KANE 2006; EIDE *et al.* 2005). Yeast utilize the proton gradient created by the V-ATPase to drive sequestration of Ca^{2+} and Zn^{2+} ions within the vacuole (KLIONSKY *et al.* 1990). A variety of proton-exchange antiporter pumps reside on the vacuolar membrane and other organelles that participate in maintaining nontoxic cytosolic levels of various ions and metals including calcium and zinc (MISETA *et al.* 1999; MACDIARMID *et al.* 2002). Deletion of any of the V-ATPase component proteins results in a number of specific growth and cellular phenotypes including sensitivity to excess metals and a lack of vacuolar acidification. This makes yeast a useful model system to study the V-ATPase complex (GRAHAM *et al.* 2003; KANE 2006). Complete disruption of V-ATPase function in yeast results in a characteristic Vma^- phenotype: failure to grow on media buffered to pH 7.5 (KANE 2006). Additionally, numerous genetic screens have demonstrated that a loss of the V-ATPase renders yeast sensitive to a variety of metals (including zinc and calcium) and drugs (KANE 2007; EIDE *et al.* 2005). Yeast lacking the V-ATPase complex do not acidify their vacuoles as shown through a lack of quinacrine staining (WEISMAN *et al.* 1987).

The V-ATPase enzyme in yeast contains 14 protein subunits within two domains: the V_1 portion is responsible for hydrolyzing ATP and the V_0 portion shuttles protons across a lipid bilayer (FORGAC 2007). The V_1 domain (subunits A, B, C, D, E, F, G,

and H) is peripherally associated, and the V_0 domain (subunits a, d, e, c, c', and c") is imbedded within the membrane except subunit d which is a peripheral membrane protein. The functional V-ATPase enzyme requires the presence of all of these subunits. Subunit a has two isoforms in yeast, the absence of one of them is not sufficient to cause a Vma^- phenotype. Yeast contain two populations of the V-ATPase complex and their localization is dictated by the incorporation of one of two isoforms of subunit a, Stv1p or Vph1p (MANOLSON *et al.* 1992, 1994). While higher eukaryotes contain numerous isoforms for many of the different V-ATPase subunits (MARSHANSKY and FUTAI 2008), Stv1p/Vph1p is the only structural difference between the two yeast enzymes. V-ATPase complexes containing the Vph1 protein are trafficked to the vacuolar membrane while Stv1p-containing V-ATPases are retained within the Golgi/endosomal network (MANOLSON *et al*. 1994). Similarly, higher eukaryotes use different isoforms of subunit a to alter the localization of the V-ATPase to specific cellular compartments (FORGAC 2007). One mechanism of V-ATPase regulation occurs through the rapid, reversible dissociation of the V_1 and V_0 domains (KANE 2006).

In the absence of any V_1 subunit, the V_0 domain is still properly assembled and targeted to the vacuole (GRAHAM *et al*. 2003). In the absence of the V_0 domain, V_1 is still assembled (TOMASHEK *et al*. 1997). Loss of any V_0 subunit protein prevents proper V_0 assembly and ER exit (GRAHAM *et al*. 2003), and Vph1p undergoes ubiquitin-dependent ER associated degradation (ERAD; HILL and COOPER 2000). Assembly of the V_0 domain occurs in the ER and requires the presence of a number of additional proteins (FORGAC 2007). Five ER-localized assembly factors have been identified in yeast that are required for full V-ATPase function yet are not part of the final

complex: Vma21p, Vma22p, Vma12p, Pkr1p, and Voa1p (DAVIS-KAPLAN *et al*. 2006; MALKUS *et al*. 2004; HILL and STEVENS, 1995; HIRATA *et al*. 1993; RYAN *et al*. 2008). Deletion of *VMA21*, *VMA12*, or *VMA22* causes a failure of the V_0 subunits to properly assembly in the ER and a complete loss of V-ATPase function, resulting in a full Vma$^-$ phenotype (GRAHAM *et al*. 2003). Yeast lacking *PKR1* show a limited amount of V_0 assembly (DAVIS-KAPLAN *et al.* 2006) and yeast lacking *VOA1* display only a slight reduction in V-ATPase enzyme activity (RYAN *et al.* 2008). Consequently, *pkr1Δ* cells score a partial Vma$^-$ phenotype while *voa1Δ* cells appear normal.

Genetic screens in *S. cerevisiae* have been critical in identifying the components of the V-ATPase and its associated factors (HO *et al.* 1993; OHYA *et al.* 1991; SAMBADE *et al.* 2005). However, the most recently discovered V-ATPase assembly factor, Voa1p, was identified by proteomics and *voa1*Δ cells have no detectable growth phenotype (RYAN *et al.* 2008). Voa1p physically associates with the Vma21p-V_0 complex early in V-ATPase assembly and deletion of *VOA1* displays a dramatic growth phenotype in conjunction with a specific mutant allele of the *VMA21* assembly factor, *vma21QQ* (RYAN *et al.* 2008). In yeast it has been shown that Vma21p plays a critical role in V-ATPase assembly and chaperones the completed V_0 subcomplex out of the ER to the Golgi (HILL and STEVENS 1994; MALKUS *et al.* 2004). Vma21p is retrieved back to the ER through a conserved, C-terminal dilysine motif and participates in multiple rounds of assembly and transport (HILL and STEVENS 1994; MALKUS *et al.* 2004). Mutation of the dilysines to diglutamine residues, as in *vma21QQ*, results in mislocalization of yeast Vma21p to the vacuolar membrane and a significant loss of V-ATPase function.

The identification of V-ATPase assembly factors like Voa1p that do not display a full Vma$^-$ are not likely to be found using traditional forward genetic screens. Also, pathways involved in promoting full V-ATPase function that may act independently of V_1 and/or V_0 assembly and require a sensitized genetic background to produce a detectible growth phenotype. However, *vma21QQ* mutant yeast and, more so, the *vma21QQ voa1*Δ double mutant are two cases where the V-ATPase is partially compromised for function (HILL and STEVENS 1994; RYAN *et al.* 2008). We have chosen to use these two assembly mutants in genome-wide enhancer screens to identify additional factors that assist in promoting full V-ATPase function by searching for genes that will cause an increase in calcium or zinc sensitivity when deleted.

Here we report the identification of *HPH1* and *ORM2* in a genome-wide search for V-ATPase effectors. We describe the characterization of these two redundant yeast gene pairs, *HPH1/HPH2*, and *ORM1/ORM2*, both of which display synthetic growth defects when deleted in combination with the *vma21QQ* mutant. Both sets of genes were found to have specific growth phenotypes on zinc and calcium media. Deletion of either gene pair did not affect vacuolar acidification or assembly of the V_0 domain. However, deletion of *ORM1* and *ORM2* results in a reduction of V-ATPase activity. The Orm proteins have very recently been shown to be negative regulators of sphingolipid synthesis (BRESLOW *et al.* 2010; HAN *et al.* 2010). Consistent with these reports, we find that disruption of sphingolipid biogenesis is able to suppress Orm-related growth defects.

2. *Materials and methods*

Plasmids and yeast strains: Bacterial and yeast manipulations were done using standard laboratory protocols for molecular biology (SAMBROOK and RUSSEL 2001). Plasmids for this study are listed in Table 1. *ORM1* plus flanking sequence was amplified by polymerase chain reaction (PCR) from BY4741 (Invitrogen, Carlsbad, CA) from genomic DNA using primers containing an upstream *BamHI* restriction site and downstream *SalI* restriction site. This fragment was inserted into pCR4Blunt-TOPO (Invitrogen), digested, and ligated into the *BamHI* and *SalI* sites of YEp351 to create pGF127. pGF87 was created using homologous recombination and *in vivo* ligation by gapping pRS415 and co-transforming a PCR fragment containing *prVPH1::VPH1::GFP::HIS3* (amplified from pGF06) with flanking sequence to the pRS415 vector.

Table 1. Plasmids used in this study.

Plasmid	Description	Reference
pRS415	*CEN, LEU2*	SIMONS *et al.* 1987
pRS316	*CEN, URA3*	SIKORSKI and HIETER 1989
YEp351	*2μ, LEU2*	HILL *et al.* 1986
pGF127	YEp351 *ORM1*	This study
pGF87	pRS415 *VPH1::GFP::HIS3*	This study
pGF06	pRS316 *VPH1::GFP::HIS3*	RYAN *et al.* 2008
pGF20	pRS316 *VMA2::mCherry::Nat^R*	This study

Yeast strains used in this study are listed in Table 2. GFY164 was created by PCR amplifying the *hph1Δ::Kan^R* cassette plus 500 base pairs flanking sequence from corresponding BY4741 strains of the genome deletion collection (Open Biosystems, Huntsville, AL). It was subcloned into pCR4Blunt-TOPO, reamplified by PCR,

transformed into SF838-1Dα, and selected on YEPD plus G418 (Gold Biotechnology, St. Louis, MO). Strains containing deletion cassettes other than Kan^R (Hyg^R or Nat^R) were created by PCR amplifying either the Hyg^R or Nat^R cassette from pAG32 or pAG25, respectively (GOLDSTEIN and MCCUSTER 1999) and transforming the fragment into the corresponding Kan^R genome deletion strain to exchange drug resistance markers. Deletions in the SF838-1Dα strain (GFY164, GFY165, GFY166, GFY168, GFY169, and GFY170) were constructed by PCR amplifying the appropriate gene locus (including 500 base pairs of 5' UTR and 3' UTR flanking sequence), transforming into wild-type SF838-1Dα, and selecting for the appropriate drug resistance. GFY167, GFY171, and GFY172 were created using LGY183 as the parental strain. GFY173 was created using MRY5 as the parental strain.

All deletion strains in SF838-1Dα were confirmed by diagnostic PCR from genomic DNA with primers complementary to the 5' UTR (750-1000 base pairs upstream of the start codon) and internal to the drug resistance gene. A disruption cassette was created to delete *TSC3* by first PCR amplifying the *TSC3* open reading frame with 500 base pairs of flanking UTR, subcloning in PCR4Blunt-TOPO, and introducing a unique restriction site within the ORF. The *TSC3* gene was subcloned into pRS316 and the entire ORF was replaced by the Nat^R cassette using homologous recombination. The deletion cassette was amplified and cloned into PCR4Blunt-TOPO for use in creating GFY174 (using SF838-1Dα as the parental strain), GFY175 (using GFY170 as the parental strain), and GFY313 (using MRY5 as the parental strain). pGF20 was created by first swapping GFP for mCherry (SHANER *et al.* 2004) in pRS316 *VMA2-GFP* and

introducing a unique PmeI restriction site downstream of mCherry using site directed mutagenesis.

Table 2. Yeast strains used in this study.

Strain	Genotype	Reference
SF838-1Dα	*MATα ura3-52 leu2-3,112 his4-519 ade6 pep4-3 gal2*	ROTHMAN and STEVENS 1986
Y7092	*MATα can1Δ::STE2pr-Sp_HIS5 lyp1Δ ura3Δ0 leu2Δ0 his3Δ1 met15Δ0 LYS2*	TONG and BOONE 2006
GFY36	Y7092; *vma21QQ::HA::Nat^R*	This study
GCY2	Y7092; *vma21QQ::HA voa1Δ::Kan^R*	This study
GCY3	Y7092; *vma21QQ::HA voa1Δ::Nat^R*	This study
GFY104	Y7092; *vma21QQ::HA voa1::Hyg^R*	This study
TASY006	SF838-1Dα; *vma21Δ::Kan^R*	COMPTON *et al.* 2006
LGY183	SF838-1Dα; *vma21QQ::HA*	RYAN *et al.* 2008
MRY5	SF838-1Dα; *vma21QQ::HA voa1::Hyg^R*	RYAN *et al.* 2008
MRY14	SF838-1Dα; *voa1::Hyg^R*	RYAN *et al.* 2008
GFY163	SF838-1Dα; *vma21QQ::HA::Nat^R*	This study
GFY164	SF838-1Dα; *hph1Δ::Kan^R*	This study
GFY165	SF838-1Dα; *hph2Δ::Kan^R*	This study
BY4741	*MATa leu2Δ ura3Δ met15Δ his3Δ*	Yeast Deletion Collection
GFY181	BY4741; *hph1Δ::Kan^R hph2Δ::Hyg^R*	This study
GFY166	SF838-1Dα; *hph1Δ::Kan^R hph2Δ::Hyg^R*	This study
GFY167	SF838-1Dα; *vma21QQ::HA hph1Δ::Kan^R hph2Δ::Nat^R*	This study
GFY168	SF838-1Dα; *orm1Δ::Kan^R*	This study
GFY169	SF838-1Dα; *orm2Δ::Kan^R*	This study
GFY170	SF838-1Dα; *orm1Δ::Hyg^R orm2Δ::Kan^R*	This study
GFY171	SF838-1Dα; *vma21QQ::HA orm2Δ::Kan^R*	This study
GFY172	SF838-1Dα; *vma21QQ::HA orm1Δ::Hyg^R orm2Δ::Kan^R*	This study
GFY173	SF838-1Dα; *vma21QQ::HA voa1::Hyg^R hph1Δ::Kan^R*	This study
GFY174	SF838-1Dα; *tsc3Δ::Nat^R*	This study
GFY175	SF838-1Dα; *orm1ΔHyg^R orm2Δ::Kan^R tsc3Δ::Nat^R*	This study
GFY304	SF838-1Dα; *VMA2::mCherry::Nat^R*	This study
GFY305	SF838-1Dα; *VMA2::mCherry::Nat^R vma21Δ::Kan^R*	This study
GFY302	SF838-1Dα; *VMA2::mCherry::Nat^R orm1Δ::Hyg^R orm2Δ::Kan^R*	This study
GFY313	SF838-1Dα; *vma21QQ::HA voa1::Hyg^R tsc3Δ::Nat^R*	This study

Secondly, *in vivo* ligation was used to insert the ADH terminator and Nat^R cassette at the 3' end of *VMA2*-mCherry. A single, C-terminal mCherry (PCR amplified from pGF20 including the Nat^R cassette) was integrated at the *VMA2* locus in strains GFY170, SF838-1Dα, and TASY006. This created yeast strains GFY302, GFY304, and GFY305, respectively.

The synthetic genetic array (SGA) query strains were created from yeast parental strain Y7092 (TONG and BOONE 2006). After PCR amplifying the *vma21QQ::HA::Nat*^{R} locus with 500 base pairs of flanking sequence from GFY163 genomic DNA, the PCR product was transformed into Y7092 to create GFY36. To create GCY3, GCY2 (*vma21QQ::HA voa1*Δ*::Kan*^{R}) was transformed with the Nat^R cassette to replace the Kan^R cassette. Both the *VMA21* and *VOA1* loci were PCR amplified with flanking sequence and the PCR product was transformed into Y7092. GFY104 was created by PCR amplifying both the *VMA21* and *VOA1* loci from MRY5 (*vma21QQ::HA voa1::Hyg*^{R}) with 500 base pairs of flanking sequence and transforming the fragment into GCY3.

Culture conditions: Yeast were cultured in YEPD (1% yeast extract, 2% peptone, and 2% dextrose), YEPD buffered to pH 5.0 using 50 mM succinate/phosphate plus 0.01% adenine, or synthetic minimal media with dextrose (SD) and the appropriate amino acids. Growth tests were performed by culturing exponentially growing yeast in rich medium to a cell density of 1.0 OD_{600}, serial diluted 5-fold, and spotted onto agar plates. Plates used included YEPD pH 5.0, YEPD + 4.0 mM or 5.0 mM $ZnCl_2$, YEPD + 100 mM $CaCl_2$, and YEPD + 25 mM or 50 mM $CaCl_2$ pH 7.5 (using 50 mM HEPES).

Synthetic genetic array screen: A synthetic genetic enhancer screen was performed as previously described (TONG *et al.* 2001; TONG and BOONE 2006). Briefly, the query strains (GFY36, GCY3, and GFY104) were mated to the MATa haploid genome deletion collection (BY4741, *his3*Δ*1 leu2*Δ*0, met15*Δ*0, ura3*Δ*0*) and double or triple haploid mutants were selected. The final haploid mutant array was spotted onto YEPD pH 5.0, YEPD + $ZnCl_2$, or YEPD + $CaCl_2$ pH 7.5 and incubated at 30°C for 2-3 days. Scans of each plate were visually scored for colony size on each plate type used; colonies were scored for increased sensitivity to calcium or zinc. The genome deletion collection was also arrayed under identical conditions and scored in the same way. Colonies that showed equivalent sensitivity to either metal as a single deletion strain and as part of the double (or triple) mutant collection were not scored as positive hits. Only mutants that displayed a synthetic growth defect that was not present (or not as strong) in either of the single mutant strains were scored as positive hits. Gene Ontology (GO) analysis was performed using the Saccharomyces Genome Database (SGD) GO Term Finder (version 0.83) using a p-value cut-off of 0.01.

Whole cell extract preparation and immunoblotting: Whole cell extracts were prepared as previously described (RYAN *et al.* 2008). Briefly, cultures were grown overnight in SD dropout media and then diluted to 0.25 OD_{600}/mL in YEPD pH 5.0 and grown to a cell density of OD_{600}=1.0. 10 OD_{600} of the culture was centrifuged, resuspended in 0.25 mL Thorner buffer (8M urea, 5% SDS, and 50 mM TRIS pH 6.8) and vortexed with 0.2 mL of glass beads. Following centrifugation, protein concentrations were determined using a modified Lowry protein assay (MARKWELL *et al.* 1978). Equal amounts of protein were separated by SDS-PAGE, transferred to

nitrocellulose membrane, and probed with antibodies. Antibodies used included monoclonal primary anti-Vph1p (10D7; Invitrogen, Carlsbad, CA), anti-Vma1p (8B1; Invitrogen), and anti-Dpm1p (5C5; Invitrogen), and secondary horseradish peroxidase-conjugated anti-mouse antibody (Jackson ImmunoResearch Laboratories, West Grove, PA). Blots were visualized by ECL detection.

Fluorescence microscopy: Yeast were stained with quinacrine as previously described (FLANNERY *et al.* 2004). Briefly, cells were grown overnight in YEPD pH 5.0 plus adenine, and diluted to a cell density of 0.25 OD_{600}/mL in YEPD. Yeast were harvested at a density of 0.8-1.0 OD_{600}/mL and one mL of culture was placed on ice for five minutes. Cells were pelleted and resuspended in 200 μM quinacrine, 100 mM HEPES pH 7.6, and 50 μg/mL of concanavalin A tetramethylrhodamine (Invitrogen) in YEPD for ten minutes at 30°C. Following staining with quinacrine, cells were placed on ice and washed three times in 100 mM HEPES pH 7.6 plus 2% glucose (4°C). Microscopy images were obtained using an Axioplan 2 fluorescence microscope (Carl Zeiss, Thornwood, NY). A 100x objective was used as well as AxioVision software (Carl Zeiss).

V-ATPase activity assay: Yeast vacuoles were isolated from wild-type (SF838-1Dα and BY4741), *vma21*Δ*::Kan*^{R} (TASY006), *vma21QQ::HA* (LGY183), *orm1*Δ*::Hyg*^{R} *orm2*Δ*::Kan*^{R} (GFY170), *vma21QQ::HA voa1::Hyg*^{R} (MRY5), *vma21QQ::HA orm1*Δ*::Hyg*^{R} *orm2*Δ*::Kan*^{R} (GFY172), and *hph1*Δ*::Kan*^{R} *hph2*Δ*::Hyg*^{R} (GFY166 and GFY181) strains as previously published (UCHIDA *et al.* 1985). Modifications to this protocol included harvesting cells at 1.8-2.2 OD_{600}/mL and use of a tighter-fitting dounce homogenizer (5 strokes). Fresh vacuoles were assayed by a

coupled spectrophotometric assay (CONIBEAR and STEVENS 2002). In this assay system ATP hydrolysis is coupled to NADH oxidation (340 nm) in a reaction mixture containing 50 μg/mL vacuole membrane protein, 25 mM MES, 25 mM MOPS, 25 mM KCl, 5 mM $MgCl_2$, 1 mM NaN_3, 0.05 mM Na_3VO_4, 2 mM phosphoenolpyruvate, 0.5 mM NADH, 30 U/mL pyruvate kinase and 37 U/mL lactate dehydrogenase; pH 7 (KOH), with and without 1 μM concanamycin A. Reactions were initiated by adding Mg^{2+}-ATP to 2 mM and thermostatted at 30 °C. For each mutant strain, one to three separate vacuole preparations were assayed, and the assay was repeated 2-6 times for each preparation. Concanamycin A-sensitive ATPase activities were determined by calculating the activity as a percentage of wild-type activity for each biological replicate. For samples with multiple vacuole preparations, these percentages were averaged and the error was presented as the standard error of the mean. For samples with only a single biological preparation, the error is presented as the standard deviations for replicate assays.

3. *Results*

Genome-wide synthetic genetic array (SGA) screen for V-ATPase effectors: To identify new genes that assist in promoting full V-ATPase function, we performed three synthetic genetic array (SGA) Vma^- enhancer screens using the *S. cerevisiae* haploid deletion mutant collection (4,741 mutants). Since a loss of *VOA1* only displayed a synthetic growth defect upon combination with the *vma21QQ* mutation, additional factors might only be identified in a sensitized genetic background. The three query mutants used were *vma21QQ::Nat^R, vma21QQ voa1Δ::Nat^R, and vma21QQ voa1::Hyg^R*

(subsequent experiments were all performed with the *voa1::Hyg*^{R} allele, designated as *voa1*Δ). The *VMA21* and *VOA1* loci are tightly linked; only 146 base pairs separate their open reading frames. We chose to use both mutants containing the *VOA1* disruption as it has been shown that a complete deletion of this open reading frame results in a decrease in the steady-state levels of Vma21p, whereas the *voa1::Hyg*^{R} allele does not lower Vma21p levels (RYAN *et al*. 2008). Therefore, the *voa1*Δ*::Nat*^{R} allele served as an additional sensitized genetic background.

Yeast that contain Vma21p having the mutated retrieval/retention signal, *vma21QQ,* show a partial growth defect on elevated calcium media buffered to pH 7.5 and have reduced V-ATPase activity (RYAN *et al.* 2008; HILL and STEVENS 1994). Additionally, *vma21QQ voa1*Δ yeast are also compromised for V-ATPase function yet do not display a full Vma^{-} phenotype (RYAN *et al.* 2008).

The haploid double or triple mutant yeast were plated onto rich media, and media containing either zinc (2.75 mM or 7.0 mM) or calcium (50 mM or 100 mM) buffered to pH 7.5 in quadruplicate. Yeast that displayed increased sensitivity to these conditions were scored as positive hits. Genes were identified from a diverse set of cellular processes such as protein modification, metabolism, chromatin remodeling, and transcriptional regulation (Figure 1, Table S1, see Appendix A). A comprehensive gene ontology (GO) analysis was performed for categories of genes that were enriched in our SGA screens (Table S2, see Appendix A). Some of most highly enriched categories included vacuolar transport (p-value of 4.94×10^{-17}), vesicle-mediated transport (p-value of 3.48×10^{-15}), and intracellular transport (p-value of 9.46×10^{-10}). Genes identified by the three SGA screens that correspond to elements of protein trafficking, vacuolar

morphology, and the V-ATPase complex are listed in Table 3 and several were chosen for further study.

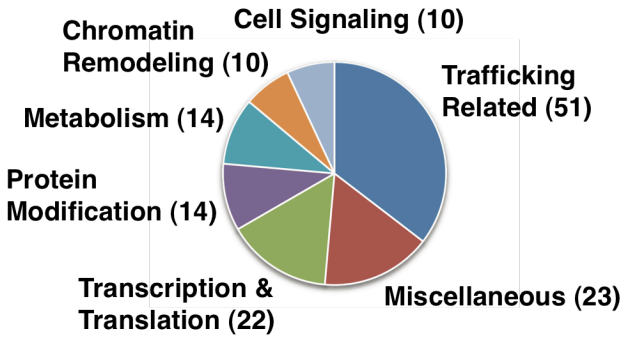

Figure 1. Molecular function of 144 genes identified in at least 2 of 3 SGA screens for an enhanced Vma$^-$ phenotype. Genes were categorized according to their presumed molecular function. The miscellaneous category includes lipids/sphingolipids, cellular morphogenesis, nuclear import, and several other processes, and also genes with no molecular characterization. A comprehensive list of all genes identified and a comprehensive GO analysis can both be found in Appendix A.

Since we were searching for genes that showed increased sensitivity to zinc or calcium when deleted in combination with *vma21QQ or vma21QQ voa1*Δ, we did not identify any of the essential V-ATPase subunits or assembly factors (those with a *VMA* designation) as expected. Also, *VOA1* was not identified in the *vma21QQ* SGA screen because it is genetically linked to the *VMA21* locus. In order for the *voa1*Δ locus to be paired with the *vma21QQ* mutation during the SGA protocol, a cross-over event would be required between these two loci. However, we did identify V-ATPase subunits *VPH1*, *STV1*, the assembly factor *PKR1*, and genes within the vacuolar transporter chaperone (VTC) and regulator of vacuolar and endosomal membrane (RAVE) complexes.

In addition, genes involved in ER-resident processes including protein folding and degradation were identified (Table 3). A number of genes were found that have been poorly characterized according to the *Saccharomyces* Genome Database (SGD) and these were most interesting to us.

Table 3. Genes found in our screens that are involved in either protein trafficking or are ER-localized are listed. A comprehensive list of all genes identified in all three screens can be found in Table S1 (see Appendix A). Screens were performed with query strains *vma21QQ voa1::Hyg*^{R} (GFY104), *vma21QQ voa1*Δ*Nat*^{R} (GCY3), and *vma21QQ-Nat*^{R} (GFY36). Colonies from the final double or triple mutant strains were analyzed for fitness defects on rich media plus 2.75 mM or 7.0 mM $ZnCl_2$ or rich media buffered to pH 7.5 plus 50 mM or 100 mM $CaCl_2$. The haploid deletion library was also tested and scored under identical media conditions. Fitness defects of single knockout strains were noted and considered when determining synthetic growth effects. *HPH1* and *ORM2* (shown in bold) were chosen for further study. A comprehensive Gene Ontology (GO) analysis for enriched categories of genes can be found in Table S2 (see Appendix A).

Trafficking Related Genes	
AP-3 (4)	*apl5*Δ, *apl6*Δ, *apm3*Δ, *aps3*Δ
Vesicle formation (5)	*arf1*Δ, *cdc50*Δ, *drs2*Δ, *vps1*Δ, *yap1801*Δ
Rabs/vesicle targeting factors (5)	*gyp1*Δ, *sro7*Δ, *vps21*Δ, *vps9*Δ, *ypt7*Δ
TGN trafficking (11)	*age2*Δ, *arl1*Δ, *arl3*Δ, *cog5*Δ, *cog6*Δ, *cog7*Δ, *cog8*Δ, *coy1*Δ, *gyp36*Δ, *sys1*Δ, *vps13*Δ
ESCRT/MVB sorting (13)	*vps2*Δ, *vps22*Δ, *vps23*Δ, *vps24*Δ, *vps25*Δ, *vps27*Δ, *vps36*Δ, *vps37*Δ, *vps4*Δ, *vps46*Δ, *vps55*Δ, *vps60*Δ, *vta1*Δ
Vacuole Inheritance (2)	*cla4*Δ, *vac8*Δ
HOPS/CORVET (4)	*vam6*Δ, *vps3*Δ, *vps33*Δ, *vps41*Δ
Endocytosis/Exocytosis (5)	*chs5*Δ, *chs6*Δ, *gsf2*Δ, *lst4*Δ, *rcy1*Δ, *drs2*Δ
ER-Golgi trafficking (12)	*bst1*Δ, *erd1*Δ, *erp3*Δ, *erv46*Δ, *gcs1*Δ, *get1*Δ, *get2*Δ, *get3*Δ, *gsg1*Δ, *pho86*Δ, *sec28*Δ, *ubp3*Δ
Autophagy (5)	*atg15*Δ, *atg21*Δ, *atg27*Δ, *atg8*Δ, *vps62*Δ
GARP (2)	*vps52*Δ, *vps53*Δ
SNAREs and fusion (8)	*gos1*Δ, *pep12*Δ, *sec22*Δ, *snx4*Δ, *swf1*Δ, *tlg2*Δ, *vam10*Δ, *vam7*Δ
Phosphatidylinositol synthesis (3)	*inp53*Δ, *sac1*Δ, *vac14*Δ
Retromer (5)	*vps17*Δ, *vps26*Δ, *vps29*Δ, *vps35*Δ, *vps5*Δ
H^+-V-ATPase (7)	*pkr1*Δ, *rav1*Δ, *rav2*Δ, *stv1*Δ, *vph1*Δ, *vtc1*Δ, *vtc4*Δ
Miscellaneous (5)	*apm1*Δ, *ccz1*Δ, *mon1*Δ, *vps19*Δ, *yck3*Δ
Genes whose protein products are ER-localized	
Protein degradation (2)	*cue1*Δ, *ubc7*Δ
Protein import and maturation (5)	*cne1*Δ, *cwh41*Δ, *emc1*Δ, *scj1*Δ, *sec66*Δ
Miscellaneous (16)	*alg6*Δ, *alg8*Δ, *bsd2*Δ, *csg2*Δ, *erg3*Δ, *erg6*Δ, *flc2*Δ, ***hph1*Δ,** *ice2*Δ, *ilm1*Δ, *mga2*Δ, ***orm2*Δ,** *ost3*Δ, *ost4*Δ, *per1*Δ, *scs2*Δ, *spf1*Δ, *sur4*Δ

We chose to examine Orm2p for further study because it was an ER-localized, integral membrane protein. Also, Hph1p has been identified as an ER-localized binding partner of calcineurin (HEATH *et al.* 2004). Due to the genetic link between calcineurin and the V-ATPase (TANIDA *et al.* 1995), we also chose *HPH1* for further study.

***HPH1*/*HPH2* or *ORM1/ORM2* null mutants cause synthetic growth defects in *vma21QQ* yeast:** The *hph1Δ* mutation was moved to the SF838-1Dα genetic background and carefully tested by serial dilution in comparison to Vma^- and Vma^-compromised strains. The growth phenotypes of *vma21QQ voa1*Δ yeast deleted for *HPH1* were tested on media containing 50 mM calcium buffered to pH 7.5 (Figure 2A). Whereas wild-type yeast were able to grow under these conditions, yeast deleted for *VMA21* were unable to grow as they lack functional V-ATPase complexes. *vma21QQ voa1*Δ yeast showed a compromised level of growth under these conditions and a deletion of *HPH1* in this strain caused a further increase in sensitivity (Figure 2A). *HPH1* has a homolog in *S. cerevisiae*, *HPH2,* and both Hph1p and Hph2p reside in the ER membrane (HEATH *et al.* 2004). It has been reported that deletions in *HPH1* and *HPH2* display a synthetic growth defect under alkaline conditions of pH 8.8 (HEATH *et al.* 2004). Since a reduction in V-ATPase function results in increased sensitivity to calcium or zinc, we determined if a loss of the *HPH* genes results in a metal-specific phenotype. Loss of either *HPH1* or *HPH2* did not result in any sensitivity to excess zinc yet deletion of both *HPH* genes caused a dramatic growth defect on 5.0 mM $ZnCl_2$ (Figure 2B). Both *HPH1* and *HPH2* were also deleted in a strain containing the *vma21QQ* mutation and tested on the less stringent conditions of 4.0 mM $ZnCl_2$. Both *vma21QQ* and *hph1*Δ *hph2*Δ yeast grew comparable to WT but the *vma21QQ hph1*Δ *hph2*Δ mutant was fully sensitive

under these conditions and unable to grow (Figure 2C). Interestingly, the *hph1*Δ *hph2*Δ double mutant did not show any sensitivity to 4.0 mM $ZnCl_2$ but displayed a dramatic shift in sensitivity between 4.0 mM and 5.0 mM $ZnCl_2$.

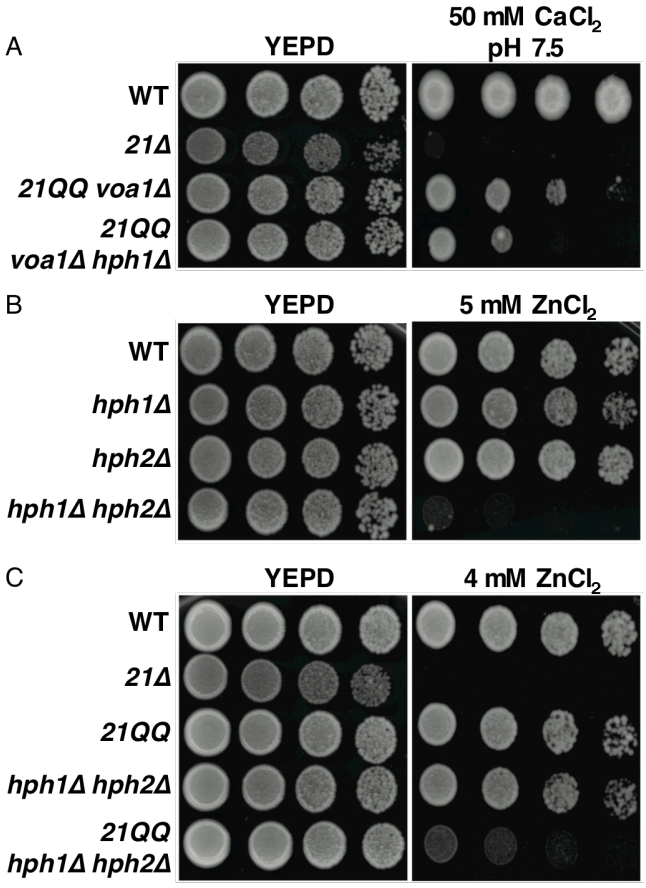

Figure 2. *HPH1* and *HPH2* display synthetic growth defects with V_0 assembly mutants. (A) Exponentially growing cultures of wild-type (WT; SF838-1Dα), *vma21*Δ (21Δ; TASY006), *vma21QQ voa::Hyg*^{R} (*21QQ voa1*Δ; MRY5), *vma21QQ voa1::Hyg*^{R} *hph1*Δ (*21QQ voa1*Δ *hph1*Δ; GFY173) were serially diluted and spotted onto rich media buffered to pH 5.0 or rich media buffered to pH 7.5 plus 50 mM $CaCl_2$. (B) Exponentially growing cultures of wild-type, *hph1*Δ (*hph1*Δ; GFY164), *hph2*Δ (*hph2*Δ; GFY165), *hph1*Δ *hph2*Δ (*hph1*Δ *hph2*Δ; GFY166) were spotted onto rich media or rich media plus 5.0 mM $ZnCl_2$. (C) Cultures of wild-type, *vma21*Δ*, vma21QQ* (*21QQ*; LGY183), *hph1*Δ *hph2*Δ, and *vma21QQ hph1*Δ *hph2*Δ (*21QQ hph1*Δ *hph2*Δ; GFY167) were serially diluted and spotted onto rich media buffered to pH 5.0 or rich media plus 4.0 mM $ZnCl_2$.

The SGA screens also identified cells lacking *ORM2* as an enhancer of the assembly factor mutant strains *vma21QQ* and *vma21QQ voa1*Δ on media containing

either zinc or calcium. The *orm2Δ* was recreated in SF838-1Dα cells expressing *vma21QQ* and tested on media containing 25 mM calcium buffered to pH 7.5. Loss of *ORM2* in *vma21QQ* yeast caused a slight increase in the sensitivity of this strain compared to *vma21QQ* yeast (Figure 3A). *ORM2* has a homolog in *S. cerevisiae, ORM1*, and the double *orm1*Δ *orm2*Δ mutant shows synthetic growth defects under various environmental stress conditions including elevated mercury or the reducing agent DTT (HJELMQVIST *et al.* 2002). We tested whether a loss of both *ORM1* and *ORM2* caused an increase in sensitivity to 25 mM calcium at pH 7.5. While deletion of *ORM1* did not result in any growth defect, yeast deleted for *ORM2* were partially sensitive under these conditions (Figure 3B). However, the *orm1*Δ *orm2*Δ double mutant displayed a synthetic growth defect under these conditions. Due to the high similarity between *ORM1* and *ORM2* (~67% identical), we tested whether *ORM1* and *ORM2* are functionally redundant. Overexpression of Orm1p was able to fully rescue the growth defect of an *orm2*Δ strain (Figure 3C). These data suggest that *ORM1* and *ORM2* are a functionally redundant gene pair; we chose to examine the effect of a loss of both Orm1p and Orm2p on the V-ATPase.

Finally, we compared the growth of *vma21QQ* and *orm1*Δ *orm2*Δ yeast to the triple *vma21QQ orm1*Δ *orm2*Δ mutant using less stringent conditions of unbuffered 100 mM $CaCl_2$. Since a loss of both *ORM1* and *ORM2* was only sensitive under stringent growth conditions, we tested whether reducing V-ATPase function using the *vma21QQ* mutant would result in a more dramatic growth phenotype. Similar to the *HPH1/2* genes, a loss of both *ORM* genes in *vma21QQ* yeast caused a severe growth defect (Figure 3D). This suggests that the *ORM* genes are required when V-ATPase activity is reduced.

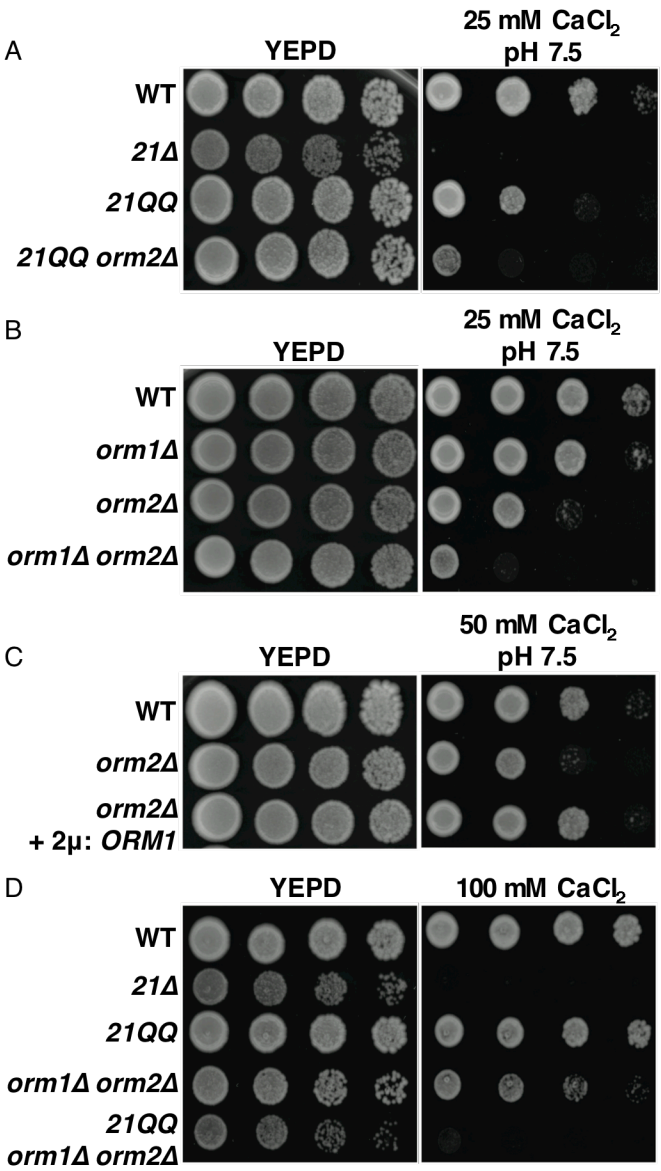

Figure 3. *ORM1* and *ORM2* display synthetic growth effects in cells expressing *vma21QQ*. (A) Exponentially growing cultures of wild-type (WT; SF838-1Dα), *vma21*Δ (*21*Δ; TASY006), *vma21QQ* (*21QQ*; LGY183), and *vma21QQ orm2*Δ (*21QQ orm2*Δ; GFY171) were serially diluted and spotted onto rich media buffered to pH 5.0 or rich media buffered to pH 7.5 plus 25 mM $CaCl_2$. (B) Cultures of wild-type, *orm1*Δ (*orm1*Δ; GFY168), *orm2*Δ (*orm2*Δ; GFY169), and orm*1*Δ *orm2*Δ (*orm1*Δ *orm2*Δ; GFY170) spotted onto rich media and rich media buffered to pH 7.5 plus 25 mM $CaCl_2$. (C) Cultures of wild-type, *orm2*Δ, and *orm2*Δ transformed with a high-copy vector expressing *ORM1* were spotted onto rich media and rich media buffered to pH 7.5 plus 50 mM $CaCl_2$. (D) Exponentially growing cultures of wild-type, *vma21*Δ*, vma21QQ, orm1*Δ *orm2*Δ*,* and *vma21QQ orm1*Δ *orm2*Δ (*21QQ orm1*Δ *orm2*Δ; GFY172) were serially diluted and spotted onto rich media buffered to pH 5.0 or rich media plus 100 mM $CaCl_2$.

Vacuolar acidification, V_0 assembly, and V-ATPase localization are normal in *HPH* and *ORM* mutants: Yeast disrupted for V-ATPase function show decreases in vacuolar acidification (DAVIS-KAPLAN *et al.* 2006; RYAN *et al.* 2008). In order to determine whether the growth defects seen with both the *HPH* and *ORM* mutants result from a loss of V-ATPase function, we assayed vacuolar acidification by fluorescent staining with quinacrine (Figure 4). Wild-type yeast displayed accumulation of quinacrine within the acidified vacuole while *vma21*Δ yeast showed no quinacrine staining. As previously shown, yeast mutant for either *vma21QQ* or *voa1*Δ displayed wild-type levels of quinacrine staining and vacuolar acidification (RYAN *et al.* 2008, Figure 4). As expected, the *vma21QQ voa1*Δ double mutant accumulated a very low level of quinacrine (Figure 4). Surprisingly, both the double mutants (*hph1*Δ *hph2*Δ and *orm1*Δ *orm2*Δ) and the triple mutant (*vma21QQ hph1*Δ *hph2*Δ) had fully acidified vacuoles (Figure 4). Only the *vma21QQ orm1*Δ *orm2*Δ mutant displayed a partial loss of quinacrine staining indicating reduced V-ATPase function.

While there was no detectable difference in vacuolar acidification, it is possible that the *HPH* and *ORM* mutants have slightly reduced levels of the V-ATPase present on the vacuole that might not be apparent using fluorescent microscopy but still be consistent with the observed growth phenotypes. We assayed the levels of Vph1p within these mutant strains by Western blotting to examine any defects in V_0 assembly (Figure 5). In wild-type yeast, Vph1 protein is extremely stable (> four hour half life; GRAHAM *et al.* 1998; HILL and COOPER 2000) and incorporated into the V_0 subcomplex. However, Vph1p is rapidly degraded (25-30 minute half life) if there is a V_0 assembly defect in the ER (GRAHAM *et al.* 1998; HILL and COOPER 2000).

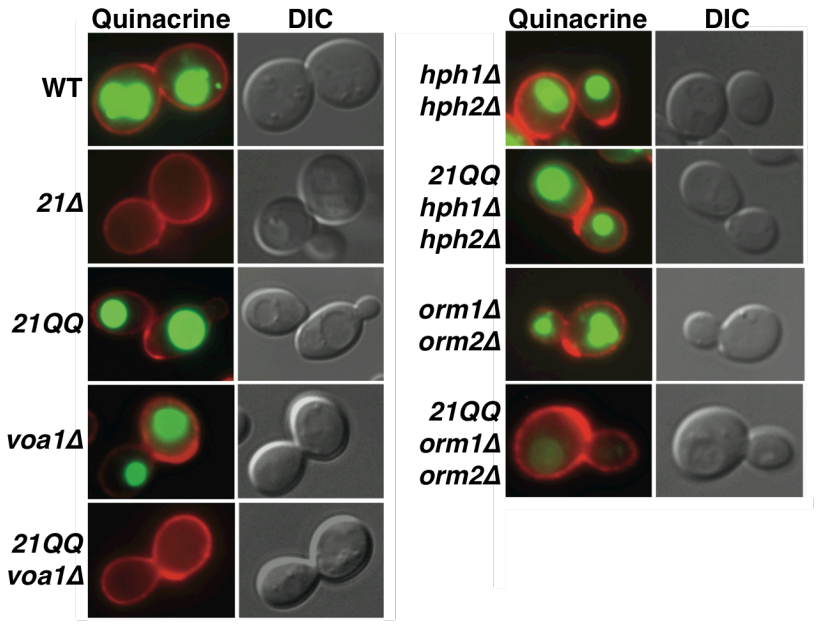

Figure 4. Loss of *HPH1/HPH2* or *ORM1/ORM2* does not result in a loss of vacuolar acidification. Exponentially growing cultures of wild-type (WT; SF838-1Dα), *vma21*Δ (*21*Δ; TASY006), *vma21QQ* (*21QQ*; LGY183), *voa1::H* (*voa1*Δ; MRY14), *vma21QQ voa1::H* (*21QQ voa1*Δ; MRY5), *hph1*Δ *hph2*Δ (*hph1*Δ *hph2*Δ; GFY166), and *vma21QQ hph1*Δ *hph2*Δ (*21QQ hph1*Δ *hph2*Δ; GFY167), *orm1*Δ *orm1*Δ (*orm1*Δ *orm2*Δ; GFY170), and *vma21QQ orm1*Δ *orm2*Δ (*21QQ orm1*Δ *orm2*Δ; GFY172) were stained with quinacrine (green) and concanavalin A-tetramethylrhodamine (red) and viewed by either fluorescent or DIC microscopy.

As predicted, the levels of Vph1p in *vma21*Δ yeast were greatly reduced compared to wild-type levels. In contrast, *voa1*Δ*, hph1*Δ *hph2*Δ*,* and *orm1*Δ *orm2*Δ yeast all displayed wild-type levels of Vph1p. This result indicates there is no V_0 assembly defect in these strains that would result in increased turnover of Vph1p. The *vma21QQ* mutant showed a slight decrease in Vph1p levels. Careful analysis has shown that this decrease was mirrored in *HPH* and *ORM* mutant strains also containing the *vma21QQ* mutation (*vma21QQ hph1*Δ *hph2*Δ and *vma21QQ orm1*Δ *orm2*Δ). Only *vma21QQ voa1*Δ yeast showed a clear reduction in Vph1p that was greater than that seen in the *vma21QQ* mutant. The ER-resident protein Dpm1p was probed as a loading control.

The steady-state levels of the V_1 subunit Vma1p did not change in any of the queried mutants.

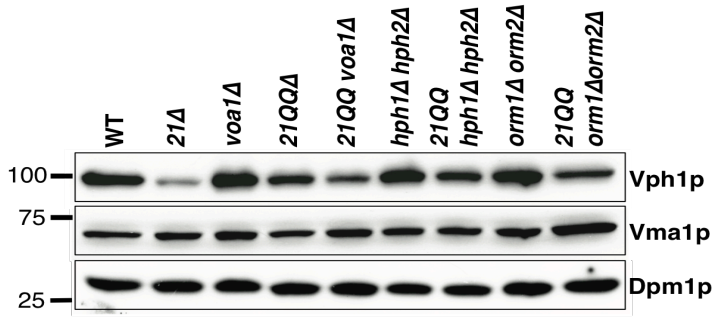

Figure 5. Vph1p levels are not reduced in strains lacking either *HPH1/HPH2* or *ORM1/ORM2*. Whole cell extracts were prepared from wild-type (WT; SF838-1Dα), *vma21*Δ (*21*Δ; TASY006), *vma21QQ* (*21QQ*; LGY183), *voa1::H* (*voa1*Δ; MRY14), *vma21QQ voa1::H* (*21QQ voa1*Δ; MRY5), *hph1*Δ *hph2*Δ (*hph1*Δ *hph2*Δ; GFY166), and *vma21QQ hph1*Δ *hph2*Δ (*21QQ hph1*Δ *hph2*Δ; GFY167), *orm1*Δ *orm1*Δ (*orm1*Δ *orm2*Δ; GFY170), and *vma21QQ orm1*Δ *orm2*Δ (*21QQ orm1*Δ *orm2*Δ; GFY172). Proteins were separated by SDS-PAGE and probed with anti-Vph1p and anti-Vma1p antibodies. Anti-Dpm1p antibody was used as a loading control. The molecular mass (kilodaltons) of the nearest marker is shown on the left.

The localization of the V-ATPase was also examined in both the *ORM* and *HPH* mutant strains. Yeast expressing both the V_0 subunit Vph1p-GFP and the V_1 subunit Vma2p-mCherry were visualized by fluorescent microscopy. In wild-type yeast, Vph1p-GFP localized to the limiting membrane of the vacuole and co-localized with Vma2p-mCherry (Figure 6). There was also a pool of Vma2p-mCherry staining within the cytosol in a diffuse pattern. In *vma21*Δ yeast, Vph1p-GFP was found in both cortical and perinuclear ER structures and Vma2p-mCherry was only localized within the cytosol. Yeast mutant for *orm1*Δ *orm2*Δ showed both V_0 and V_1 localized to the vacuolar membrane similar to wild-type cells (Figure 6). Strains mutant for *hph1*Δ *hph2*Δ localized Vph1p-GFP to the vacuole (data not shown).

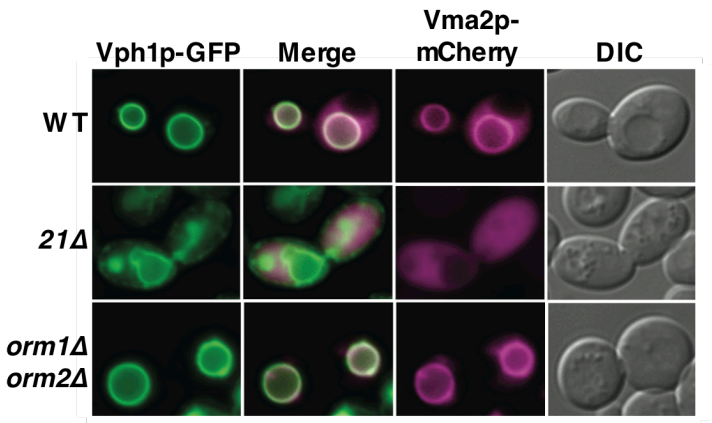

Figure 6. V_1 and V_0 are localized to the vacuole membrane in *Orm* mutant yeast. A single mCherry was integrated at the *VMA2* locus in the following strains: wild type (WT; GFY304), *vma21*Δ (*21*Δ; GFY305), and *orm1*Δ *orm2*Δ (*orm1*Δ *orm2*Δ; GFY302). Yeast strains also contained a vector expressing Vph1p-GFP (pGF87). Exponentially growing cells were visualized by fluorescent and DIC microscopy.

Loss of the *ORM* genes (but not the *HPH* genes) results in reduced V-ATPase enzyme activity: Since it is possible that the growth defects seen in the *HPH* and *ORM* strains could result from defects in V-ATPase enzyme function (rather than from assembly defects), we performed V-ATPase activity assays on isolated vacuole membranes in these mutant strains. We measured vacuole membranes from the *hph1*Δ *hph2*Δ strain to have 88% V-ATPase activity, whereas the *orm1*Δ *orm2*Δ mutant had 67% activity relative to wild-type yeast (Table 4). We also tested V-ATPase enzyme activity for the *hph1*Δ *hph2*Δ mutant in a separate genetic background (BY4741) and found no difference from wild-type vacuole membranes (116% of WT; Table 4). We determined the *vma21QQ* mutant activity to be 22% of wild-type yeast despite the appearance of fully acidified vacuoles. The double *vma21QQ voa1*Δ mutant showed a dramatic decrease to 9%. The *vma21QQ orm1*Δ *orm2*Δ triple mutant had a comparable reduction of V-ATPase activity to 8% relative to wild-type yeast. These results indicate

that the Hph proteins do not affect the activity of the V-ATPase and that the Orm proteins are required for full V-ATPase function.

Table 4. V-ATPase activity and quinacrine staining of mutants. Loss of both *ORM1* and *ORM2* results in a decrease in V-ATPase activity. Activity assays were performed for wild-type strains (WT; SF838-1Dα and WT; BY4741), *vma21*Δ (*21*Δ; TASY006), *vma21QQ* (*21QQ*; LGY183), *voa1::H* (*voa1*Δ; MRY14), *orm1*Δ *orm1*Δ (*orm1*Δ *orm2*Δ; GFY170), *vma21QQ voa1::H* (*21QQ voa1*Δ; MRY5), *hph1*Δ *hph2*Δ SF838-1Dα (*hph1*Δ *hph2*Δ; GFY166), *hph1*Δ *hph2*Δ BY4741 (*hph1*Δ *hph2*Δ; GFY181) and *vma21QQ orm1*Δ *orm2*Δ (*21QQ orm1*Δ *orm2*Δ; GFY172). A continuous, coupled spectrophotometric assay (CONIBEAR and STEVENS 2002) was used to assay freshly prepared vacuole membranes for concanamycin A-sensitive ATPase activity. The wild-type strain SF838-1Dα had an average specific activity of 0.817 μmol min^{-1} mg^{-1} (average of n = 7 independent vacuole isolations) and the wild-type strain BY4741 has a specific activity of 0.836 μmol min^{-1} mg^{-1} (1 vacuole isolation). The specific activity of mutant samples was divided by the wild-type specific activity measurement for each independent vacuolar preparation to produce a relative percentage. For samples prepared more than once (biological replicates indicated in parentheses), the different percentages were averaged to produce the percentage wild-type activity measurements +/- the standard error of the mean. Quinacrine staining is derived from Figure 3.

Strain	% wild type ATPase activity	Quinacrine
Wild type (SF838-1Dα)	100	++++
Wild type (BY4741)	100	++++[a]
*vma21*Δ	1 +/- 0.3 (1)[d]	-
*hph1*Δ *hph2*Δ (SF838-1Dα)	88 +/- 6 (4)[b]	++++
*hph1*Δ *hph2*Δ (BY4741)	116 +/- 0.7 (1)[d]	++++[a]
*orm1*Δ *orm2*Δ	67 +/- 6 (3)	++++
*voa1*Δ	75[c]	++++
vma21QQ	22 +/- 1 (3)	++++
*vma21QQ voa1*Δ	9 +/- 0.5 (2)	+
*vma21QQ orm1*Δ *orm2*Δ	8 +/- 0.5 (2)	++

[a] Data not shown.
[b] 3 of 4 measurements for *hph1*Δ *hph2*Δ (SF838-1Dα) averaged 97% of wild-type.
[c] From RYAN *et al.* 2008.
[d] For stains with only a single biological preparation, the error is expressed as the standard deviation of technical replicates.

The Orm proteins function in sphingolipid regulation: Two reports have recently demonstrated that Orm1p and Orm2p are negative regulators of the serine palmitoyltransferase (SPT) complex responsible for the first and rate-limiting enzymatic

step of sphingolipid synthesis (BRESLOW *et al.* 2010; HAN *et al.* 2010). Since loss of Orm1p and Orm2p has been shown to result in increased sphingolipid production (BRESLOW *et al.* 2010; HAN *et al.* 2010), we tested whether inhibition of the SPT complex alleviated the defects seen in an *orm1*Δ *orm2*Δ mutant. Tsc3p is a small protein that associates with the SPT enzyme and is required for full activity of this complex (GABLE *et al.* 2000). We deleted *TSC3* in the *orm1*Δ *orm2*Δ mutant and tested the triple mutant strain on media containing elevated calcium and buffered to pH 7.5 (Figure 7A). Yeast lacking *TSC3* did not display any growth defect under these conditions. However, loss of *TSC3* allowed for increased growth of the *orm1*Δ *orm2*Δ strain. Additionally, suppression by deletion of *TSC3* was specific to the *orm1*Δ *orm2*Δ mutant, as loss of this regulator did not suppress the calcium sensitivity of the *vma21QQ voa1*Δ mutant (Figure 7B). These results suggest that the growth defects seen in the *orm1*Δ *orm2*Δ mutant strain are due to perturbation of sphingolipid synthesis.

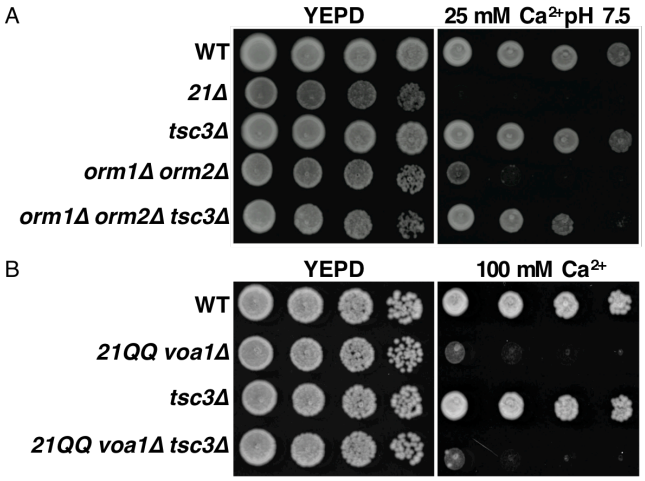

Figure 7. Orm sensitivity to buffered calcium media can be suppressed by inhibition of sphingolipid biogenesis. A) Cultures of wild-type (WT; SF838-1Dα), *vma21*Δ (*21*Δ; TASY006), *tsc3*Δ (*tsc3*Δ; GFY174), *orm1*Δ *orm2*Δ (*orm1*Δ *orm2*Δ; GFY170), and *orm1*Δ *orm2*Δ *tsc3*Δ (*orm1*Δ *orm2*Δ *tsc3*Δ; GFY175) were spotted onto rich media and media containing 25 mM $CaCl_2$ buffered to pH 7.5. B) Wild-type, *vma21QQ voa1*Δ (*21QQ voa1*Δ; MRY5), *tsc3*Δ, and *vma21QQ voa1*Δ *tsc3*Δ (*21QQ voa1*Δ *tsc3*Δ; GFY313) yeast were spotted onto rich media and media containing 100 mM $CaCl_2$.

4. *Discussion*

The goal of this study was to identify additional factors that contribute to V-ATPase function that may have been missed by previous forward genetic screens. The power of enhancer and suppressor screens is evident from work in both *D. melanogaster* and *C. elegans* where it is often necessary to use a sensitized background to uncover new genetic pathways (ST JOHNSTON 2002; JORGENSEN and MANGO 2002). In the case of the yeast V-ATPase, parallel genetic pathways are most likely not the main obstacles for identifying subtle effectors of this complex. Instead, the V-ATPase enzyme within the cell requires a dramatic decrease in enzyme function or assembly before cellular growth phenotypes become evident (RYAN *et al.* 2008). The discovery of the fourth and fifth factors that participate in V_0 assembly (Pkr1p and Voa1p) demonstrates the complexity of the assembly processes required for the V-ATPase enzyme complex. While Voa1p has been shown to physically associate with the V_0 subcomplex in the ER (RYAN *et al.* 2008), no physical association has been characterized for Pkr1p despite a strong genetic link to the assembly factor Vma21p (DAVIS-KAPLAN *et al.* 2006; data not shown, GRAHAM and STEVENS). Growth phenotypes associated with perturbation of the V-ATPase are only evident upon a significant reduction in enzyme activity to about 20% of wild-type as in the case of the mutant assembly factor allele, *vma21QQ* (HILL and STEVENS 1994). This retrieval-defective mutant allele of the highly conserved assembly factor, Vma21p, is a unique scenario to serve as a genetic tool for enhancer (and suppressor) screens because (i) the levels of functional V-ATPase are sufficiently low to allow for phenotypic scoring, and (ii) the V-ATPase is not

compromised for enzyme function, but rather, is defective for assembly due to the limited supply of Vma21p in the ER.

In performing genome-wide enhancer screens with the *vma21QQ* and *vma21QQ voa1*Δ alleles, a large number of genes involved in vesicular trafficking pathways, endosomal ESCRT machinery, vesicle formation, and vacuolar morphology were identified. Deletion of some trafficking-related genes has been shown to result in sensitivity to zinc, calcium, or alkaline conditions (PAGANI *et al.* 2007; SAMBADE *et al.* 2005; SERRANO *et al.* 2004). Our strategy for screening effectively detected reduced V-ATPase activity levels to ~10% of wild-type yeast (scored as <50% of activity in the *vma21QQ* mutant strain). It is therefore not surprising that we have identified additional genes involved in trafficking pathways that were not previously found in forward genetic screens. For instance, many of the vacuolar protein sorting (VPS) genes have not been identified in previous genome-wide screens for Vma^{-} phenotypes (SAMBADE *et al.* 2005). The genetic relationship between these sorting pathways and vacuolar acidification most likely results from aberrant sorting of the V-ATPase. There are many ways by which disruption of vesicular trafficking can result in mislocalization of the V-ATPase enzyme. For example, loss of the AAA-ATPase Vps4p results in an aberrant multivesicular body that traps vacuole-bound cargo in this compartment (RAYMOND *et al.* 1992). In addition, loss of the syntaxin Pep12p (another class of trafficking mutants) results in mislocalization of Vph1p (GERRARD *et al.* 2000). If the V-ATPase is not targeted to the vacuolar membrane, the pH gradient necessary to drive the sequestration of excess metals is not established, and the result is an increased sensitivity in our screen. Due to the complexity of protein sorting from the Golgi to the

vacuole, there are many components that are required for proper transport of the V-ATPase to the vacuole membrane (BOWERS and STEVENS 2005). It will be of interest to determine if disruption of other trafficking pathways is able to affect metal sensitivity without perturbation of V-ATPase localization and function.

We chose to characterize two gene families, *HPH1* and *ORM2*, whose protein products had been previously reported to localize to the ER; both have homologs within budding yeast, *HPH2* and *ORM1*, respectively (HEATH *et al.* 2004; HJELMQVIST *et al.* 2002). *HPH1* and *HPH2* have been characterized as new components of calcineurin signaling (HEATH *et al.* 2004). Genetic screens have also found that deletion of any of the essential subunits of the V-ATPase is synthetic lethal with a loss of calcineurin (TANIDA *et al.* 1995; PARSONS *et al.* 2004). We therefore investigated the involvement of the Hph proteins in the function and/or assembly of the V-ATPase complex in the ER.

HPH1 and *HPH2* have been previously reported to be functionally redundant and sensitive to high salinity or alkaline conditions (HEATH *et al.* 2004). We have found a unique set of growth phenotypes associated with a loss of *HPH1* and *HPH2* on media containing excess metals. The *hph1*Δ *hph2*Δ mutant did not display any sensitivity to elevated calcium (data not shown) yet displayed a non-linear shift in zinc sensitivity. This was unusual, as our previously observed V-ATPase mutants with a partial reduction in function, *pkr1Δ*, *vma21QQ*, and *vma21QQ voa1Δ* (data not shown), exhibit growth defects on *both* zinc and calcium to varying degrees, and have a gradual response to increasing concentrations of $ZnCl_2$. Preliminary work has also demonstrated that the zinc sensitivity of the *hph1*Δ *hph2*Δ mutant was not completely dependent on calcineurin (data

not shown). Based on our results, we propose that the growth defect of *hph1*Δ *hph2*Δ yeast on $ZnCl_2$ likely results from a V-ATPase independent mechanism. It is unclear if the zinc sensitivity in *Hph* mutants results from an effect on vacuole-localized Zn^{2+} transportation or some other mechanism.

Genome-wide screens for zinc or calcium (at pH 7.5) sensitivity have found genes that do not directly contribute to V-ATPase function yet show sensitivity to excess metals (PAGANI *et al.* 2007; SAMBADE *et al.* 2005). An example is deletion of the vacuolar zinc transporter Zrc1p that confers zinc sensitivity even though vacuolar acidification is normal (data not shown). Also, a loss of the serine protease Kex2p results in both calcium and zinc sensitivity yet does not cause any defect in vacuolar acidification (SAMBADE *et al.* 2005). Identifying which genetic pathways are directly linked to metal sensitivity independent of V-ATPase function will require further study.

The Orm proteins are also functionally redundant, integral membrane proteins that localize to the ER in yeast (data not shown). Since loss of both *ORM* genes caused a reduction in vacuolar acidification and V-ATPase enzyme activity in the context of the *vma21QQ* mutation, we propose that Orm1p and Orm2p are necessary for full V-ATPase function. However, the phenotype associated with disruption of only the *ORM* genes does not completely phenocopy a loss of other assembly factors (such as *PKR1* or the combination *vma21QQ voa1*Δ). Key differences highlight the potential mechanism through which the Orm proteins may impact the V-ATPase including the lack of an apparent V_0 assembly defect. It is unlikely that the Orm proteins transiently participate in V_0 assembly of the V-ATPase, as we were unable to determine any physical association of Orm2p with the Vma21p-V_0 subcomplex (data not shown).

We also examined whether a variety of cargo proteins (including both subdomains of the V-ATPase) were aberrantly targeted upon a loss of the Orm proteins. Resident ER (Vma21p), Golgi (Vps10p), plasma membrane (Pma1p, Ste3p, and Snf3p), and vacuolar proteins (Sna3p, Zrt3p, Vcx1p, ALP, and Cps1p) did not display changes in localization patterns compared to wild-type yeast (data not shown). Consistent with these data, we found normal V_1V_0 localization of the V-ATPase to the vacuole membrane; these suggested an indirect involvement of Orm1p and Orm2p. A more likely scenario involves perturbation of V-ATPase function through other cellular pathways.

Recently, two studies have characterized Orm1p and Orm2p as negative regulators of sphingolipid synthesis (BRESLOW *et al.* 2010; HAN *et al.* 2010). Both groups have reported that the Orm proteins physically associate with and regulate the SPT complex in the ER. Interestingly, inhibition of the SPT enzyme complex was found to alleviate phenotypes associated with a loss of *ORM1* and *ORM2* including cold sensitivity and sensitivity to tunicamycin (HAN *et al.* 2010). Our data are consistent with these findings and it is likely that *ORM1* and *ORM2* indirectly affect V-ATPase function through perturbation of sphingolipid production. This interpretation is in agreement with the effect of the lipid environment on the assembly, transport or function of various enzymes including the amino acid permease Gap1p (LAUWERS *et al.* 2007), uracil permease Fur4p (HEARN *et al.* 2003), and plasma membrane H^+-ATPase Pma1p (WANG and CHANG 2002; GAIGG *et al.* 2006).

Also, deletion of two components of the fatty acid elongation pathway required for sphingolipid C26 acyl group synthesis (*fen1*Δ *and sur4*Δ) resulted in perturbation of vacuolar acidification, a decrease in V-ATPase enzyme activity, and a functionally

compromised V_1 domain (CHUNG *et al.* 2003). This previous study reported destabilization of the V-ATPase, specifically a portion of the V_1 subdomain dissociates from the membrane during vacuole membrane preparation of the *sur4*Δ mutant. Since loss of the Orm proteins results in a similar change in the lipidome as *sur4*Δ yeast (Breslow et al., 2010), loss of the V_1 subdomain during vacuolar preparation could explain why *vma21QQ orm1*Δ *orm2*Δ cells display levels of V-ATPase activity similar to *vma21Q voa1*Δ yeast but higher vacuolar acidification *in vivo.* Since they are negative regulators, deletion of *ORM1* and *ORM2* results in an increase in the sphingolipid composition of the cell (BRESLOW *et al.* 2010). Loss of the Orm proteins results in a subtle decrease in V-ATPase function and this differs from both the *sur4*Δ and *fen1*Δ mutations. However, this connection between sphingolipid regulation and V-ATPase function would have been missed in previous forward genetic screens. Overproduction of sphingolipids likely results in an altered lipid environment for the V-ATPase as sphingolipids play crucial roles for many cellular functions (HANADA 2003; COWART and OBEID 2007).

The use of sensitized genetic backgrounds to identify factors that have subtle effects on V-ATPase function has revealed genes involved in a variety of cellular pathways. We have identified the Orm proteins and implicated sphingolipid regulation as important contributors to full V-ATPase enzyme activity. Future genome-wide screens that specifically assay V-ATPase function will aid in separating genes, like *HPH1* and *HPH2*, which do not directly affect enzyme activity, from those that are dedicated effectors of V-ATPase assembly, transport, or enzyme function. Finally, further characterization of the precise mechanism by which alteration of sphingolipids and the

cellular lipid composition affect function of the V-ATPase will be of great interest and provide a more complete understanding of this crucial molecular machine.

The work from this Chapter presents a connection between the lipid composition of the cell and V-ATPase enzyme function. This work is consistent with other reports that have documented the impact that changes to the lipidome have on other molecular cargo include the V-ATPase. Additionally, these genome wide screens have implicated a number of trafficking-related genes and processes in V-ATPase function.

For mutants that have lost *ORM1*/*ORM2*, there does not seem to be an effect either assembly or trafficking of the V-ATPase. Therefore, it is possible that the local lipid environment is affecting either (i) enzyme activity of the enzyme complex and/or (ii) regulation of the complex. Understanding the link between lipids and the V-ATPase will require further study. However, previous observations have shown that the two isoforms of the V-ATPase (containing either Stv1p or Vph1p) are differentially regulated and have different coupling efficiencies. It is possible that some of these biochemical differences can be attributed to the specific cellular compartments where these enzymes reside. In order to further explore the differences between the Stv1p and Vph1p V-ATPase complexes, I have taken an evolutionary approach. Characterization of the trafficking, assembly, and regulation of these two isoforms of the V-ATPase will provide additional insight into the effects of local cellular environments can have on enzyme function.

CHAPTER III

THE RECONSTRUCTED ANCESTRAL SUBUNIT A FUNCTIONS AS BOTH V-ATPASE ISOFORMS VPH1P AND STV1P IN EXTANT *S. CEREVISIAE*

The phylogenetic analysis and ancestral reconstruction was performed by V. Hanson-Smith (affiliated with the Center for Ecology and Evolutionary Biology and Department of Computer Science, University of Oregon, Eugene, OR, 97403). B. D. Houser and H. J. Park (both from the Department of Chemsitry, University of Oregon, Eugene, OR 97403) contributed to several figures and unpublished data. G. C. Finnigan performed all other experiments and did all of the writing. V. Hanson-Smith and T. H. Stevens provided editorial comments. This manuscript has been submitted to *Molecular Biology of the Cell* and is in the first revision. G. C. Finnigan and T. H. Stevens are affiliated with the University of Oregon (Eugene, OR, 97403).

Abbreviations used: V-ATPase, vacuolar-type proton translocating ATPase; Anc.a, the reconstructed, ancestral subunit a of the vacuolar H^+-ATPase within the fungal clade; YEPD, yeast extract peptone dextrose; HA, hemagglutinin; BPS, bathophenanthrolinedisulfonic acid; GFP, green fluorescent protein; ALP, yeast alkaline phosphatase encoded by the *PHO8* gene; CPY, vacuolar carboxypeptidase Y encoded by the *PRC1* gene; mDsRed, monomeric form of a red fluorescent protein from the genus *Discosoma*; mCherry, a mutated form of monomeric red fluorescent protein; ML, maximum likelihood; PP, posterior probability.

1. *Introduction*

The vacuolar H^+-ATPase (V-ATPase) is a multisubunit molecular machine responsible for organelle acidification in eukaryotes (Forgac, 2007). The V-ATPase enzyme couples hydrolysis of ATP with proton translocation across membranes using a conserved rotary mechanism (Marshansky and Futai, 2008). The electrochemical gradient generated by the V-ATPase is required for a diverse set of biological processes including vesicular trafficking, exocytosis, membrane fusion, ion homeostasis, development, and pH regulation (Kane 2006; Forgac 2007). The V-ATPase has also been implicated in a number of disease models including cancer cell migration (Martinez-Zaguilan *et al*., 1999), osteopetrosis (Frattini *et al*., 2000), viral entry into cells (Gruenberg and van der Goot, 2006), and renal tubular acidosis (Karet *et al*., 1999).

The budding yeast *S. cerevisiae* serves as an excellent model system to study the V-ATPase because the enzyme complex is not required for viability. Yeast use the proton gradient generated by the V-ATPase to maintain pH levels and regulate ion homeostasis (Kane, 2006). Toxic levels of metals are sequestered within the yeast vacuole by proton-exchange antiporter pumps (Klionsky *et al*., 1990). Disruption of V-ATPase function results in a loss of vacuolar acidification and renders cells sensitive to excess levels of metals such as calcium or zinc. The yeast V-ATPase complex contains 14 different subunits, some of which are present in multiple copies (Forgac, 2007). The enzyme contains two subdomains: the cytosolic V_1 portion is responsible for hydrolysis of ATP whereas the membrane-bound V_0 portion transports protons across the lipid bilayer (Graham et al., 2003). The V_1 domain contains subunits A, B, C, D, E, F, G, and H whereas the V_0 domain contains subunits a, d, e, c, c' and c"; all of these subunits are

required for V-ATPase function. Assembly of the V_0 subdomain occurs within the endoplasmic reticulum (ER) and requires the presence of five dedicated assembly factors: Vma21p, Vma22p, Vma12p, Pkr1p, and Voa1p (Hirata *et al*., 1993; Hill and Stevens, 1995; Malkus *et al*., 2004; Davis-Kaplan *et al*., 2006; Ryan *et al*., 2008). These ER-resident proteins aid in chaperoning components of the V_0 and are required for full enzyme function. Regulation of V-ATPase function can occur through rapid, reversible dissociation of the V_1 and V_0 subcomplexes, differential assembly, or differences in the localization of the enzyme complex (Kane 2006; Forgac 2007).

Yeast contain two different V-ATPase complexes depending on the incorporation of one of two isoforms of the V_0 subunit a, Vph1p or Stv1p (Figure 1; Manolson *et al*., 1992, 1994). The subunit composition of the V-ATPase is identical between these two populations yet there are dramatic functional and phenotypic differences for each protein complex (Qi and Forgac, 2007; Manolson *et al*., 1994). In yeast, subunit a is responsible for targeting of the V-ATPase to distinct subcellular compartments; complexes containing Vph1p (Vph1p-complex) reside on the vacuolar membrane whereas Stv1p-containing complexes (Stv1p-complex) are found within the Golgi/endosomal network (Manolson *et al*., 1994). The cytosolic, N-terminal portion of Stv1p and Vph1p contains the targeting information necessary for trafficking of the V-ATPase to these organelles (Kawasaki-Nishi *et al*., 2001a). Complexes containing the Stv1p isoform (Stv1p-complex) are retained and/or retrieved between the late Golgi and endosome (Kawasaki-Nishi *et al*., 2001a). Aside from the difference in localization, the Stv1p and Vph1p complexes have been shown to differ in transcript expression, protein abundance, assembly, coupling efficiency, and reversible dissociation. The Stv1p-complex is found

at much lower protein levels, has a lower ATP coupling efficiency, and does not undergo reversible dissociation of V_1 and V_0 upon glucose starvation compared to the Vph1p-complex (Manolson *et al*., 1992, 1994; Kawasaki-Nishi *et al*., 2001b; Perzov *et al*., 2002).

There is a relative paucity of information describing the evolutionary mechanisms responsible for the presence of multiple isoforms of various V-ATPase subunits. Phylogenetic analysis suggests that gene duplication events played a significant role in the evolution of subunit a and the entire V-ATPase enzyme in eukaryotes (Müller and Grüber, 2003; Cross and Müller, 2004). Characterization of the two subunit a isoforms within budding yeast revealed a number of key biochemical differences in regulation, assembly, and trafficking between the V-ATPase complexes. However, it is unclear how subunit a in *S. cerevisiae* evolved from a pre-duplicated, single isoform into the two contemporary Vph1p and Stv1p subunits.

Eukaryotes outside of fungi also have multiple genes and many isoforms of various V-ATPase subunits including subunit a (Forgac, 2007). For instance, *C. elegans* has four isoforms of subunit a (Oka *et al*., 2001b), mice have four isoforms including one present on the plasma membrane (Oka *et al*., 2001a; Toyomura *et al*., 2003), and *Paramecium tetraurelia* is reported to have 17 distinct subunit a isoforms (Wassmer *et al*., 2006). The increasing number of separate isoforms allows for a high degree of specialization in the subcellular localization of the V-ATPase as well as cell-specific expression and regulation (Toei *et al*., 2010).

Although most eukaryotes use several distinct V-ATPase isoforms of subunit a, there are groups of species that have only a single isoform. How are eukaryotes with

only one V-ATPase complex able to properly acidify various cellular compartments? Fungal species basal to the clade of budding yeast belong to a group that contains only a single subunit a isoform (Chavez *et al*., 2006). However, attempts to characterize homologs of subunit a from *A. thaliana* and *S. pombe* within budding yeast for V-ATPase function have been met with no success (Aviezer-Hagai *et al*., 2000; unpublished results) because difficulties in this horizontal evolutionary approach often result from differences in genetic background (Harms and Thornton, 2010). This approach does not address (i) sequence changes that have accumulated over evolutionary time that did not contribute to protein function and (ii) the effects of epistatic interactions between mutational changes that have occurred along lineage-specific evolutionary trajectories (Harms and Thornton, 2010).

To address these questions, we reconstructed the most recent common ancestor of Vph1p and Stv1p and tested its function as the only isoform of subunit a in *S. cereviaise.* The ancestral subunit a (Anc.a) functionally replaces both Vph1p and Stv1p through acidification of both the Golgi/endosomal network and vacuole. Anc.a displays a dual localization pattern to both of these cellular compartments. Additionally, trafficking of Anc.a does not utilize the sorting machinery that has evolved to retain and/or retrieve Stv1p within the *trans* Golgi. Rather, it is likely that Anc.a localizes to both structures through slowed anterograde transport *en route* to the yeast vacuole.

2. *Materials and methods*

***In silico* reconstruction of ancestral protein sequences:** GenBank was queried for all fungal V-ATPase subunit a sequences and protein sequences for sixty-eight

isoforms were returned (Supplemental Table S1, see Appendix B). The non-fungal subunit a sequences for *D. discoideum* and *A. thaliana* were also retrieved and used as a phylogenetic outgroup. Sequences were aligned using PRANK v0.081202 (Loytynoja and Goldman, 2005, 2008). This alignment was best-fit by the Whelan-Goldman matrix (WAG) with gamma-distributed rate variation (+G) and proportion of invariant sites (+I), according to the Akaike Information Criterion as implemented in PROTTEST (Whelan and Goldman, 2001, Abascal *et al*., 2005). In-house code modification of PhyML v3.0 was used to infer the maximum likelihood (ML) topology, branch lengths, and model parameters (Guindon and Gascuel, 2003). Specifically, the topology was optimized by using the best result from Nearest-Neighbor-Interchange and Subtree Pruning and Regrafting (using PhyML's implementation). All other free parameters using our implementation of the limited-memory Broyden-Fletcher-Goldfarb-Shanno multidimensional optimization algorithm were also optimized (Liu and Nocedal, 1989). Phylogenetic branch support was calculated as the approximate likelihood ratio based on a Shimodaira-Hasegawa-like procedure (Anismova and Gascuel, 2006).

ML ancestral states were reconstructed at each site for all ancestral nodes in the ML phylogeny using a set of Python scripts, called *Lazarus* (Hanson-Smith *et al*., 2010), which wraps PAML version 4.1 (Yang, 2007). Lazarus parsimoniously placed ancestral gap characters according to Fitch's algorithm (Fitch, 1971). The overall support for the reconstructed Anc.a sequence was characterized by binning the posterior probability of the ML state at each ancestral site into 5%-sized bins and counting the proportion of total sites within each bin (Supplemental Figure S1, see Appendix B).

Plasmids and yeast strains: Standard molecular biology procedures were used in this study (Sambrook and Russel, 2001). Plasmids that were used can be found in Table 1. To construct pGF35, plasmid pAAC200 (Cooper and Stevens, 1996) was digested with StuI. Next, a polymerase chain reaction (PCR) product of the C-terminal portion of the *VPS10* open reading frame (ORF) fused to GFP, the *S. pombe HIS5* cassette (Yeast GFP Collection; Invitrogen, Carlsbad, CA), and *VPS10* 3' untranslated region was obtained. Using homologous recombination and *in vivo* ligation, the PCR fragment and gapped vector were co-transformed into wild-type (BY4741) yeast and selected for growth on media lacking histidine to create pGF35. The Anc.a sequence was synthesized by GenScript (Piscataway, NJ) with a yeast codon bias. A double hemagglutinin (HA) epitope tag was included after site 171 in Anc.a. This corresponds to the same position as the double HA tags found in both Stv1p (site 219) and Vph1p (site 185) (Kawasaki-Nishi *et al*., 2001). The Anc.a gene was subcloned to a single-copy, *CEN*-based yeast vector and tagged with either the *ADH* terminator sequence (247 base pairs) and Nat^R drug resistance cassette (Goldstein and McCuster, 1999) or *GFP::ADH::Hyg*^{R} cassette (amplified from pGF123) using *in vivo* ligation. A second round of *in vivo* ligation was used to place the Anc.a gene (with or without the GFP tag) under control of either the *STV1* promoter (500 base pairs) or *VPH1* promoter (380 base pairs) to create pGF243-pGF246. To create pGF341-342, the *VPH1* promoter and Anc.a gene (containing codons 1-736) were PCR amplified (from pGF245), propagated in pCR4Blunt-TOPO (Invitrogen), and subcloned to pRS316. Similarly, the C-terminal portion of Anc.a (codons 737-stop) including the *ADH::Nat*^{R} cassette was cloned into a TOPO vector. The R737Q or R737A mutation was introduced into primers that

contained 40 base pairs of sequence homology to the Anc.a coding region and downstream vector sequence. *In vivo* ligation was used to recreate a full-length Anc.a gene containing the two mutational changes. For construction of pGF242, the mCherry tag (Shaner *et al*., 2004) was amplified, cloned into TOPO, subcloned to a CEN-vector, and tagged with *ADH::Nat*^{R} using *in vivo* ligation. The mCherry tag was placed behind the promoter of *VPH1* (380 base pairs) and included a start codon. Subsequent subcloning removed the *ADH::Nat*^{R} marker. The *PHO8* gene (ALP) was amplified from genomic DNA (SF838-1Dα), propagated in TOPO, subcloned to pRS316, and tagged with *ADH::Nat*^{R} as previously described. Finally, the *PHO8::ADH::Nat*^{R} sequence was amplified and *in vivo* ligated behind the *prVPH1::mCherry* sequence to create pGF242. Constructs were verified by diagnostic PCR and DNA sequencing.

Table 1. Plasmids used in this study.

Plasmid	Description	Reference
pRS415	*CEN, LEU2*	Simons *et al*. (1987)
pRS316	*CEN, URA3*	Sikorski and Hieter (1989)
GFP-ALP	pRS426 Pr$_{CPY}$*::GFP::ALP*	Cowles *et al*. (1997)
pGF35	pRS315 *VPS10::GFP::Sp-HIS5*	This Study
pGF244	pRS415 Pr$_{STV1}$*::Anc.a::2xHA::ADH::Nat*^{R}	This Study
pGF245	pRS415 Pr$_{VPH1}$*::Anc.a::2xHA::ADH::Nat*^{R}	This Study
pGF243	pRS415 Pr$_{STV1}$*::Anc.a::2xHA::GFP::ADH::HYG*^{R}	This Study
pGF246	pRS415 Pr$_{VPH1}$*::Anc.a::2xHA::GFP::ADH::HYG*^{R}	This Study
pGF342	pRS316 Pr$_{VPH1}$*::Anc.a::2xHA::ADH::Nat*^{R} *R737Q*	This Study
pGF341	pRS316 Pr$_{VPH1}$*::Anc.a::2xHA::ADH::Nat*^{R} *R737A*	This Study
pGF242	pRS316 Pr$_{VPH1}$*::mCherry::ALP::ADH::Nat*^{R}	This Study

Yeast strains can be found in Table 2. Yeast strains GFY270 and GFY271 were created by first switching the drug resistance cassette of *vph1*Δ*::Kan*^{R} (LGY120) to either *vph1*Δ*::Hyg*^{R} or *vph1*Δ*::Nat*^{R}. The *Hyg*^{R} or *Nat*^{R} cassettes were amplified by PCR, transformed into LGY120, and selected for Hyg or Nat resistance and loss of Kan

resistance. Next, the *STV1* locus from KEBY4 (*stv1*Δ*::Kan*^{R}) was amplified with 500 base pairs of flanking, untranslated sequence and transformed into *vph1*Δ*::Hyg*^{R} or *vph1*Δ*::Nat*^{R} to create GFY270 and GFY271, respectively. To construct GFY251, the Anc.a gene was integrated into the genome at the *STV1* locus; the parent yeast strain was GFY270. The Anc.a gene (including the double HA tag) was amplified from pGF244 including the full promoter of *STV1* and the *ADH::Nat*^{R} cassette. Following treatment with the restriction enzyme DpnI, the PCR product was transformed into *vph1*Δ*::Hyg*^{R} *stv1*Δ*::Kan*^{R} yeast, selected for Nat resistance, and the loss of Kan resistance. The drug resistance cassettes all contain 239 base pairs of the same downstream terminator allowing for homologous recombination. Yeast strains GFY250, GFY253, GFY255, and GFY256 were all created using a similar method. The *vma21*Δ*::Kan*^{R} deletion cassette was PCR amplified from pLG139 and transformed into GFY256 to generate GFY300. GFY308 was constructed by first tagging *VPH1::2xHA* (pSKN12; Kawasaki-Nishi *et al*., 2001) with a *GFP::ADH::Hyg*^{R} cassette using *in vivo* ligation to create pGF336. The *VPH1* promoter, coding sequence and *GFP::Hyg*^{R} cassette were amplified and transformed into *vph1*Δ*::Kan*^{R} yeast (LGY120) as previously described to create GFY308. For GFY310, *STV1* (from pJG2) was tagged with *GFP::ADH::Nat*^{R} (amplified from pGF02) using *in vivo* ligation. *STV1::GFP::Nat*^{R} was then integrated into *stv1*Δ*::Kan*^{R} yeast (KEBY4). For GFY307, *VPH1::GFP::Hyg*^{R} was amplified without any promoter sequence from pGF336 and *in vivo* ligated downstream of the *STV1* promoter to create pGF332. Finally, the *VPH1* locus including the GFP tag and drug cassette were amplified and integrated at the *STV1* locus in LGY120 yeast. For construction of GFY314, the sequence of mDsRed was amplified from pERGmDsRed

(Binns *et al*., 2006), propagated into TOPO, subcloned to pRS316, and tagged with *ADH::Nat*^{R}. A PCR fragment of *mDsRed::ADH::Nat*^{R} was then generated with a forward primer containing homology to the coding region of Anc.a and the product was transformed into GFY255 to exchange the GFP tag for mDsRed. For GFY315-317, the drug marker in GFY310 was first switched to *Kan*^{R}. Next, *VPH1* was deleted with the *Hyg*^{R} cassette (using genomic DNA from GFY270). Finally, *VPH1::2xHA::ADH::Nat*^{R} (from pGF339), *STV1::2xH::ADH::Nat*^{R} (from pGF337), and *Anc.a::2xHA::ADH::Nat*^{R} (from pGF245) were PCR amplified and integrated at the *VPH1* locus to create GFY315, GFY316, and GFY317, respectively. *S*trains were confirmed by diagnostic PCR, Western blots (when applicable), and growth tests.

Culture conditions: Yeast were cultured in YEPD (1% yeast extract, 2% peptone, and 2% dextrose), YEPD pH 5.0 buffered using 50 mM succinate/phosphate plus 0.01% adenine, or synthetic drop-out media containing dextrose (SD) and supplemented with amino acids. Growth assays were performed by spotting 3-5 μL of exponentially growing cells onto agar media. Five-fold serial dilutions were used; the first spot corresponds to an OD_{600} of approximately 0.8-1.0. For growth tests on media containing bathophenanthrolinedisulfonic acid (BPS; Sigma-Aldrich, USA), cells were grown overnight to saturation in YEPD pH 5.0 plus 25 μM BPS. Cultures were back-diluted to an OD_{600} of 0.25-0.30 in YEPD pH 5.0 plus 100 μM BPS for 6 hours before being spotted (2-3 μL) onto agar media. Conditions used include YEPD pH 5.0, YEPD + 100 mM Ca2+, YEPD + 3.5 mM Zn2+, and YEPD + 95 μM BPS. Plates were incubated at 30˚C for 2-5 days.

Table 2. Yeast strains used in this study.

Strain	Description	Reference
SF838-1Dα	*MATα ura3-52 leu2-3,112 his4-519 ade6 pep4-3 gal2*	Rothman and Stevens (1986)
KEBY4	SF838-1Dα *stv1*Δ*::Kan*^{R}	Kawasaki-Nishi *et al*. (2001a)
LGY120	SF838-1Dα *vph1*Δ*::Kan*^{R}	Davis-Kaplan *et al*. (2006)
GFY270	SF838-1Dα *vph1*Δ*::Hyg*^{R} *stv1*Δ*::Kan*^{R}	This study
GFY271	SF838-1Dα *vph1*Δ*::Nat*^{R} *stv1*Δ*::Kan*^{R}	This study
GFY251	SF838-1Dα *vph1*Δ*::Hyg*^{R} Pr$_{STV1}$*::Anc.a::2xHA::ADH::Nat*^{R}	This study
GFY250	SF838-1Dα Pr$_{VPH1}$*::Anc.a::2xHA::ADH::Nat*^{R} *stv1*Δ*::Kan*^{R}	This study
GFY253	SF838-1Dα *vph1*Δ*::Nat*^{R} Pr$_{STV1}$*::Anc.a::2xHA::GFP::ADH::Hyg*^{R}	This study
GFY255	SF838-1Dα Pr$_{VPH1}$*::Anc.a::2xHA::GFP::ADH::Hyg*^{R} *stv1*Δ*::Kan*^{R}	This study
GFY308	SF838-1Dα *VPH1::2xHA::GFP::ADH::Hyg*^{R}	This study
GFY310	SF838-1Dα *STV1::GFP::ADH::Nat*^{R}	This study
GFY310	SF838-1Dα *STV1::GFP::ADH::Nat*^{R}	This study
GFY307	SF838-1Dα Pr$_{STV1}$*::VPH1::GFP::ADH::Hyg*^{R} *stv1*Δ*::Kan*^{R}	This study
GFY314	SF838-1Dα Pr$_{VPH1}$*::Anc.a::2xHA::mDsRed::ADH::Nat*^{R} *STV1::GFP::Kan*^{R}	This study
GFY315	SF838-1Dα *VPH1::2xHA::ADH::Nat*^{R} *STV1::GFP::Kan*^{R}	This study
GFY316	SF838-1Dα Pr$_{VPH1}$*::STV1::2xHA::ADH::Nat*^{R} *STV1::GFP::Kan*^{R}	This study
GFY317	SF838-1Dα Pr$_{VPH1}$*::Anc.a::2xHA::ADH::Nat*^{R}	This study
GFY256	SF838-1Dα Pr$_{VPH1}$*::Anc.a::2xHA::GFP::ADH::Hyg*^{R}	This study
GFY300	SF838-1Dα Pr$_{VPH1}$*::Anc.a::2xHA::GFP::ADH::Hyg*^{R} *vma21*Δ*::Kan*^{R}	This study

Whole cell extract preparation and immunoblotting: Extracts from yeast cells were harvested as previously described (Ryan *et al*., 2008). Briefly, cultures were growth to saturation overnight in rich media, diluted to an OD_{600} of 0.25, and grown for an additional 4-6 hours to an optical density of 1.0. Cells from 10 mL of this culture were

harvested, resuspended into Thorner buffer (8M urea, 5% SDS, and 50 mM TRIS pH 6.8), and vortexed with glass beads for 8-10 minutes. A modified Lowry assay was used to determine the amount of protein within each extract (Markwell *et al*., 1978). Equal loads of protein were probed by SDS-PAGE, moved to nitrocellulose, and incubated with antibodies. Antibodies included monoclonal anti-HA (Sigma-Aldrich), anti-Vma2p (13D11B2; Molecular Probes, Inc.), anti-Dpm1p (5C5; Invitrogen), and secondary horseradish peroxidase-conjugated anti-mouse antibody (Jackson ImmunoResearch Laboratories, West Grove, PA). Western blots were visualized using ECL detection.

Fluorescence microscopy: Cells were stained with quinacrine as previously described (Flannery *et al*., 2004). Briefly, cells were grown overnight in YEPD pH 5.0 + adenine and then back-diluted to an OD_{600} of 0.25 in YEPD (unbuffered) for 4-6 hours. 1 mL of exponentially growing yeast was harvested, incubated on ice for 5 minutes, and resuspended in 200 µM quinacrine, 100 mM HEPES pH 7.6, and 50 µg/mL of concanavalin A tetramethylrhodamine (Invitrogen) in YEPD for 10 minutes at 30˚C. Cells were washed 3-4 times in 100 mM HEPES plus 2% glucose (on ice) and then visualized by fluorescent microscopy within 30 minutes of quinacrine treatment.

For visualization of fluorescently-tagged proteins (GFP, mcherry, mDsRed), strains were grown overnight in the appropriate media (minimal media if containing a vector) and then back-diluted to an OD_{600} of 0.25 in rich media at pH 5.0. Exponentially growing cells were harvested by centrifugation, washed once with water, and visualized by fluorescent and DIC microscopy.

For yeast treated with cycloheximide, cultures were grown overnight in rich media, back-diluted to an OD_{600} of 0.25, and grown at 30˚C for 4 hours to a density of

approximately 0.7-0.8. 10 mL of samples were treated with 20 µg/mL cycloheximide (Sigma-Aldrich, USA) or 0.02% DMSO (mock treatments) and incubated at 30˚C for 0-2 hours. At specific time points, 1 mL of cells was centrifuged, washed with water, and visualized on the microscope. Cycloheximide-treated cells were quantified by scoring the subcellular localization for 150-400 cells for control strains (Vph1p-GFP, Vph1p-GFP under control of the *STV1* promoter, Stv1p-GFP, GFP-ALP, or Vps10p-GFP) and 400-600 cells for experimental strains (Anc.a-GFP under control of either the *VPH1* or *STV1* promoter). Experiments were performed in triplicate. Error is expressed as the standard deviation.

All images were taken using a 100x objective on an Axioplan 2 fluorescence microscope (Carl Zeiss, Thornwood, NY) and analyzed using Axiovision software (Car Zeiss) and Adobe Photoshop CS (v. 8.0).

3. *Results*

Anc.a functions in extant *S. cerevisiae* as part of a hybrid V-ATPase complex: It is likely the two subunit a isoforms in yeast (Vph1p and Stv1p; Figure 1, Chapter II) evolved from a gene duplication event within the fungal clade (Figure 1). We tested the function of most recent common ancestor of Vph1p and Stv1p (referred to as "Anc.a") in extant *S. cerevisiae*. The sequence of this ancient protein was determined by calculating the maximum likelihood sequence from the phylogeny of a large set of subunit a isoforms from modern species (Supplemental Table S1, see Appendix B). Anc.a shares a high degree of sequence identity to the C-termini of both Stv1p and Vph1p (Figure 2A). However, Anc.a is only 38% and 53% identical to the N-termini of Stv1p and Vph1p,

respectively (Figure 2A). Secondary structure predictions of the N-terminal, cytosolic domains of Vph1p, Stv1p, and Anc.a revealed a very similar overall structure of the three proteins (Figure 2B).

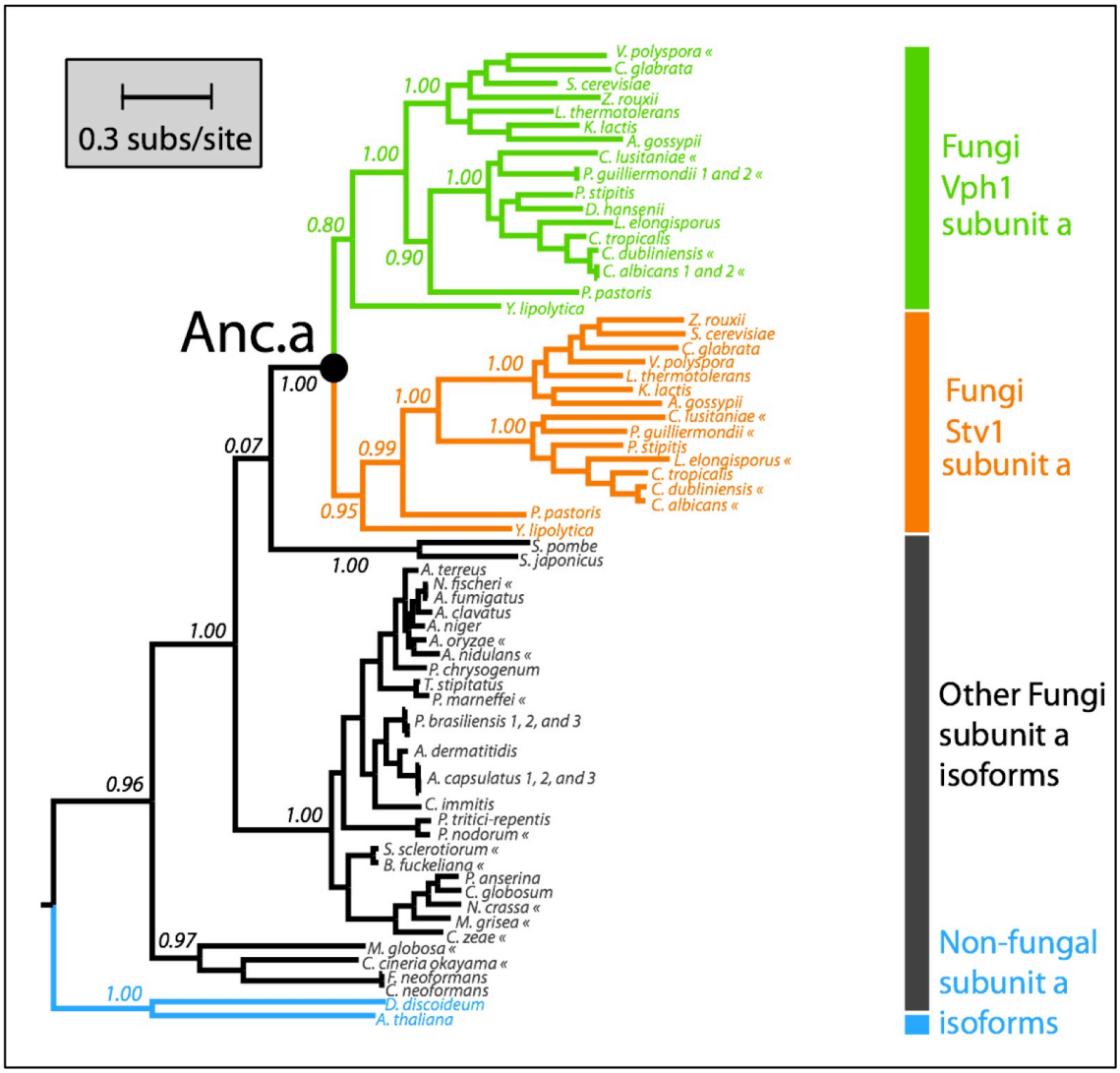

Figure 1. The maximum likelihood phylogeny of fungal V-ATPase subunit a. The tree was rooted using subunit a sequences from *D. discoideum* (Amoebozoa) and *A. thaliana* (Plantae) as outgroups. The position of the reconstructed fungal ancestral subunit a protein is labeled as "Anc.a." Extant taxa marked with *«* indicate predicted subunit a sequences according to GenBank annotations, whereas all other sequences have been functionally assayed. Branch support values are approximate-likelihood ratio test values based on a Shimodaira-Hasegawa-like procedure. Statistical support for the Anc.a sequence can be found in Supplemental Figure S1 (see Appendix B).

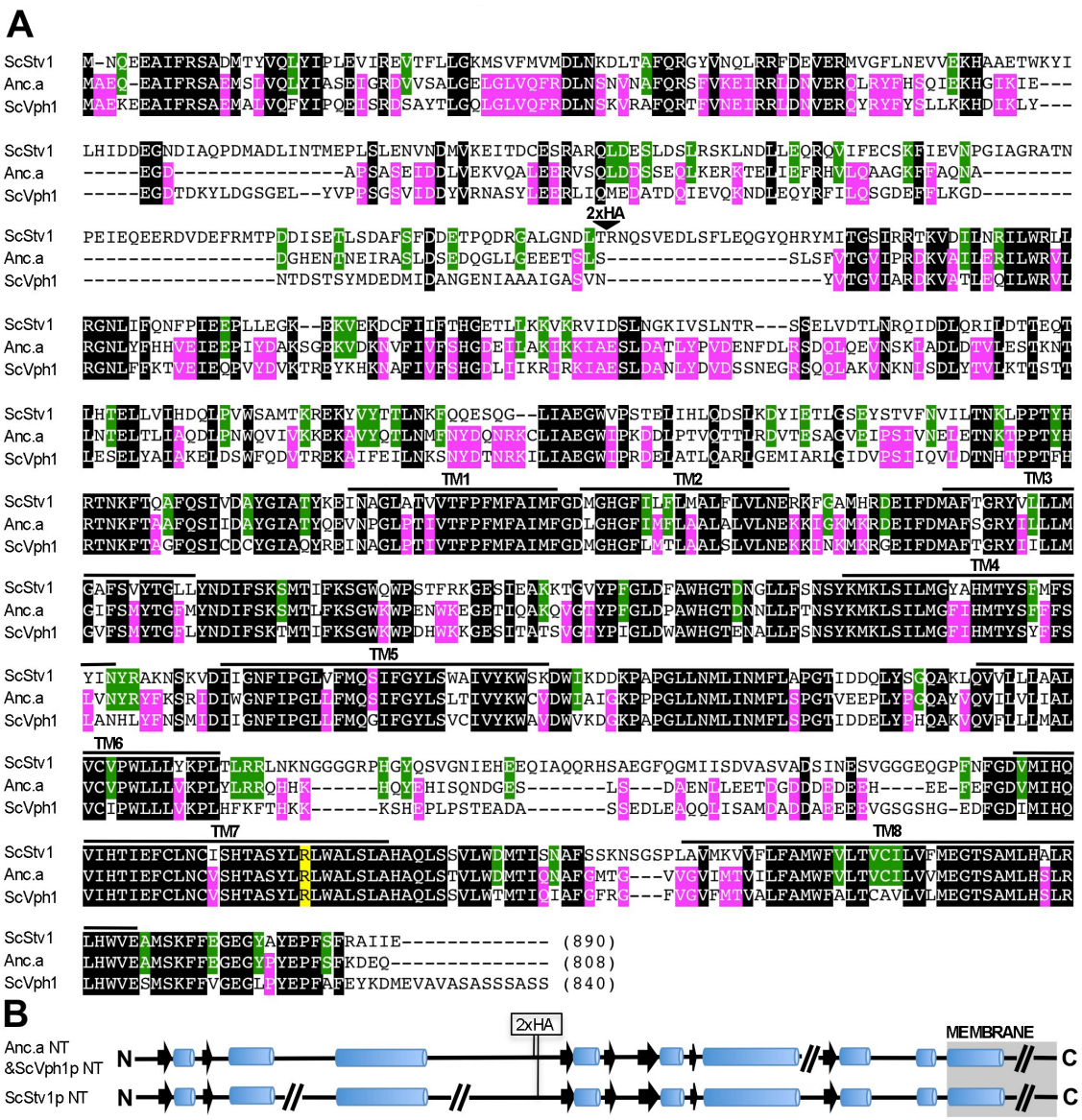

Figure 2. Alignment of *S. cerevisiae* Stv1p, Vph1p, and Anc.a amino acid sequences. (A) Identical residues between all three proteins are shown against a black background. Residues identical between only Vph1p and Anc.a are shown against a magenta background. Residues identical between Stv1p and Anc.a are shown against a green background. The alignment was performed using the CLUSTALW program (Thompson *et al*., 1994). Potential transmembrane domains are marked with black bars above the alignment (modeled from Wang *et al*., 2008). The critical arginine residues (Stv1p R795, Vph1p R735, and Anc.a R737) are marked against a yellow background. The position of the double HA epitope tag is indicated by a triangle (beginning after residue 171 for Vph1p, 227 for Stv1p, and 185 for Anc.a). (B) Secondary structure prediction of the N-termini of Stv1p, Vph1p, and Anc.a by the PSIPRED program (University College London). α-helices are shown as cylinders, ß-sheets are shown as black arrows, and coiled-coil regions are shown as black lines. The breaks in the lines represent short insertions that have no predicted structure.

Since the expression level of the ancestral subunit a is unknown, we chose to test the expression of an integrated copy of Anc.a under control of either the *STV1* or *VPH1* promoter; the coding region of Anc.a replaced the entire coding region of either yeast gene. We assayed the ancestral isoform in yeast lacking both contemporary Vph1p and Stv1p on media buffered with either excess calcium or zinc (Figure 3A). Yeast deleted for both isoforms do not acidify their vacuoles and are unable to survive on media containing excess metals (Manolson *et al.*, 1994). Cells deleted for *STV1* (*stv1*Δ) are not sensitive to either calcium or zinc as they still contain a functioning vacuolar isoform. However, yeast lacking *VPH1* (*vph1*Δ) grow in the presence of 100 mM Ca^{2+} but cannot survive on media containing 3.5 mM Zn^{2+}. Resistance to calcium depends on proton antiporters present on both the vacuole and Golgi apparatus; cells containing an acidified Golgi/endosome are therefore able to survive on excess calcium (Rudolph *et al*., 1989; Miseta *et al*., 1999). Resistance to zinc depends on the presence of proton/zinc antiporters present on the vacuolar membrane (MacDiarmid *et al*., 2000). Expression of Anc.a under control of either promoter that replaced the endogenous integrated copy of either *STV1* or *VPH1* was sufficient to promote growth on toxic levels of calcium or zinc (Figure 3A). Western blots to the HA epitope tag revealed the difference in steady-state levels of Anc.a under control of either the *STV1* or *VPH1* promoters; strains differed in levels of Anc.a protein by approximately 20-fold (Figure 3B). The levels of the V_1 subunit Vma2p did not change in either of these strains. These results indicate that Anc.a allows for V-ATPase function on the yeast vacuole.

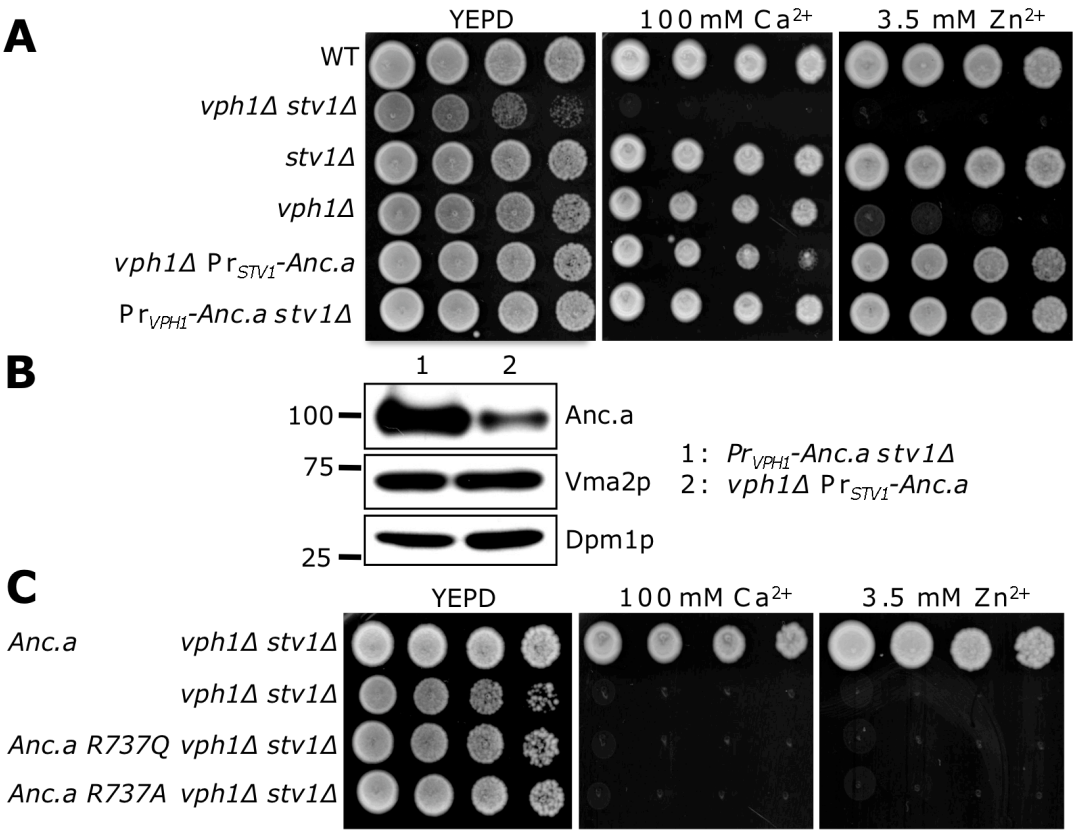

Figure 3. Ancestral subunit a complements a loss of both *VPH1* and *STV1*. (A) Exponentially growing cultures of wild-type (WT; SF838-1Dα), *vph1*Δ *stv1*Δ (GFY271), *stv1*Δ (KEBY4), *vph1*Δ (LGY120), *vph1*Δ Pr$_{STV1}$-*Anc.a* (GFY251), and Pr$_{VPH1}$-*Anc.a* *stv1*Δ (GFY250) were spotted onto rich media and media containing either 100 mM calcium or 3.5 mM zinc. (B) Western blot analysis of strains (*vph1*Δ *stv1*Δ*)* expressing epitope-tagged Anc.a protein (GFY250 and GFY251). Samples were separated by SDS-PAGE, transferred to nitrocellulose, and probed with antibodies to the HA epitope tag and V_1 subunit, Vma2p. Antibodies to Dpm1p served as a loading control. The position of the closest molecular marker is indicated. (C) Yeast deleted for *VPH1* and *STV1* (GFY271) were transformed with vectors expressing Anc.a (pGF245), Anc.a R737Q (pGF342), or Anc.a R737A (pGF341) and tested on media containing calcium and zinc as described in Part A. Vectors used were under control of the *VPH1* promoter.

Our ancestral reconstruction included 134 residues that were poorly supported by our maximum likelihood phylogenetic algorithm (with posterior probability < 0.8) and had plausible secondary alternate states (with posterior probability > 0.2). Posterior probability (PP) is a measure of the confidence of each ancestral state expressed as a probability (Hanson-Smith *et al*., 2010). Given the statistical support for alternative

amino acids within the Anc.a sequence, we sampled 50 independent, single amino acid substitutions to Anc.a; sites were chosen randomly across the entire protein sequence. Point mutations were introduced into the protein sequence of Anc.a and each alternative state was tested in *vph1*Δ *stv1*Δ yeast by growth assays on calcium and zinc. We determined that our reconstruction was robust to uncertainty as all changes to Anc.a still allowed for full complementation (Supplemental Table S2, see Appendix B).

Previous work has highlighted the importance of the arginine residue at site 735 in Vph1p and the corresponding arginine at site 795 in Stv1p (Kawasaki-Nishi *et al*., 2001c). This amino acid is essential for proton translocation and it is highly conserved in eukaryotic sequences. Complementation by Anc.a in *vph1*Δ *stv1*Δ yeast was fully dependent on the presence of this critical arginine residue within the C-terminus. It is also strongly supported in our reconstruction with a posterior probability of 1.0. Substitution of Vph1p arginine 735 for glutamine (which allows for V_0 assembly) or alanine (which disrupts V_0 assembly) has been shown to completely abolish V-ATPase activity (Kawasaki-Nishi *et al*., 2001c). When these mutational changes were introduced into Anc.a in cells lacking *VPH1* and *STV1* we observed no complementation on media containing either calcium or zinc (Figure 3C) yet Western blots revealed that the Anc.a R737Q mutant protein was stable (unpublished results). This demonstrates that Anc.a functions within a hybrid V-ATPase complex and is required for proton translocation.

The yeast isoforms of subunit a are subject to degradation upon loss of Vma21p or any of the other essential assembly factors (Graham *et al*., 1998; Hill and Cooper, 2000). Stability of the Anc.a protein was also fully dependent on the presence of the dedicated V-ATPase assembly factor, Vma21p (Supplemental Figure S2, see Appendix

B). These data demonstrate that assembly of the hybrid ancestral V-ATPase complex requires the modern-day yeast assembly machinery.

Anc.a functionally replaces yeast Stv1p and Vph1p: We assayed whether expression of Anc.a properly acidified the yeast vacuole by staining with the dye quinacrine. Quinacrine is a weakly basic, fluorescent dye that accumulates within acidified compartments. Staining of *vph1*Δ or *vph1*Δ *stv1*Δ mutants showed that these cells do not acidify their vacuoles (Figure 4).

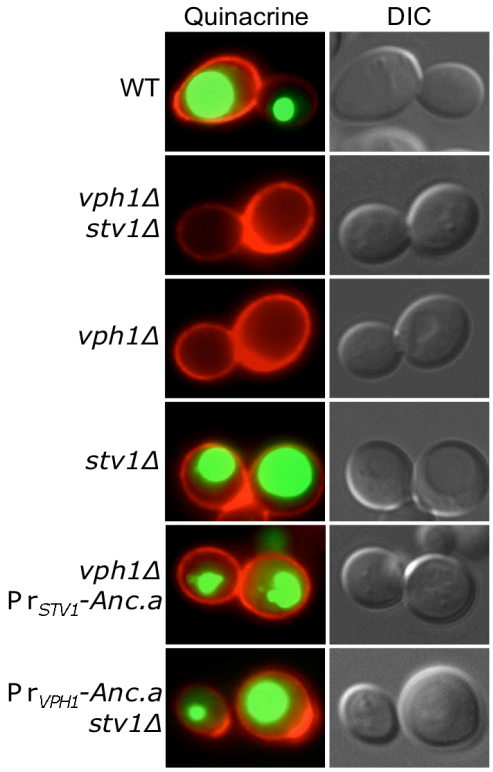

Figure 4. Expression of Anc.a results in acidification of the yeast vacuole. Cultures of wild-type (WT; SF838-1Dα), *vph1*Δ *stv1*Δ (GFY271), *vph1*Δ (LGY120), *stv1*Δ (KEBY4), *vph1*Δ Pr$_{STV1}$-*Anc.a* (GFY251), and Pr$_{VPH1}$-*Anc.a stv1*Δ (GFY250) were stained with quinacrine (green; acidified compartments) and concanavalin A-tetramethylrhodamine (red; stains the yeast cell wall) and viewed by fluorescent or DIC microscopy.

Yeast lacking the Golgi-isoform, Stv1p properly acidify their vacuoles as they contain the vacuolar isoform, Vph1p. Expression of Anc.a was sufficient to confer wild-

type levels of acidification in cells lacking both *STV1* and *VPH1* (Figure 4). These data suggest that the ancestral protein can function in place of the vacuolar isoform.

Quinacrine staining is not sensitive enough to visualize Golgi/endosomal acidification in yeast. Also, conventional growth assays (on elevated calcium or zinc) do not differentiate between wild-type yeast and yeast lacking *STV1,* as the vacuolar isoform compensates for a loss of the Stv1p-containing complex (Figure 3A). However, a recent report described a phenotypic difference between wild-type yeast and the *stv1*Δ mutant on media containing the iron chelator, BPS (Jo *et al*., 2009). Acidification of the Golgi/endosomal network is critical for iron metabolism/homeostasis (Philpott and Protchenko, 2008). We utilized low iron conditions to determine if Anc.a could functionally substitute for Stv1p *in vivo.* Cells lacking the V-ATPase (*vph1*Δ *stv1*Δ) were fully sensitive to media containing 95 μM BPS (Figure 5). While yeast lacking Vph1p survived under these conditions, cells lacking the Golgi isoform, Stv1p, were fully sensitive. Expression of Anc.a under control of the *STV1* promoter was not sufficient to promote growth on media buffered with BPS. However, expression of Anc.a under control of the *VPH1* promoter conferred growth under these low iron conditions (Figure 5). These results demonstrate that Anc.a is also sufficient to substitute for the Golgi isoform, Stv1p.

Anc.a localizes to both the Golgi/endosome and vacuole in yeast: Since Anc.a could complement the loss of either Stv1p or Vph1p, we assayed the cellular localization of the ancestral V-ATPase complex in yeast. Tagging of subunit a isoforms with GFP at the C-terminus did not compromise V-ATPase function (our unpublished results).

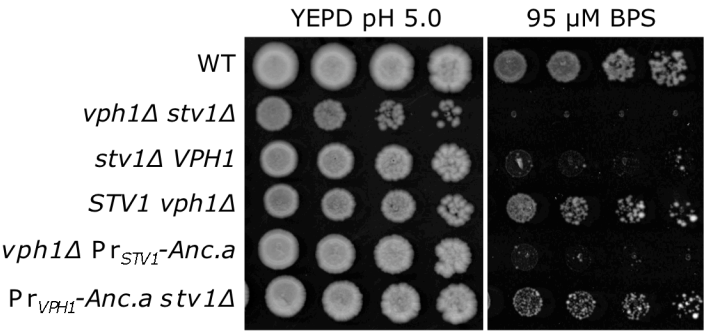

Figure 5. Expression of Anc.a complements the low iron growth defect of *stv1*Δ yeast. Cultures of wild-type (WT; SF838-1Dα), *vph1*Δ *stv1*Δ (GFY271), *vph1*Δ (LGY120), *stv1*Δ (KEBY4), *vph1*Δ Pr$_{STV1}$-*Anc.a* (GFY251), and Pr$_{VPH1}$-*Anc.a stv1*Δ (GFY250) were grown to saturation in YEPD pH 5.0 plus 25 µM BPS, back diluted into YEPD pH 5.0 plus 100 µM BPS, and grown for 6 hours before being spotted onto rich media or media containing 95 µM BPS.

Vph1p-GFP localized to the limiting membrane of the vacuole whereas Stv1p-GFP localized to punctate structures (Figure 6A). Stv1p co-localizes with the late-Golgi marker, A-ALP, and, to a lesser extent, the endosomal marker, Pep12p (Kawasaki-Nishi *et al*., 2001a). A-ALP is a reporter protein containing a fusion between the cytosolic portion of Ste13p and alkaline phosphatase (Nothwehr *et al*., 1997). The majority of Stv1p resides within the late Golgi although it has previously been shown to cycle through the endosome (Kawasaki-Nishi *et al*., 2001a). Overexpression of Stv1p results in its missorting to the vacuolar membrane (Manolson *et al*., 1994). Since the ancient expression level of the ancestral isoform is unknown, we tested whether altering the expression level of the contemporary yeast subunit Vph1p would result in a different localization pattern. We tested the localization of Vph1p-GFP under control of the weaker *STV1* promoter. Whereas the intensity of the fluorescent signal was greatly decreased, we found no difference in the localization of Vph1p-containing V-ATPase complex, as it was still present on the vacuolar membrane. Interestingly, Anc.a localized to both punctate stuctures and the vacuolar membrane (Figure 6A). The localization

pattern did not change when Anc.a was expressed under either the *STV1* or *VPH1* promoters suggesting that localization is not dependent on expression levels for this isoform.

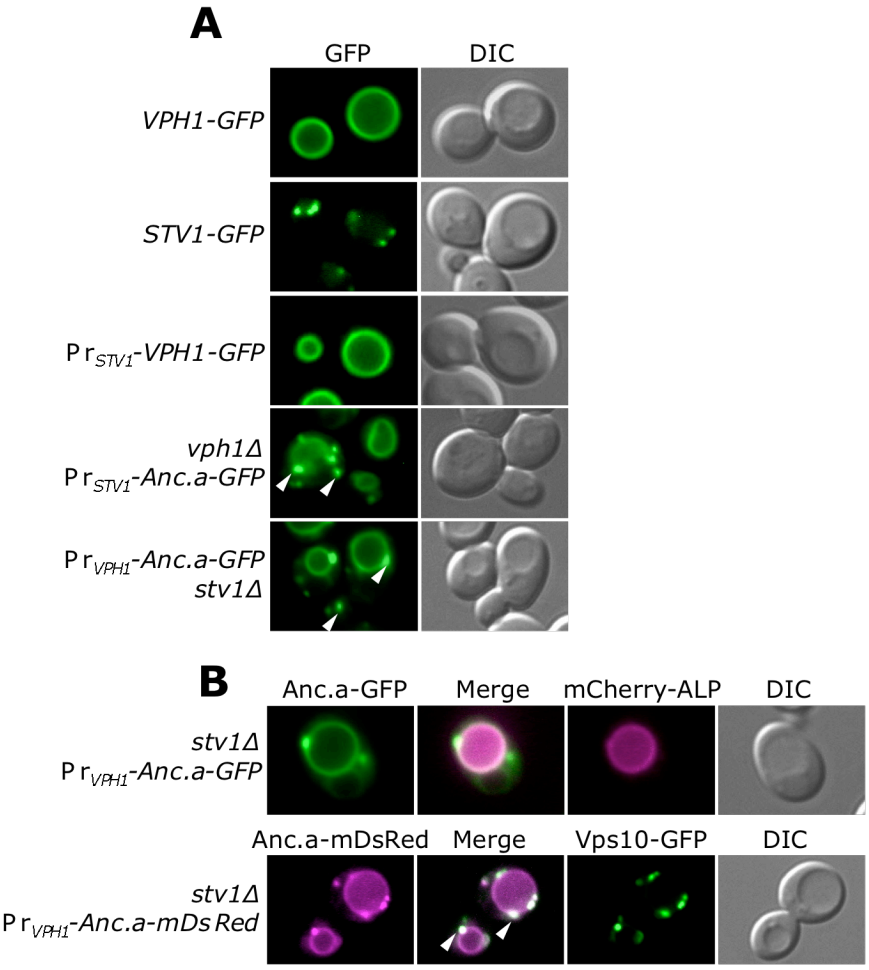

Figure 6. Anc.a localizes to the vacuole membrane and Golgi/endosomal network. (A) Yeast cultures expressing Vph1p-GFP (GFY308), Stv1p-GFP (GFY310), Vph1p-GFP at the *STV1* locus (GFY307), *vph1*Δ Pr$_{STV1}$-*Anc.a-GFP* (GFY253), and Pr$_{VPH1}$-*Anc.a-GFP stv1*Δ (GFY255) were visualized by fluorescent or DIC microscopy. White arrows label several of the punctate structures seen in strains expressing Anc.a protein. (B) Cultures of Pr$_{VPH1}$-*Anc.a-GFP stv1*Δ (GFY255) were transformed with a vector expressing mCherry-ALP and visualized by fluorescent microscopy. The merged image shows the overlay of the GFP (green) and mCherry (magenta) channels as a white signal. Cultures *of stv1*Δ Pr$_{VPH1}$-*Anc.a-mDsRed* (GFY314) were transformed with a CEN-based plasmid expressing Vps10p-GFP (under control of the *VPS10* promoter) and visualized by fluorescent microscopy. The merged image between the mDsRed (magenta) and GFP (green) channels presents overlap as a white color. White arrows indicate the presence of several distinct, punctate structures in the merged image.

We next determined the precise cellular compartments that contained the ancestral V-ATPase. Alkaline phosphatase (ALP) served as a marker for the vacuolar membrane. ALP traffics to the vacuole using a different route (ALP pathway) than the V-ATPase (CPY pathway) (Raymond *et al*., 1992; Cowles *et al*., 1997; Piper *et al*., 1997; Stepp *et al*., 1997). In Figure 6B we show colocalization of mCherry-tagged ALP with Anc.a-GFP on the limiting membrane of the vacuole. Vps10p, the receptor for carboxypeptidase Y (CPY), cycles between the late Golgi and endosome and served as a marker for the late Golgi (Marcusson *et al*., 1994; Cooper and Stevens, 1996). We assayed the localization of Anc.a-mDsRed in yeast also expressing Vps10p-GFP (Figure 6B). Vps10p-GFP localized to punctate structures as expected and the punctate structures containing Anc.a colocalized with Vps10p. These data demonstrate that the Anc.a-containing V-ATPase complex is localized to both the *trans*-Golgi network as well as the vacuolar membrane.

The Anc.a V-ATPase complex utilizes slowed anterograde trafficking to the vacuole membrane: We investigated the different trafficking mechanisms that might describe the dual localization pattern of Anc.a. It is possible that Anc.a could be retrieved from the endosome back to the Golgi (similar to yeast Stv1p). Alternatively, rather than retrograde transport, Anc.a could utilize slowed anterograde transport *en route* to the vacuole. Either of these models would account for the steady-state localization of Anc.a to both vacuolar and Golgi/endosomal compartments.

To differentiate between these models, we treated cells expressing Anc.a-GFP with cycloheximide to inhibit protein synthesis yet still allow for continued vesicular transport of cargo proteins. Cargo that is actively retrieved from the endosome to the

Golgi should continue to localize to the Golgi/endosome upon treatment with cycloheximide. However, proteins lacking a retrieval signal should be transported to the vacuole after protein synthesis is inhibited. Yeast treated with cycloheximide showed a dramatic shift in the localization pattern of Anc.a-GFP (Figure 7A). While the mock treatment displayed dual localization to both the vacuolar membrane and punctate structures, cells treated with cycloheximide only showed strong GFP signal on the vacuolar membrane. Control treatments did not show any detectible difference in localization pattern. We also tested to ensure that the shift in localization was not due to a decrease in steady-state protein levels of Anc.a-GFP. Western blots demonstrated that there was no significant change in Anc.a protein levels during the cycloheximide treatment compared with control samples (Figure 7B). Finally, we quantified the localization of Anc.a-GFP compared to a number of other resident Golgi proteins (Stv1p and Vps10p) or resident vacuolar proteins (Vph1p and ALP) upon treatment with cycloheximide (Figure 7C). Cells were scored for the presence of the fluorescent proteins in punctate structures. Upon drug treatment, ALP, Vph1p, or Vph1p expressed from the *STV1* locus did not show any shift in the percentage of cells containing puncta (Figure 7C). Similarly, we did not see any shift in the localization pattern for the late-Golgi membrane proteins Stv1p and Vps10p. However, there was a dramatic difference in the localization pattern of Anc.a-GFP under either the *VPH1* (50% reduction) or *STV1* (61% reduction) promoters. In addition, the fluorescence intensity of the remaining puncta was also decreased (data not shown). These experiments indicate that the trafficking of Anc.a likely involves slow, anterograde transport *en route* to the vacuole and is likely not to involve active retrieval/retention within the Golgi/endosome.

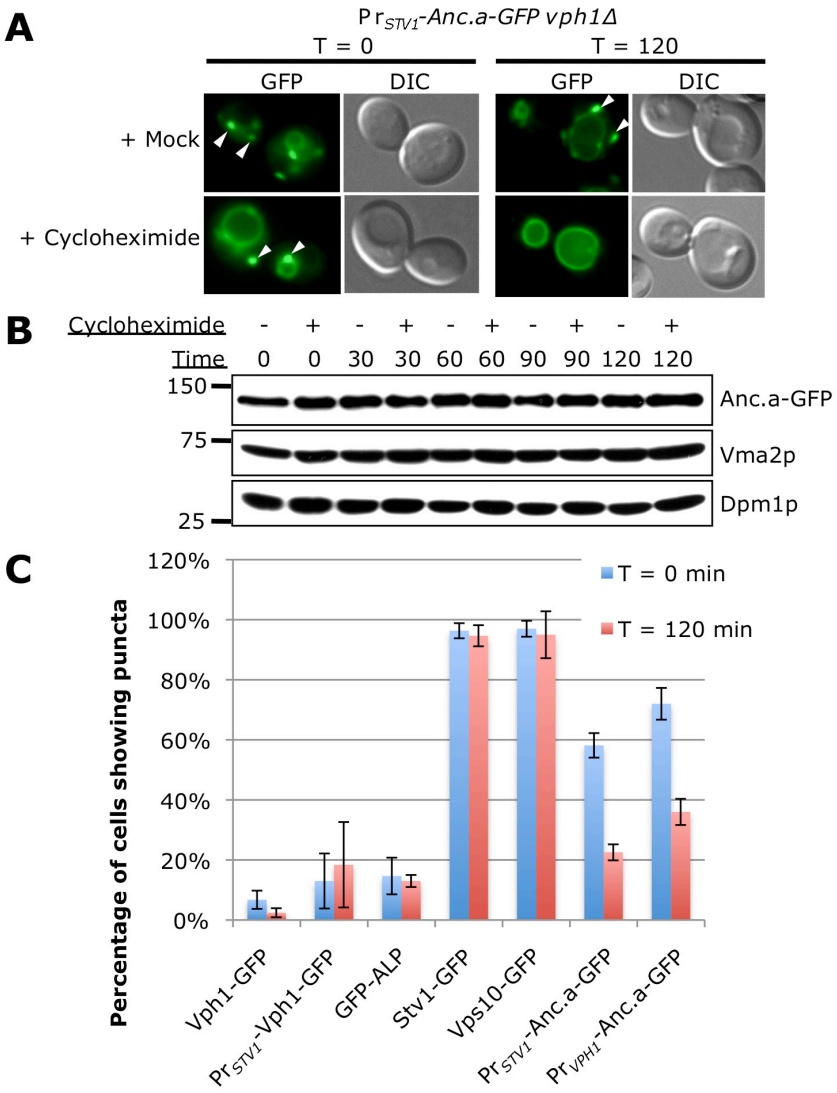

Figure 7. Anc.a localization shifts to the vacuole membrane after treatment with cycloheximide. (A) An exponentially growing culture of Pr$_{STV1}$-*Anc.a-GFP vph1*Δ (GFY253) was treated with either 0.02% DMSO (mock) or 20 µg/mL cycloheximide. Cells were visualized immediately after treatment and two hours following treatment by fluorescent and DIC microscopy. White arrows indicate the presence of multiple puncta. (B) Cultures of Pr$_{STV1}$-*Anc.a-GFP vph1*Δ (GFY253) were treated with DMSO or cycloheximide as described in Part A. Whole cell extracts were prepared at 30-minute intervals, separated by SDS-PAGE and probed with anti-HA, Vma2p, and Dpm1p antibodies. (C) Strains containing the following GFP-tagged constructs were treated with DMSO or cycloheximide: Vph1p-GFP (GFY308), Stv1p-GFP (GFY310), Vph1p-GFP at the *STV1* locus (GFY307), wild-type yeast expressing GFP-ALP, or Vps10p-GFP (pGF35), *vph1*Δ Pr$_{STV1}$-*Anc.a-GFP* (GFY253), and Pr$_{VPH1}$-*Anc.a-GFP stv1*Δ (GFY255). The percentage of cells showing punctate fluorescent staining was quantified. Between 150-400 cells were counted for each control strain and the 400-600 cells were counted for stains containing Anc.a. Experiments were performed in triplicate and the error is expressed as the standard deviation.

Finally, since Anc.a also localizes to the Golgi/endosomal network, we tested whether Anc.a would utilize the same sorting machinery as the Stv1p isoform. The retrieval machinery that sorts the Stv1p-containing V-ATPase is saturable; overexpression of Stv1p results in its mislocalization to the yeast vacuole (Manolson *et al*., 1994). Therefore, we tested whether expression of Anc.a would saturate the Stv1p-sorting machinery and cause endogenous levels of Stv1p to be missorted to the vacuolar membrane. Stv1p-GFP localized to punctate structures when *VPH1* was also present (Figure 8, row 1). When *VPH1* was replaced with an untagged copy of *STV1* (resulting in overexpression of Stv1p), the endogenous copy of Stv1p-GFP was mislocalized to the vacuole (Figure 8, row 2). Finally, high-level expression of Anc.a did not cause a shift in the localization of endogenous Stv1p-GFP (Figure 8, row 3). These data imply that trafficking of Anc.a does not utilize the same sorting machinery as the Stv1p isoform.

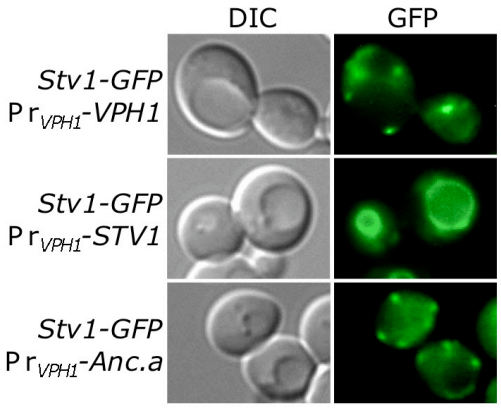

Figure 8: Anc.a does not perturb Stv1p sorting in budding yeast. Strains expressing Stv1p-GFP that contained either *VPH1* (GFY315), *STV1*, (GFY316), or Anc.a (GFY317) integrated at the *VPH1* locus were visualized by fluorescent and DIC microscopy.

4. *Discussion*

Like other large, multiprotein complexes, the V-ATPase enzyme has undergone radical architectural changes through evolutionary time while maintaining a conserved

enzymatic function. The high degree of homology between specific V-ATPase subunit pairs such as V_1 subunits A and B, V_0 subunit a isoforms, and V_0 proteolipid ring subunits c, c', and c" across all eukaryotes suggest that gene duplication events have played a significant role in the increasing complexity of this multiprotein enzyme (Müller and Grüber, 2003; Cross and Müller, 2004). Within the V_0 subdomain, subunit a is unique within budding yeast because it is the only complex-specific subunit isoform of the V-ATPase. Within *S. cerevisiae*, Stv1p and Vph1p are solely responsible for the phenotypic differences seen between the two isoforms of the V-ATPase. One of the most dramatic differences can be seen in the distinct subcellular localizations of Stv1p-complex (Golgi/endosome) and Vph1p-complex (vacuole).

We sought to describe the evolutionary origins of the Stv1p and Vph1p isoforms in budding yeast using ancestral gene reconstruction. Previous work has been unsuccessful at characterizing other V-ATPase subunit a isoforms from various eukaryotes within budding yeast (Aviezer-Hagai *et al*., 2000; unpublished results). This type of horizontal approach fails to provide the specific genetic background for mutational changes that have accumulated within extant nodes along different evolutionary trajectories. Ancestral reconstruction incorporates mutational information from modern sequences to infer the most probable ancestral state of a gene.

Several evolutionary models of gene duplication events followed by subfunctionalization might describe the phenotypes of contemporary subunits Stv1p and Vph1p (Innan and Kondrashov, 2010). For instance, it is possible that the ancestral subunit a was exclusively localized to either the vacuole or the Golgi apparatus and that the derived function of the duplicated subunit was to occupy a second compartment. Our

in vivo analysis of Anc.a in *S. cerevisiase* suggest that the pre-duplicated subunit a functioned on both the Golgi/endosomal and vacuolar compartments. Surprisingly, extant yeast are able to properly assemble the ancestral subunit as part of a hybrid V-ATPase complex. Furthermore, yeast allow for efficient transport of the V-ATPase and *in vivo* acidification despite differences in the primary amino acid sequence between Anc.a, Stv1p, and Vph1p. These results highlight the conservation of overall structural identity of subunit a, which makes contacts with a number of both V_0 and V_1 subunits and interacts with various assembly factors in yeast (Landolt-Marticorena *et al*., 2000; Wilkens *et al*., 2004; Zhang *et al*., 2008; Qi and Forgac, 2008; Ediger *et al*., 2009). This is also evident when examining the support values for the Anc.a reconstruction; despite 23.9% of all sites having less than 80% posterior probability, our reconstruction resulted in a high degree of complementation and function *in vivo.*

Interestingly, trafficking of the Anc.a-containing V-ATPase does not utilize the extant, Stv1p-sorting machinery. Therefore, rather than being specifically targeted for retrieval from the endosome back to the *trans*-Golgi, Anc.a is likely being slowed *en route* to the vacuole through these compartments. Also, contemporary yeast contain the necessary machinery required to cause slowed anterograde trafficking of Anc.a. Many of the components of vesicular trafficking pathways (including the TRAPP, COG, ESCRT, and GARP complexes) are highly conserved among eukaryotes including humans (Field and Dacks, 2009; Bonifacino and Hierro, 2010; Reynders *et al*., 2010; Barrowman *et al*., 2010). We have described a unique mechanism for localization of the hybrid Anc.a-containing V-ATPase enzyme in budding yeast to two different cellular compartments.

Given the localization of Anc.a in yeast as well as previous insights into the biochemical differences between the contemporary yeast subunits, we propose a model of subfunctionalization for subunit a following the gene duplication event that took place within the fungal lineage. A number of other factors have contributed to the evolution of Stv1p and Vph1p that have allowed for the shift in V-ATPase localization. A common evolutionary trend following subfunctionalization is the difference in gene expression of the two duplicated genes (Force *et al*., 1999). Differences in the relative levels of transcript and/or differential regulation can lead to alterations in spatial and temporal control of the two genes following the duplication event. In the case of Stv1p and Vph1p, previous work has determined the difference in mRNA transcripts (5 fold) between the two genes (Manolson *et al.*, 1994). However, this is not sufficient to completely explain the difference in steady-state levels between yeast Stv1p and Vph1p (Vph1p ~20 fold higher). One possibility includes differences in V_0 assembly between the two isoforms. Upon a loss of Vph1p, there is a reproducible increase in the levels of Stv1p protein (Perzov *et al*., 2002; data not shown). Additionally, preliminary results have shown that there is a difference in the steady-state levels between Anc.a and Stv1p protein when under the control of the *STV1* promoter; Anc.a shows a higher protein level (unpublished results). This suggests a possible reduction in assembly for the Stv1p isoform following the duplication event from Anc.a. Since our results demonstrate that Anc.a functions on the vacuole, it is possible that the expression of Anc.a was similar to modern *VPH1*. Therefore, a reduction in the levels of Stv1p protein had to accompany a shift in the localization of the evolving Stv1p isoform to the Golgi/endosome because the modern Stv1p-sorting machinery is saturable (Manolson *et al*., 1994).

It is unknown why the two post-duplication gene products were maintained in budding yeast while other fungi contain only a single subunit a isoform. However, work on other eukaryotes has provided insight into the importance of V-ATPase specialization using subunit a. This involves both the localization of this critical enzyme to specific subcellular compartments (including the plasma membrane) and a variety of additional functional roles for subunit a including membrane fusion, pH sensing, development, and V-ATPase regulation (Adams *et al*., 2006; Marshansky, 2007; Baars *et al*., 2007; Forgac, 2007). There may have been a selective fitness advantage to evolving a dedicated Golgi/endosomal isoform of the V-ATPase in budding yeast. The importance of iron uptake and metabolism under varying environmental conditions is evident in almost every organism (Philpott and Protchenko, 2008). Yeast may have evolved the Stv1p isoform to specifically acidify the Golgi and endosomal compartments to allow for essential processes including iron homeostasis that utilize an acidified endosomal network.

The process of ancestral gene reconstruction has been a powerful tool providing insight into the evolution of enzyme-substrate specificity and the directionality of evolutionary change (Ortlund *et al*., 2007; Dean and Thornton, 2007; Bridgham *et al*., 2009). Anc.a serves as a useful platform to perform future structural and mutational analyses to address questions regarding other biochemical differences between Stv1p and Vph1p including assembly, coupling efficiency, and *in vivo* dissociation. Further experiments will also characterize the evolutionary trajectory of the Stv1p-dependent sorting signal(s). Preliminary analyses have found that residues necessary for Stv1p trafficking are not found within the Anc.a N-terminus (Cronan and Stevens, unpublished

results). Anc.a also provides a scenario where it is the sole V-ATPase isoform, similar to other fungal species such as *N. crassa* and *S. pombe*. Additional experimentation will provide insight into how organisms with a single isoform are able to efficiently traffic the V-ATPase to multiple cellular compartments. Anc.a has provided a model for the evolutionary origins of the two yeast isoforms. Future ancestral reconstructions will allow for a more complete understanding of the molecular mechanisms responsible for the diverse set of V-ATPase isoforms seen in many eukaryotes.

The use of ancestral reconstruction has been a powerful tool allowing for an evolutionary analysis of the two yeast V-ATPase isoforms. This type of work will allow for a plethora of additional experiments that utilize a historical perspective to classical molecular techniques. Future studies could aid in characterizing the regulation, coupling efficiency, and trafficking signal(s) within subunit a in yeast or other organisms. Additionally, other subunits of the V-ATPase might be interesting candidates for ancestral reconstructions. One obvious and intriguing target is the protolipid ring of the V_0 subdomain.

The mechanism of the proteolipid ring is highly conserved across all lineages within both the V-type ATPase enzymes as well as the distantly related F-type and A-type ATPase complexes. However, given the restrictions on the overall enzymatic function of this subdomain, there is great diversity in the number, composition, and stoichiometry of the subunits that make up the proteolipid ring across the three domains of life. We chose to explore evolutionary questions regarding the origins of the three-subunit ring found in fungi with respect to the two proteolipid system used in metazoans.

This work uses the V-ATPase as a model protein complex to examine how increasing protein complexity might arise while conserving overall enzyme function. While the data presented in Chapter III examines a fungal-specific duplication event, we chose to characterize ancestral subunits that existed at the split between fungi and metazoans.

CHAPTER IV

THE EVOLUTION OF MULTI-PARALOG PROTEIN COMPLEXITY IN THE VACUOLAR H^+-ATPASE V_0 PROTEOLIPID RING

This work was done in collaboration with several co-authors. G. C. Finnigan, T. H. Stevens, and V. Hanson-Smith conceived the experiments. V. Hanson-Smith performed the phylogenetic analysis and statistical ancestral reconstructions. G. C. Finnigan performed all functional experiments. G. C. Finnigan, T. H. Stevens, V. Hanson-Smith, and J. W. Thornton interpreted the results, wrote, and edited the manuscript. V. Hanson-Smith is affiliated with the Center for Ecology and Evolutionary Biology and Department of Computer Science at the University of Oregon (Eugene, OR, 97403). J. W. Thornton is affiliated with the Center for Ecology and Evolutionary Biology at the University of Oregon (Eugene, OR, 97403) and the Howard Hughes Medical Institute. G. C. Finnigan and T. H. Stevens are affiliated with the Institute of Molecular Biology at the University of Oregon (Eugene, OR, 97403).

1. *Introduction*

A central challenge of evolutionary biology is to understand the relationship between genotypes and physiological phenotypes. A growing body of investigation has articulated precise molecular and evolutionary mechanisms for several cases in which gene duplications followed by amino acid substitutions gave rise to contemporary phenotypic diversity[1-6]. However, there is a relative paucity of evidence demonstrating the molecular mechanisms of the converse situation, in which duplicated genes were conserved without significantly changing their concomitant phenotype from its pre-

duplicated---ancestral---state. The V-ATPase illustrates this puzzle. The V-ATPase is a multi-subunit protein complex that acidifies cellular organelles by coupling ATP hydrolysis with proton translocation across membranes; this enzymatic function is required for intracellular protein trafficking, coupled transport of small molecules, and receptor-mediated endocytosis[3]. The V-ATPase V_0 subdomain contains a hexameric proteolipid ring that functions through a rotary mechanism[7,8] (Figure 1, see Chapter I). Although the V-ATPase is found in species across the Eukaryote domain, the V_0 proteolipid ring varies in subunit composition among lineages: Fungi use three different proteolipid subunits (designated c, c', and c") whereas other Eukaryotes---including metazoans---use only two subunits[3] (c and c") (Figure 1). Contemporary yeast build proteolipid rings using one copy of c", one c', and multiple copies of c[9]. Although all three subunits are required for the V-ATPase to function in Fungi, the evolutionary processes and underlying molecular mechanisms that led to a fungal preservation of duplicated subunit c' are unknown9[9-11]. Understanding the evolutionary history of the V-ATPase is of biomedical importance: V-ATPase been implicated in human osteopetrosis, multidrug resistance in squamous cell carcinoma, and virulence strategies in *Legionella pneumophila*[12-14].

In order to determine why the duplicated gene was preserved in Fungi---rather than accumulating deleterious mutations and psuedogenizing---we functionally compared the pre-duplicated Opisthokont ancestral V-ATPase proteolipid ring with a contemporary post-duplication fungal proteolipid ring.

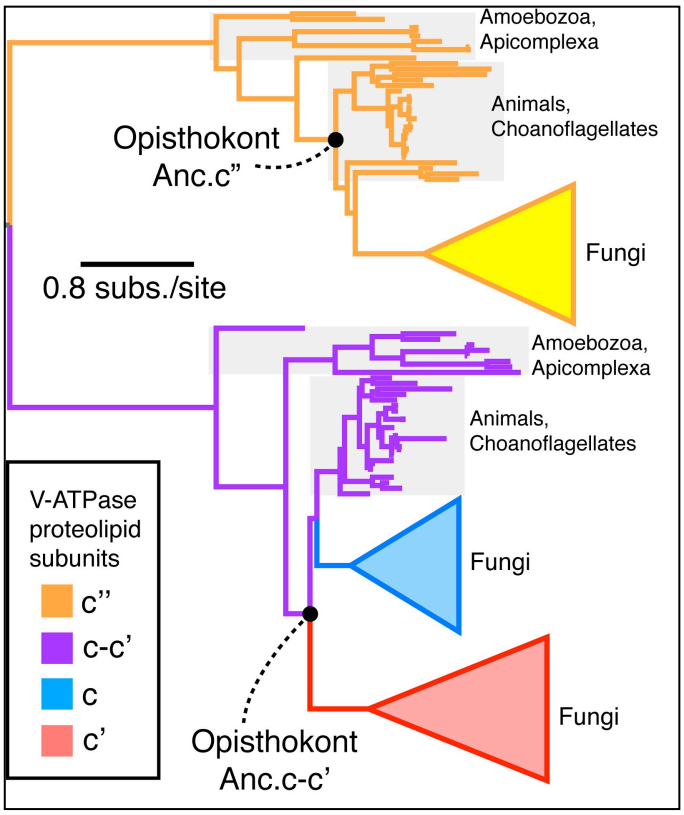

Figure 1. Evolution of the V-ATPase proteolipid ring. The maximum likelihood phylogeny of V-ATPase subunits c, c’, and c”. Amoebozoa, Apicomplexa, Animals, and Choanoflagellates contain subunits c-c’ (typically labelled as just c in most V-ATPase literature) and c”, whereas Fungi contain subunits c, c’, and c”. The positions of the four reconstructed ancestral proteins are labeled as Opisthokont Anc.c”, Anc.c-c’, Anc.c, and Anc.c’. A more comprehensive phylogeny with support values for ancestral nodes and ancestral state reconstructions is found in Figure 2. A comparison of ancestral protein sequences to extant sequences is found in Figure 3 and Figure 7.

First, we reconstructed the maximum likelihood phylogeny of all known eukaryotic proteolipid subunits c, c’, and c” (Figure 2), and then we resurrected the ancestral Anc.c-c’ (the most-recent shared ancestral protein of Opisthokont proteolipid subunits c and c’) and Anc.c” (the most-recent-common shared ancestral protein of Opishthokont subunit c”) (Figure 3). We assayed the function of the reconstructed ancestral proteins *in vivo* using extant yeast *S. cerevisiae.*

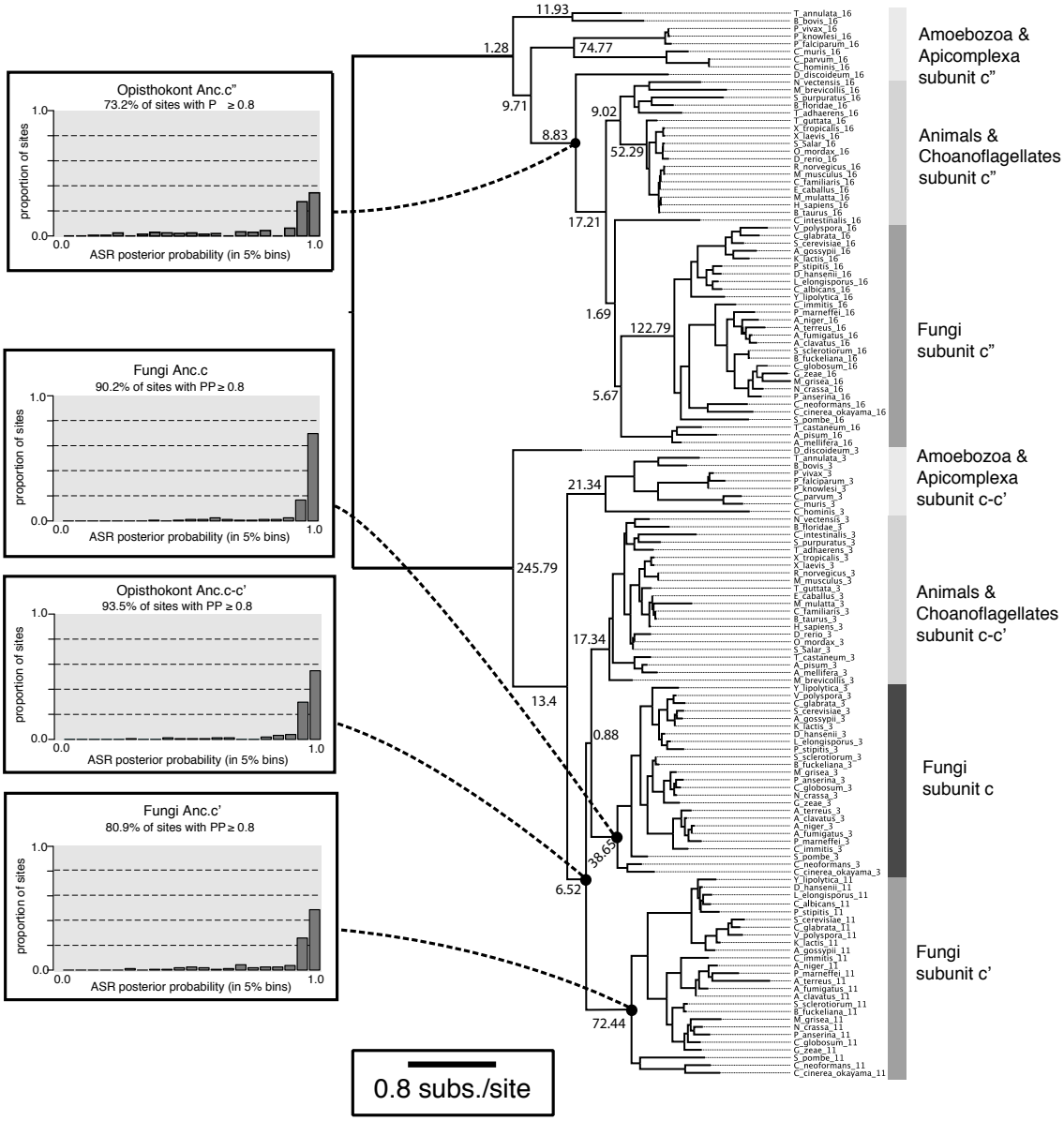

Figure 2. Maximum likelihood phylogeny of V-ATPase subunits c, c', and c" protein sequences. Decimals on internal nodes are approximate likelihood ratio support for the monophyly of the clade. The inset bar graphs show support for ancestral reconstructions. The locations of Anc.c-c', Anc.c", Anc.c, and Anc.c' are noted.

2. *Methods summary*

Protein sequences of the Anc.c-c' and Anc.c" were inferred using maximum-likelihood phylogenetics from an alignment of 139 protein sequences of extant c, c', and c" from Amobebozoa, Apicomplexa, Metazoa, Choanoflagellates, and Fungi.

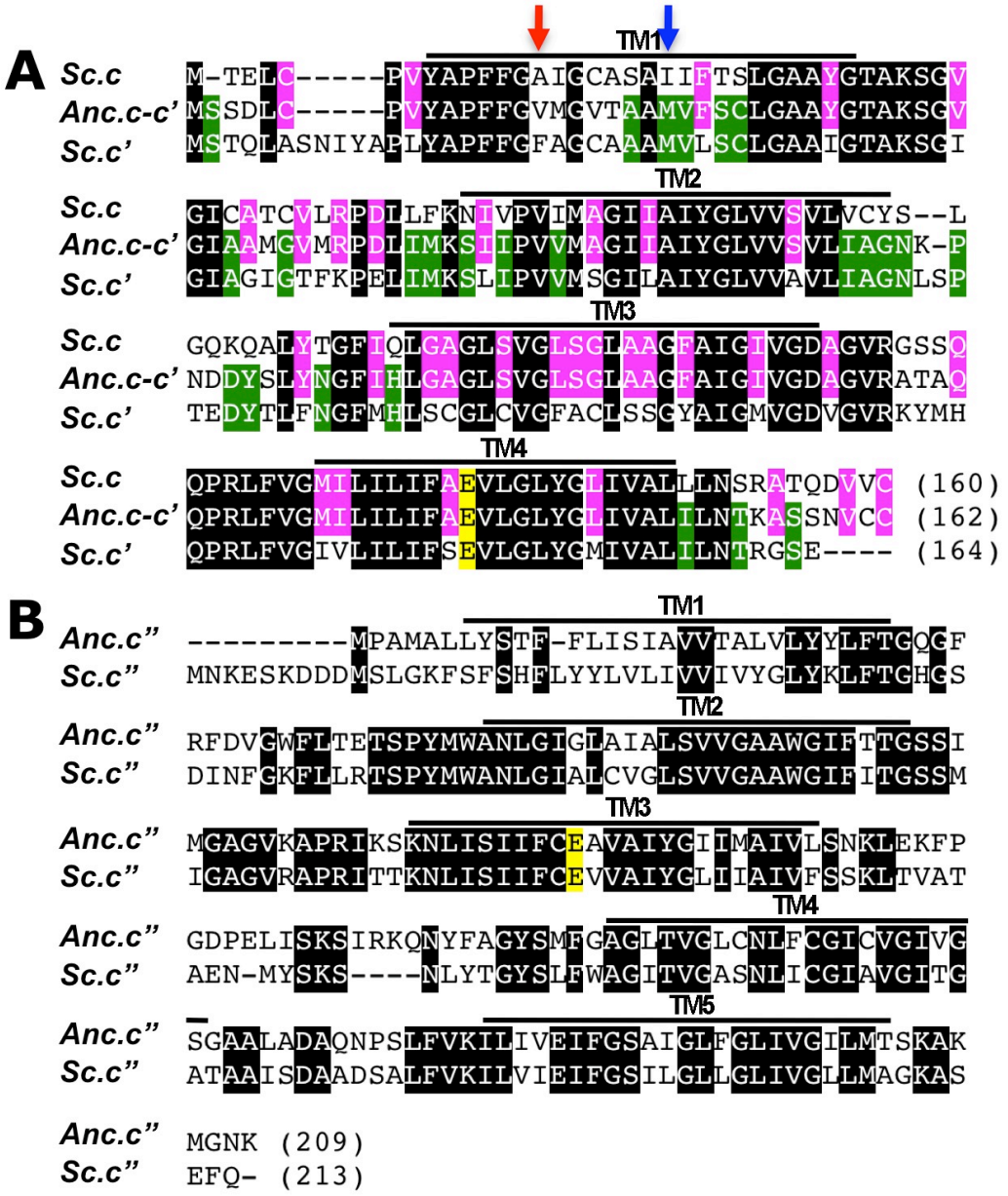

Figure 3. Protein sequence alignment of the *S. cerevisiae* proteolipids Vma3, Vma11, and Vma16 to the Anc.c-c' and Anc.c" subunits. Alignments were performed using CLUSTAL[15]. Potential transmembrane domains are marked with black bars above the protein sequences according to SOSUI[16]. (A) Identical residues between all three proteins are shown against a black background. Residues identical between only Vma3 and Anc.c-c' are shown against a magenta background. Residues identical between only Vma11 and Anc.c-c' are shown against a green background. Glutamic acid residues critical for V-ATPase enzyme function are highlighted in yellow (Vma3 E137, Vma11 E145, Anc.c-c' E139). A blue arrow indicates the position of Vma3 I21 and Anc.c-c' M22. A red arrow indicates the position of Vma11 F20 and Anc.c-c' V15. (B) Identical residues between Vma16 and Anc.c" are shown against a black background. The critical glutamic acid residues (Vma16 E108 and Anc.16 E98) are highlighted in yellow.

Ancestral genes were synthesized, cloned into yeast expression vectors, and tested for complementation in various *S. cerevisiae* mutants. V-ATPase function was assayed by growth tests on media buffered with $CaCl_2$ (as described by previously[17]). Steady-state levels of Vph1 were determined by Western blotting[17]. Quinacrine staining and Vph1-GFP fusion constructs were visualized by fluorescent microscopy[17].

3. *Expanded methods*

***In silico* reconstruction of ancestral protein sequences:** We queried GenBank for all Eukaryote V-ATPase V_0 proteolipid sequences. Our query returned c, c', and c" protein sequences for twenty-six species in Fungi, and c and c' sequences for thirty-five species in Metazoa, Amoebozoa, and Apicomplexa. We aligned the sequences using PRANK v0.081202[18,19]. This alignment is best-fit by the Whelan-Goldman matrix (WAG) with gamma-distributed rate variation (+G) and proportion of invariant sites (+I), according to the Akaike Information Criterion as implemented in PROTTEST[20,21]. Using WAG+G+I, we used PhyML v3.0 to infer the maximum likelihood (ML) topology, branch lengths, and model parameters[22]. We optimized the topology using the best result from Nearest-Neighbor-Interchange and Subtree Pruning and Regrafting; we optimized all other free parameters using the default hill-climbing algorithm in PhyML. Phylogenetic support was calculated as the approximate likelihood ratio[23]. Our ML analysis inferred the Nematoda c and c' sequences to be basal to the Chromalveolata lineages; this result is inconsistent with our expectation that Nematoda are animals[24] and we therefore excluded Nematoda data from further downstream analysis.

We reconstructed ML ancestral states at each site for all ancestral nodes in our ML phylogeny using our own set of Python scripts, called *Lazarus*, which wraps PAML version 4.1[25]. Lazarus parsimoniously places ancestral gap characters according to Fitch's algorithm[26]. We characterized the overall support for Anc.c-c' and Anc.c" by binning the posterior probability of the ML state at each site into 5%-sized bins and then counting the proportion of total sites within each bin (Figure 2).

Robustness to alignment uncertainty: In order to assess if our ancestral reconstructions are robust to alignment uncertainty, we aligned our proteolipid protein sequences using four different alignment algorithms: CLUSTAL version 2.0.10[15] MUSCLE v3.7[27], AMAP v2.2[28], and PRANK v0.081202[18]. We then inferred the ML phylogeny and branch lengths for each alignment, using the methods described above. The resultant alignments varied in length from 347 sites (using CLUSTAL) to 683 sites (using PRANK), but all four alignments yielded the same ML topology with nearly identical ML branch lengths.

In order to determine which alignment algorithm yields the most accurate ancestral inferences under V-ATPase phylogenetic conditions, we simulated sequences across the V-ATPase ML phylogeny using insertion and deletion rates ranging from 0.0 to 0.1 indels per site. For each indel rate, we generated ten random unique indel-free ancestral sequences 400 amino acids in length and then used INdelible[29] to simulate the ancestral sequence evolving along the branches of our ML phylogeny under the conditions of WAG+I+G model with indel events randomly injected according to the specified indel rate. The size of each indel event was drawn from a Zipfian distribution with coefficient equal to 1.1 and the maximum length limited to 10 amino acids. We

aligned each replicate's descendant sequences using AMAP, CLUSTAL, MUSCLEs, and PRANK; for each alignment, we inferred the ML topology, branch lengths, and model parameters using the methods described above. We used Lazarus to reconstruct all ancestral states, and queried Lazarus for the most-recent shared ancestor for Opisthokont c/c' and Opisthokont c" sequences. We measured the error of ancestral reconstructions as the proportion of ancestral sites that incorrectly contained an indel character (Figure 4).

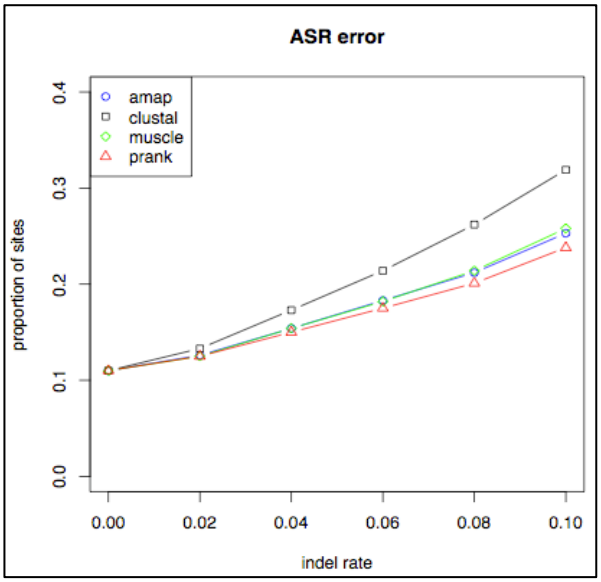

Figure 4. Ancestral sequence reconstruction (ASR) error as a function of insertion-deletion rate. Replicate sequences were simulated on the phylogeny shown in Figure 1B, and aligned using four different algorithms (AMAP, Clustal, MUSCLE, and Prank). We reconstructed the most-recent shared ancestors for the Opishtokont c-c' sequences and Opishtokont c" sequences. Ancestral sequence reconstruction was measured as the proportion of sites that incorrectly contained an indel character.

Plasmids and yeast strains: Bacterial and yeast manipulations were performed using standard laboratory protocols for molecular biology[30]. Plasmids used can be found in Table 1. Ancestral sequences (pGF140, pGF139, pGF506, and pGF508) were synthesized by GenScript (Piscataway, NJ) with a yeast codon bias. Triple hemagglutinin (HA) epitope tags were included prior to each stop codon. The Anc.c-c', Anc.c", Anc.c, and Anc.c' genes were subcloned to single-copy, *CEN*-based yeast

vectors. The *ADH* terminator sequence (247 base pairs) and Nat^R drug resistance marker[31] were polymerase chain reaction (PCR) amplified with 40 bp tails homologous to the 3' end of each coding region and vector sequence. Vectors were gapped, co-transformed into SF838-1Dα yeast with PCR fragments, and cells were selected for Nat^R. A second round of *in vivo* ligation was used to place the ancestral genes under 500 bps of the *VMA3* or *VMA16* promoters to create pGF140 and pGF139, respectively. pGF141 was created using *in vivo* ligation to move *VPH1::GFP::HIS3* (from pGF06) to pRS415. The following vectors all used a similar cloning strategy: pGF213, pGF240 - pGF41, pGF252 - pGF254, pGF499 - pGF501, pGF503 - pGF508, pGF510, pGF512 - pGF515, pGF517 - pGF519, pGF521, pGF523, pGF525, pGF528, pGF529, pGF531, pGF534 - pGF537, and pGF542. Briefly, the relevant locus (*VMA21*, *VMA3*, *VMA11*, Anc.c-c', Anc.c", or Anc.c) was PCR amplified with 5' and 3' untranslated flanking sequence and cloned into pCR4Blunt-TOPO (Invitrogen, Carlsbad, CA). If necessary, a modified Quikchange protocol[32] was used to introduce point mutations before the gene was subcloned into a yeast vector (pRS316, pRS415, or the high-copy vector, YEp351). To generate pGF502, codon 31 through the stop codon of Anc.c" were amplified with the *ADH::*Nat^R cassette from pGF139, cloned into TOPO, and *in vivo* ligated downstream of the *VMA16* promoter (including a start codon) in pRS415.

A triple-fragment *in vivo* ligation was used to generate pGF646 - pGF651. Gapped vector containing the *VMA16* promoter was transformed into yeast with two PCR fragments of the proteolipid genes to be fused. For pGF646, the coding region of (i) *VMA16* (without codons 2-41) and (ii) the coding region of Anc.c' (without codons 2-5) were amplified by PCR.

Table 1. Yeast strains and plasmids in this study.

Strain	Genotype	Reference
SF838-1Dα	*MATα ura3-52 leu2-3,112 his4-519 ade6 pep4-3 gal2*	33
LGY113	SF838-1Dα; *vma3*Δ*::Kan*^{R}	17
LGY114	SF838-1Dα; *vma11*Δ*::Kan*^{R}	17
LGY115	SF838-1Dα; *vma16*Δ*::Kan*^{R}	17
LGY125	SF838-1Dα; *vma3*Δ*::Kan*^{R} *vma11*Δ*::Hyg*^{R}	This study
LGY143	SF838-1Dα; *vma3*Δ*::Kan*^{R} *vma11*Δ*::Hyg*^{R} *vma16*Δ*::Nat*^{R}	This study
LGY124	SF838-1Dα; *vma11*Δ*::Kan*^{R} *vma16*Δ*::Nat*^{R}	This study
LGY139	SF838-1Dα; *vma3*Δ*::Kan*^{R} *vma16*Δ*::Nat*^{R}	This study

Plasmid	Description	Reference
pRS415	*CEN, LEU2*	34
pRS316	*CEN, URA3*	35
pYEP351	*2μ, LEU2*	36
pGF06	pRS316 *VPH1::GFP::HIS5*	17
pGF141	pRS415 *VPH1::GFP::HIS5*	This study
pGF140	pRS316 *prVMA3::Anc.c-c'::3xHA::ADH::Nat*^{R}	This study
pGF139	pRS415 *prVMA16::Anc.c"::3xHA::ADH::Nat*^{R}	This study
pGF252	pRS316 *prVMA3::Anc.c-c'::3xHA::ADH* A41C, E139Q	This study
pGF253	pRS316 *prVMA16::Anc.c"::3xHA::ADH* E98Q	This study
pGF254	pRS316 *VMA3*	This study
pGF499	pRS316 *VMA3* I21A	This study
pGF500	pRS316 *VMA11*	This study
pGF501	pRS316 *VMA11* F20A	This study
pGF241	pRS316 *prVMA3::Anc.c-c'::3xHA::ADH* V15F	This study
pGF239	pRS316 *prVMA3::Anc.c-c'::3xHA::ADH* A41S	This study
pGF240	pRS316 *prVMA3::Anc.c-c'::3xHA::ADH* A120G	This study
pGF502	pRS415 *prVMA16::Anc.c"(2-30*Δ*)::3xHA::ADH::Nat*^{R}	This study
pGF503	pRS316 *prVMA16::Anc.c"::3xHA::ADH* I58L	This study
pGF504	pRS316 *prVMA16::Anc.c"::3xHA::ADH* M77I	This study
pGF505	pRS316 *prVMA16::Anc.c"::3xHA::ADH* K87R	This study
pGF213	pYEP351 *VMA21*	This study
pGF506	pRS316 *prVMA3::Anc.c::3xHA::ADH::Nat*^{R}	This study
pGF507	pRS415 *prVMA3::Anc.c::3xHA::ADH::Nat*^{R}	This study
pGF508	pRS316 *prVMA3::Anc.c'::3xHA::ADH::Nat*^{R}	This study
pGF510	pRS316 *prVMA3::Anc.c-c'::3xHA::ADH* V15A	This study
pGF512	pRS316 *prVMA3::Anc.c-c'::3xHA::ADH* M22I	This study
pGF513	pRS316 *prVMA3::Anc.c-c'::3xHA::ADH* S25T	This study
pGF514	pRS316 *prVMA3::Anc.c-c'::3xHA::ADH* V38I	This study
pGF515	pRS316 *prVMA3::Anc.c-c'::3xHA::ADH* A42G	This study

Table 1. (continued).

Plasmid	Description	Reference
pGF517	pRS316 *prVMA3::Anc.c-c'::3xHA::ADH* V45T	This study
pGF518	pRS316 *prVMA3::Anc.c-c'::3xHA::ADH* M46L	This study
pGF519	pRS316 *prVMA3::Anc.c-c'::3xHA::ADH* M46F	This study
pGF521	pRS316 *prVMA3::Anc.c-c'::3xHA::ADH* I55L	This study
pGF523	pRS316 *prVMA3::Anc.c-c'::3xHA::ADH* A61S	This study
pGF525	pRS316 *prVMA3::Anc.c-c'::3xHA::ADH* K79L	This study
pGF528	pRS316 *prVMA3::Anc.c-c'::3xHA::ADH* Y87F	This study
pGF529	pRS316 *prVMA3::Anc.c-c'::3xHA::ADH* N88T	This study
pGF531	pRS316 *prVMA3::Anc.c-c'::3xHA::ADH* H92Q	This study
pGF534	pRS316 *prVMA3::Anc.c-c'::3xHA::ADH* F108Y	This study
pGF535	pRS316 *prVMA3::Anc.c-c'::3xHA::ADH* T121Y	This study
pGF536	pRS316 *prVMA3::Anc.c-c'::3xHA::ADH* A122M	This study
pGF537	pRS316 *prVMA3::Anc.c-c'::3xHA::ADH* I132V	This study
pGF542	pRS316 *prVMA3::Anc.c-c'::3xHA::ADH* N159D	This study
pGF646	pRS415 *prVMA16::VMA16(2-41Δ)::Anc.c'(2-5Δ)::3xHA::ADH::Nat^R*	This study
pGF647	pRS415 *prVMA16::Anc.c'(162-164Δ)::VMA16(1-41Δ)::3xHA::ADH::Nat^R*	This study
pGF648	pRS415 *prVMA16::VMA16(2-41Δ)::Anc.c-c'(1-2Δ)::3xHA::Nat^R*	This study
pGF649	pRS415 *prVMA16::Anc.c-c'(162Δ)::VMA16(1-49Δ)::3xHA::Nat^R*	This study
pGF650	pRS415 *prVMA16::VMA16(2-41Δ)::Anc.c(1-2Δ)::3xHA::Nat^R*	This study
pGF651	pRS415 *prVMA16::Anc.c(161-162Δ)::VMA16(1-49Δ)::3xHA::Nat^R*	This study

The proteolipid on the C-terminal portion of the gene fusion also contained the *ADH* terminator and Nat^R cassette; the amplified products contained PCR tails with homology to link the genes to both the gapped vector and to each other. Gene fusions were modeled after a previous experimental design[37] where the lumenal protein sequence linking the two proteolipids was designed to be exactly 14 amino acids. To meet these criteria, additional amino acids were inserted in the following vectors linking the two subunits: pGF646 (TRVD), pGF648, pGF650 (TR), pGF649, pGF651 (GS).

Yeast strains used can be found in Table 1. Strains containing deletion cassettes other than Kan[31] were constructed by PCR amplifying the *Hyg*^{R} or *Nat*^{R} cassette from pAG32 or pAG25, respectively, with primer tails with homology to flanking sequences to the *VMA11* or *VMA16* loci. *11*Δ*::Kan*^{R} and *16*Δ*::Kan*^{R} strains (SF838-1Dα) were transformed with the *Hyg*^{R} and *Nat*^{R} PCR fragments, respectively, and selected for drug resistance. The *11*Δ*::Hyg*^{R} locus was amplified and transformed into LGY113 (to create LGY125) and LGY115 (to create LGY124). This was repeated with the *16*Δ*::Nat*^{R} locus to create LGY139 and LGY143.

Yeast growth assays: Yeast were grown in liquid culture, diluted five-fold, and spotted onto YEPD media buffered to pH 5.0 or media containing 25 mM or 30 mM $CaCl_2$ (as previously described[17]).

Whole cell extract preparation and immunoblotting: Yeast extracts and Western blotting were performed as previously described[17]. Antibodies used in this study included monoclonal primary anti-Vph1 (10D7; Invitrogen), anti-Vma1 (8B1; Invitrogen), and anti-Dpm1 (5C5; Invitrogen), and secondary horseradish-conjugated anti-mouse antibody (Jackson ImmunoResearch Laboratory, West Grove, PA).

Fluorescence microscopy: Staining with quinacrine was performed as previously described[17,38,39]. Visualization of GFP-tagged proteins was conducted as previously described[17]. Microscopy images were obtained using an Axioplan 2 fluorescence microscope (Carl Zeiss, Thornwood, NY). A 100x objective was used as well as AxioVision software (Carl Zeiss).

4. *Results*

The reconstruction ancestor functions as subunit c, c' or both c and c' in extant budding yeast: Our reconstructions show that V-ATPase's function of vacuolar acidification was indeed conserved over evolutionary time, despite the Fungi-specific conservation of the duplicated proteolipid gene. In our growth assays, the reconstructed Anc.c-c' functionally substituted for the *S.cerevisiae* ortholog of subunit c (Vma3), the ortholog of subunit c' (Vma11), and both Vma3 and Vma11 (Figure 5A). Yeast cells lacking Vma3 (designated as *3*Δ) or lacking Vma11 (designated as *11*Δ*)* were unable to grow in the presence of elevated $CaCl_2$ because they lack a functional V-ATPase necessary for vacuolar acidification, but they were able to survive on permissive media. Expressing Anc.c-c' in *3*Δ rescued cellular growth; these cells were only partially sensitive to $CaCl_2$. Expressing Anc.c-c' in *11*Δ also rescued growth, as well as in double-delete *3*Δ*11*Δ. The reconstructed Anc.c" functionally substituted for *S. cerevisiae* subunit c" (Vma16) (Figure 5B). Furthermore, co-expression of Anc.c-c' and Anc.c" permitted cell growth in yeast lacking all three proteolipid subunits Vma3, Vma11, and Vma16 (Figure 5C). We stained cells with the dye quinacrine and observed that yeast expressing Anc.c-c' and Anc.c" properly acidified the vacuolar lumen---as is expected of a properly functioning yeast V-ATPase complex---while cells lacking the V-ATPase failed to show any staining (Figure 5D).

Previous observations showed that V-ATPase function requires the presence of critical glutamic acid residues at specific sites[9,40]; these residues are strongly supported in our reconstructions with 1.0 posterior probability at sites 139 in Anc.c-c' and 98 in

Anc.c". Mutating these glutamic acids to glutamines (E139Q and E98Q) destroyed ancestral function, thus demonstrating the necessity of E139 and E98 (Figure 6).

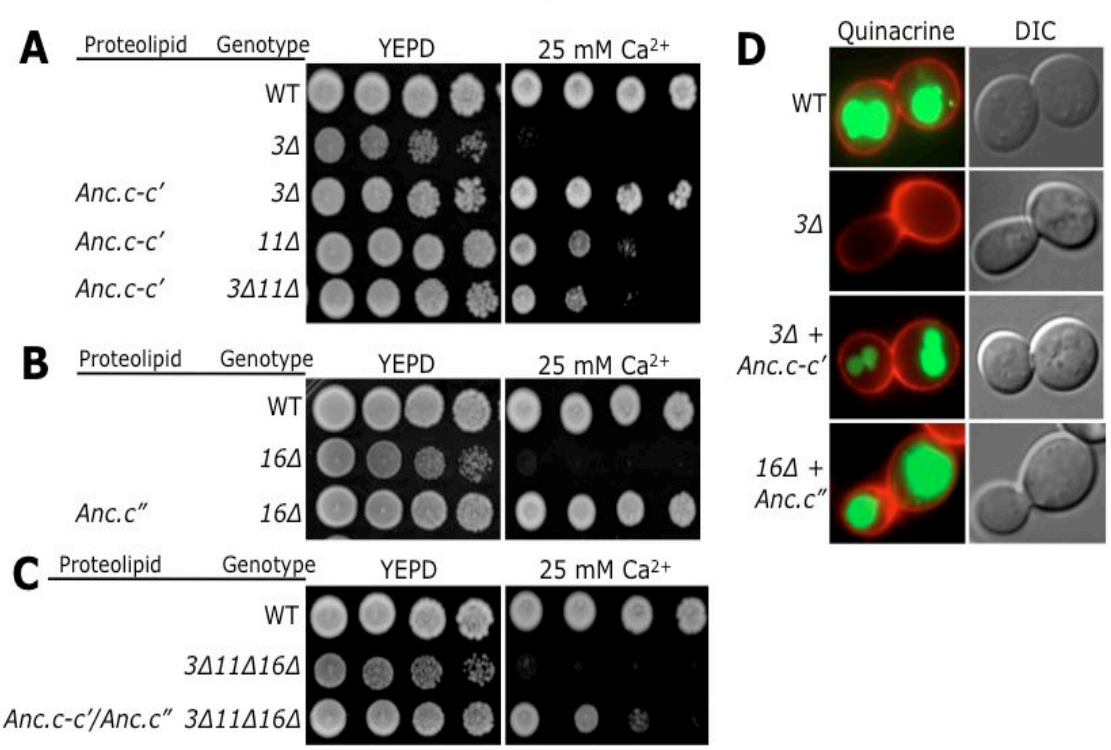

Figure 5. Functional growth assays of ancestral V-ATPase subunits expressed in contemporary *S. cerevisiae* mutants. Yeast were plated on permissive media (YEPD) and media buffered with 25 mM Ca^{2+}. (A) Anc.c-c' was expressed in yeast lacking Vma3 (*3*Δ), Vma11 (*11*Δ), and both Vma3 and Vma11 (*3*Δ*11*Δ). Growth was compared with wild-type (WT) and *3*Δ yeast. (B) Anc.c" was expressed in yeast lacking Vma16 (*16*Δ) and growth was compared to the appropriate controls. (C) Dual-expression of Anc.c-c' and Anc.c" in *3*Δ*11*Δ*16*Δ yeast was compared with controls. (D) Anc.c-c' in *3*Δ yeast and Anc.c" in *16*Δ yeast were stained with quinacrine (green; acidified compartments) and concanvalin A-tatramethylrhodamine (red; binds to yeast cell wall) and viewed by either fluorescent or DIC microscopy. Wild-type (WT) and *3*Δ yeast serve as controls. Variable levels of quinacrine staining were observed for *3*Δ yeast containing Anc.c-c'.

The observed functions of Anc.c-c' and Anc.c" are robust to uncertainty about the inferred ancestral sequences; we reconstructed alternate versions of Anc.c-c' and Anc" using secondary amino acid states with support greater than 0.2 posterior probability and we observed no qualitative difference in function compared to the ML reconstruction (Table 2).

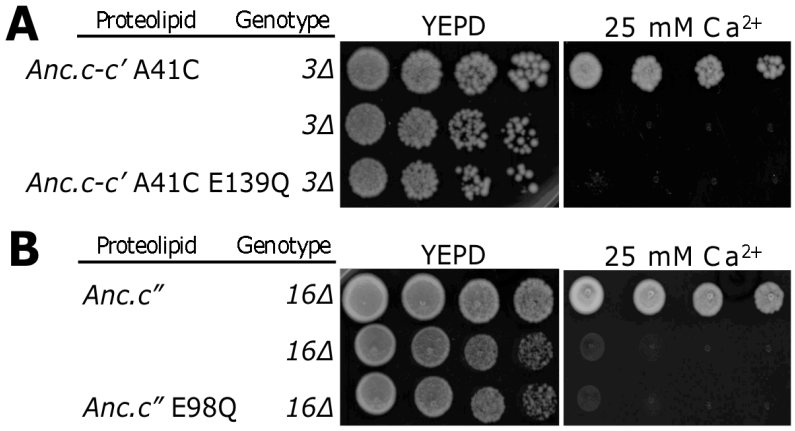

Figure 6. Functional growth assays of Anc.c-c' and Anc.c" lacking critical glutamic acid residues in contemporary *S. cerevisiae*. Yeast were plated on permissive media (YEPD) and media buffered with 25 mM Ca^{2+}. (A) A particular allele of Anc.c-c' (A41C) was used to illustrate the dramatic growth difference when the E139Q mutation is introduced. Anc.c-c' A41C, and Anc.c-c' A41C E139Q, were expressed in yeast lacking Vma3 (*3*Δ). (B) Anc.c" and Anc.c" E98Q, were expressed in yeast lacking Vma16 (*16*Δ) and tested under similar conditions.

Intermediate ancestors Anc.c and Anc.c' function as subunit c and c', respectively: We next reconstructed intermediate ancestral protelipid subunits (Figure 7), and observed that the subunit identities of c and c' diverged very soon after the Anc.c-c' gene duplication event. Specifically, we reconstructed Anc.c (the most-recent-shared ancestor of all Fungi subunit c) and Anc.c' (the most-recent-shared ancestor of all Fungi subunit c'), and tested their function in extant yeast.

Anc.c identified as subunit c while Anc.c' identified as subunit c' (Figure 8). Anc.c' functioned in place of extant yeast Vma11, and did not function as yeast Vma3 (Figure 8A). Anc.c functioned in place of yeast Vma3, and very poorly functioned as Vma11 (Figure 8B). Co-expression of both Anc.c and Anc.c' in *3*Δ *11*Δ increased the V-ATPase function as compared to the single ancestral chimeras (Figure 8C). Anc.c' in *11*Δ yeast and Anc.c in *3*Δ yeast properly acidified the vacuole (Figure 8D).

Table 2. Robustness to uncertainty for Anc.c-c' and Anc.c" sequences. The following residues were chosen from Anc.c-c' and Anc.c" that had a posterior probability of less than 80%. Regions corresponding to lumenal portions of either ancestral proteolipid (as predicted by SOSUI, Figure 3) were excluded from this analysis. The Anc.c" 2-30Δ mutant contained 23 residues that had a posterior probability of less than 80%. These alternate reconstructions were transformed into *vma3*Δ, *vma11*Δ, and *vma3*Δ *vma11*Δ strains (for Anc.c-c') and *vma16*Δ yeast (for Anc.c") and tested for growth on rich media and media containing 25 mM Ca^{2+}. Wild-type yeast scored five pluses and any yeast strain lacking a proteolipid subunit (*3*Δ, *11*Δ, *3*Δ*11*Δ, or *16*Δ) all scored zero under these conditions.

Proteolipid	*Genotype*		
	***vma3*Δ**	***vma11*Δ**	***vma3*Δ *vma11*Δ**
Anc.c-c'	+++	++	+++
Anc.c-c' V15F	++	++++	++
Anc.c-c' A41S	++	+	++
Anc.c-c' A120G	++	+	++
	***vma16*Δ**		
Anc.c"	+++++		
Anc.c" I58L	+++++		
Anc.c" M77I	+++++		
Anc.c" K87R	+++++		
Anc.c" 2-30Δ	+++++		

Also, the hybrid V-ATPase complexes containing either Anc.c or Anc.c' properly localized to the vacuole membrane (Figure 8E). The two phylogenetic branches leading to Anc.c and Anc.c' contain 25 and 31 mutations, respectively. Although it is impractical to characterize the function of all 20^{25} (=$1.55x10^{25)}$ and 20^{31} (=$8.22x10^{33}$) possible substitution combinations, we can conclude that the substitutions necessary for c and c' subunit identities are included in these sets.

Single amino acid substitutions affect the evolutionary trajectory of the c and c' subunits: We further analyzed the amino acid substitutions leading to Anc.c and Anc.c' and observed that no single substitution completely shifted the identify of Anc.c-

c' into either subunit c or c', but a small subset of substitutions individually affected a strong---but not complete---change.

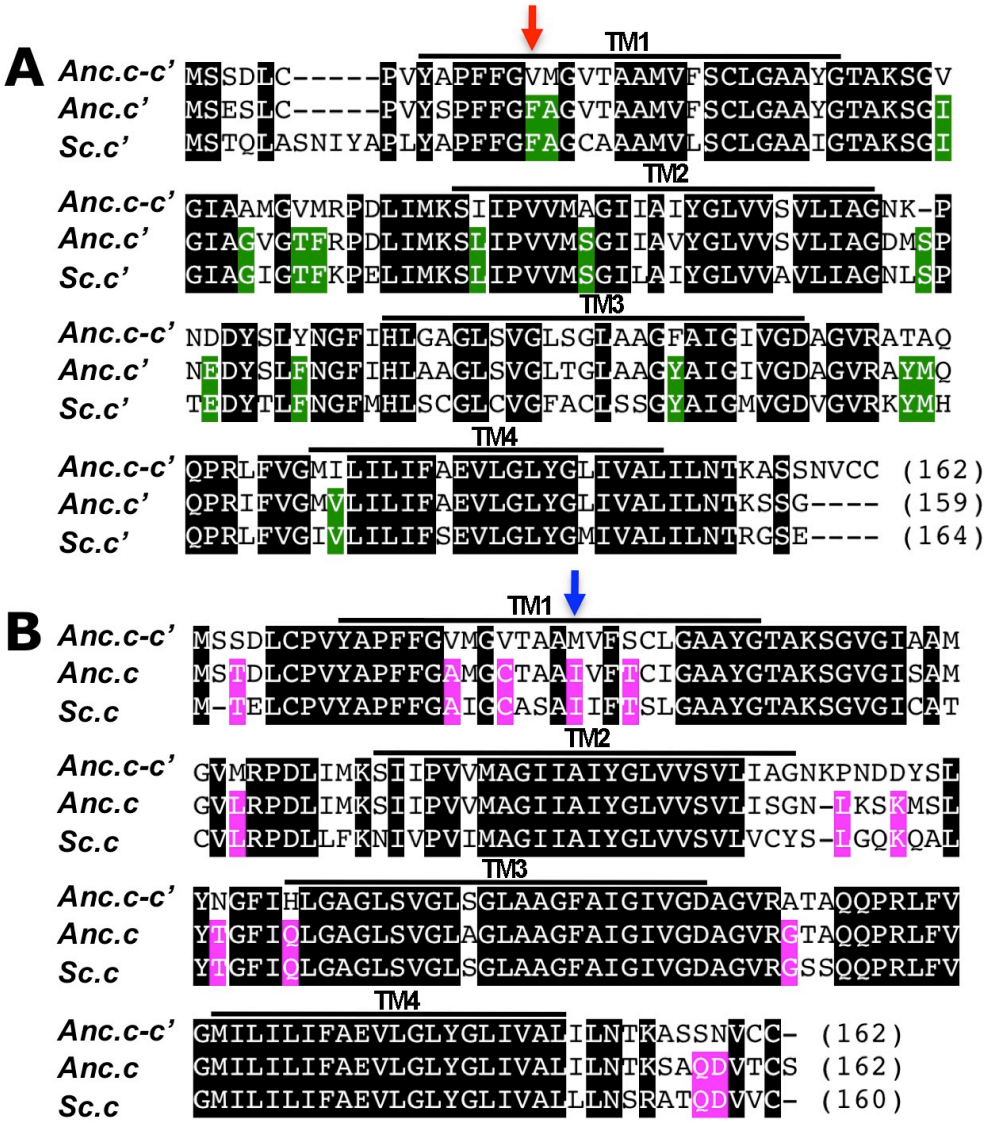

Figure 7. Protein sequence alignment of Anc.c-c', Anc.c, Anc.c' and yeast Vma3 and Vma11 subunits using CLUSTAL[15]. Potential transmembrane domains are indicated. A) Identical residues between all three proteins are shown against a black background. Residues identical between Anc.c' and *S. cerevisiae* Vma11 are shown against a green background. B) Identical residues between all three proteins are shown against a black background. Residues identical between Anc.c and yeast Vma3 are highlighted against a magenta background.

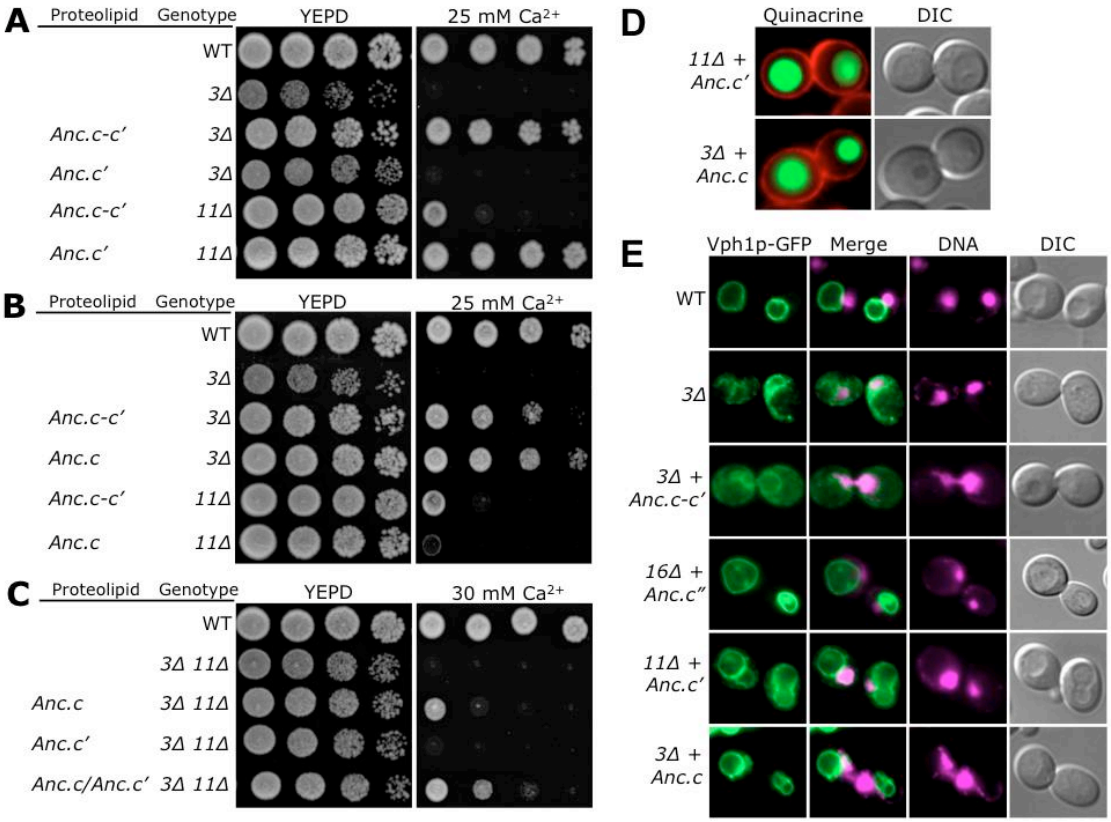

Figure 8. Functional growth assays of intermediate ancestors Anc.c and Anc.c'. Yeast were plated on permissive media (YEPD) and media buffered with 25 mM or 30 mM Ca^{2+}. (A) Anc.c-c' and Anc.c' were expressed in yeast lacking Vma3 (*3*Δ) or Vma11 (*11*Δ) and tested with controls; (B) we performed an identical analysis using Anc.c rather than Anc.c'. (C) Anc.c, Anc.c' or the combination of both Anc.c and Anc.c' were expressed in yeast lacking both Vma3 and Vma11 (*3*Δ *11*Δ) and plated with controls. (D) Yeast lacking Vma11 (*11*Δ) expressing Anc.c' and yeast lacking Vma3 (*3*Δ) expressing Anc.c were stained with quinacrine. Controls were as described in Figure 2. (E) Yeast deleted for Vma3 expressing Anc.c-c', *16*Δ yeast expressing Anc.c", *11*Δ yeast expressing Anc.c', and *3*Δ yeast expressing Anc.c were transformed with a vector containing Vph1-GFP. Controls incuded a wild-type strain and *3*Δ mutant. Strains were treated with the DNA-binding dye Hoechst 33342 (shown as magenta) and viewed by fluorescent or DIC microscopy. Merged images show the localization of Vph1-GFP (green) to either the ER perinuclear and cortical membranes (*3*Δ and *3*Δ yeast expressing Anc.c-c') or to the limiting membrane of the vacuole (*16*Δ expressing Anc.c", *11*Δ expressing Anc.c', and *3*Δ expressing Anc.c).

We selected diagnostic residues that are highly conserved in either---but not both---of the contemporary Fungi proteolipid subunit c and c' sequences, and we tested the

functional effect of introducing each residue as a single substitution into the sequence of Anc.c-c' (Table 3).

Table 3. All single amino acid changes made to Anc.c-c'. These were tested in yeast lacking either Vma3 or Vma11. Growth was assayed on rich media buffered with 25 mM Ca^{2+}. The predicted identity of each residue (based on the high conservation within sampled fungal subunits) is listed. K79L is predicted to contribute to both yeast Vma3 and Vma11 identity as it is identical between these extant subunits. The wild-type strain scored five pluses under these conditions. Yeast lacking either Vma3 or Vma11 (not containing any ancestral proteolipid) scored zero. Residues that were tested were restricted to those present within either Anc.c or Anc.c'. M22I and V15F are noted in bold and were chosen for further characterization.

Proteolipid	**Genotype**		**Predicted 3 and/or 11 "identity"**	**Found in Either Anc.c or Anc.c'**
	***3*Δ**	***11*Δ**		
Anc.c-c'	++++	++	N/A	N/A
-	0	0	N/A	N/A
Anc.c	++++++	0/+	3	N/A
Anc.c'	0	++++++	11	N/A
V15A	+	+++	3	Anc.c
M22I*	+++++	+	3	Anc.c
S25T	+++	++	3	Anc.c
M46L	+++	++	3	Anc.c
K79L	++++++	++++	3 & 11	Anc.c
N88T	++	+	3	Anc.c
H92Q	++	++	3	Anc.c
A120G	++	++	3	Anc.c
N159D	++	++	3	Anc.c
V15F*	++	++++	11	Anc.c'
M16A	++	++	11	Anc.c'
V38I	++++	++	11	Anc.c'
A42G	+++	++	11	Anc.c'
V45T	++	++	11	Anc.c'
M46F	++	++	11	Anc.c'
I55L	+++++	+++	11	Anc.c'
A61S	++++	++	11	Anc.c'
Y87F	++	++	11	Anc.c'
F108Y	+	++	11	Anc.c'
T121Y	++++	++	11	Anc.c'
A122M	+	++	11	Anc.c'
I132V	+++++	++	11	Anc.c'

Two noteworthy substitutions are Val to Phe at site 15 (V15F), and Met to an Iso at site 22 (M22I). V15F partially shifted ancestral identity towards subunit c' while compromising c identity. M22I partially shifted identity towards subunit c while partially destroying c' identity (Figure 9). Interestingly, Phe at site 15 is not necessary in extant

yeast subunit c', and Iso at site 21 is not necessary in extant subunit c (Figure 9 B,F); this observation suggests that genetic background and epistasis play crucial roles in protein evolution, consistent with previous findings in other protein families[41].

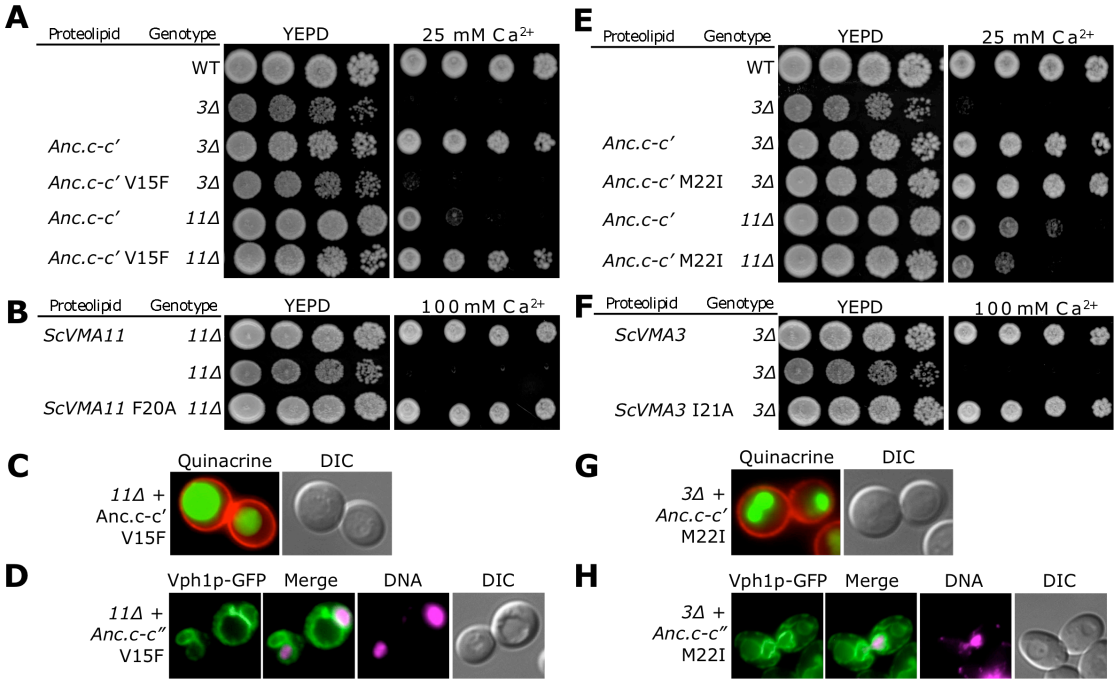

Figure 9. Two single amino acid changes contribute towards subunit c and c' identity. Introduction of V15F in to the Anc.c-c' increases function in *vma11*Δ yeast and Anc.c-c' with M22I increases complementation in *vma3*Δ yeast. (A) Growth tests were performed with Anc.c-c' and Anc.c-c' V15F in yeast lacking either Vma3 or Vma11. (B) Growth assays of extant yeast Vma11 and Vma11 containing F20A mutation were performed on rich media containing 100 mM Ca^{2+}. (C) Quinacrine staining was performed on *vma11*Δ yeast expressing Anc.c-c' V15F. (D) The localization of Vph1-GFP was assayed by fluorescence microscopy in cells expressing Anc.c-c' V15F. The nucleus was stained with DAPI. (E through H) We performed an identical analysis of the Anc.c-c' subunit containing the M22I substitution as the V15F mutant.

5. *Discussion*

Our ancestral reconstructions---combined with previous results---support a model of subfunctionalization following the gene duplication of Anc.c-c'. Subfunctionalization is strongly suggested by the fact that Anc.c-c' can function as either subunit c or c' (Figure 5), but Anc.c' cannot function as c and Anc.c functions very poorly as c' (Figure

8). Previous observations show the complementarity of these two subunits is conserved in contemporary yeast, as extant subunits c and c' cannot be functionally interchanged[9-11]. Furthermore, previous observations showed that yeast subunits are confined in their ring arrangement such that c' cannot interface with the clockwise side of c", c cannot interface with the counterclockwise side of c", and c' cannot interface with itself[37]. A synthesis of these two ideas---functional complementarity and structural specificity---implies an evolutionary model in which Anc.c-c' subfunctionalized its ability to interface with itself and with Anc.c". The structural model in Wang *et al*. (2007 implies the proteolipid ring is assembled using three interfaces, which we designate P, Q, and R (Figure 10A,B).

In this model, every subunit participates in at least two interfaces: one on its clockwise side and another on its counterclockwise side. Subunit Anc.c", for example, participated in interface Q clockwise and interface R counterclockwise (when viewed from the luminal side of the membrane). We tested this model using the intermediate ancestral ring containing Anc.c' (immediately following the duplication of Anc.c-c'). We created two reciprocal gene fusions between yeast subunit c" and Anc.c'---using an experimental strategy developed by Wang *et al*. (2007)---that constrains the ring position of Anc.c' to be either immediately clockwise or counterclockwise to subunit c". We observed that Anc.c' only functioned on the counterclockwise side of subunit c"; V-ATPase was nonfunctional when Anc.c' is forced to occupy the clockwise side (Figure 11).

The following evolutionary history emerges: immediately after Anc.c-c' duplicated, the two descendant subunits were functionally identical and we presume the

proteolipid ring could be formed from many possible combinations of the two descendants (i.e., one and four copies, two and three copies, etc.).

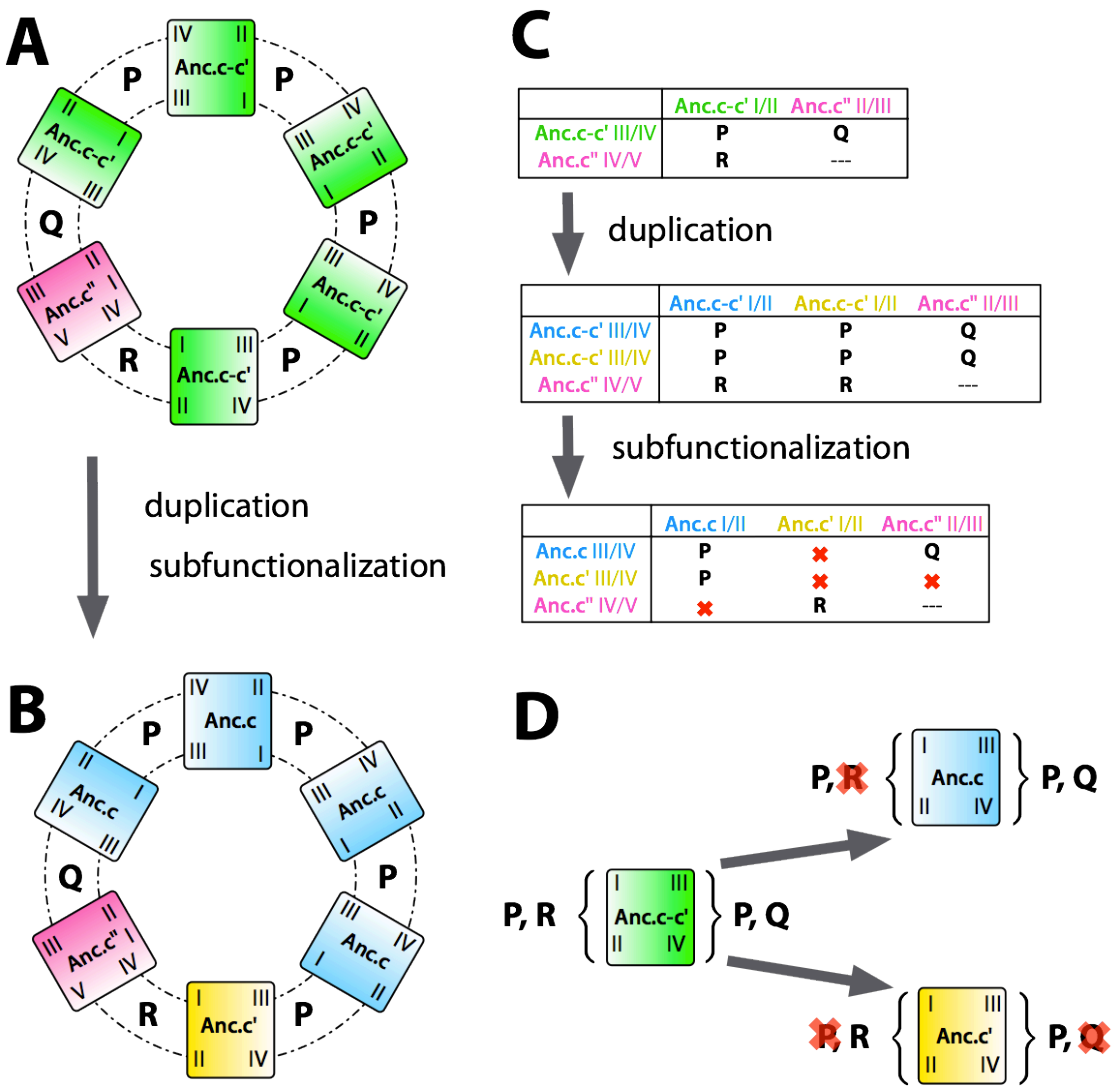

Figure 10. A model of subfunctionalization in the fungal V_0 proteolipid ring. (A) The pre-duplicated ring included two subunits: Anc.c-c' and Anc.c". The roman numerals indicate putative placement of transmembrane helices (numbered I through V) as predicted (Figure 3). Intersubunit interfaces are labeled P, Q, and R. (B) After duplication of Anc.c-c' and subfunctionalization, the proteolipid ring included three subunits arranged according to a previous model[37]. (C) All predicted intersubunit interfaces are described in tabular form. Red Xs indicate lost interfaces. (D) Anc.c-c' participated in interfaces P and R on its I/II side and interfaces P and Q on its III/IV side. Participation in R (I/II) was lost along the lineage leading to Anc.c; participation in P (I/II) and Q (III/IV) was lost along the lineage leading to Anc.c'.

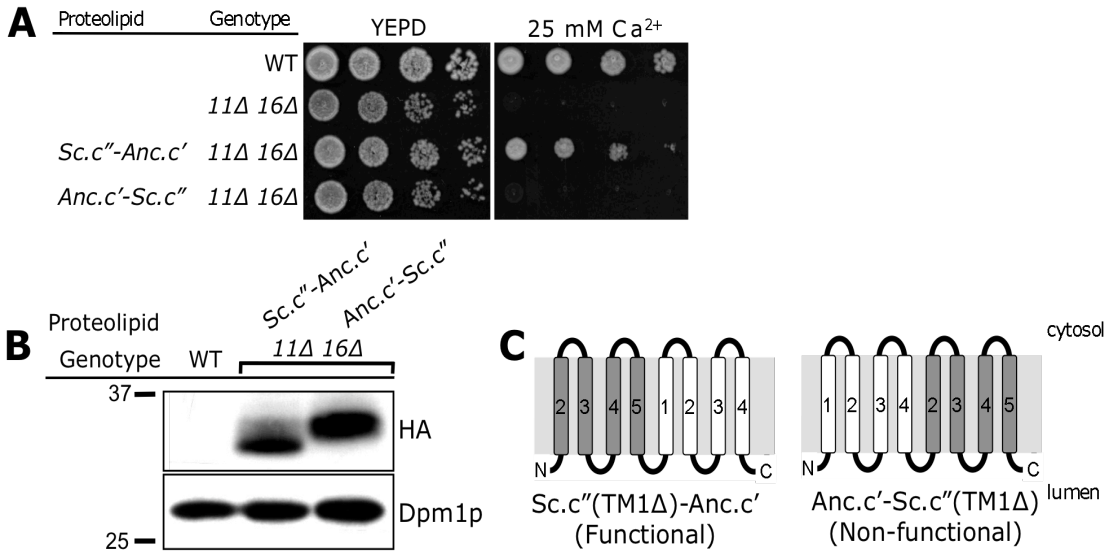

Figure 11. Translation fusions between contemporary yeast c" and Anc.c' demonstrate the positioning of these two subunits within the V-ATPase proteolipid ring. (A) Yeast deleted for *VMA11* and *VMA16* (*11Δ 16Δ*) were transformed with vectors containing a gene fusion between yeast c" lacking the first transmembrane domain followed by Anc.c' (Sc.c"-Anc.c') or a gene fusion between Anc.c' followed by yeast c" lacking the first transmembrane domain (Anc.c'-Sc.c") and tested on permissive media and media containing 25 mM Ca^{2+}. (B) Whole cell extracts were prepared from strains expressing either gene fusion construct and probed using anti-HA antibodies or anti-Dpm1 antibodies (loading control). Extracts from wild-type yeast served as a negative control. (C) Construction of the proteolipid gene fusions followed a similar strategy performed by Wang et al. (2007). The first transmembrane domain of yeast subunit c" was deleted in both gene fusions. Constructs contained a C-terminal, triple HA epitope tag and were expressed under control of the yeast *VMA16* promoter. Both constructs are fused using a 14 amino acid linker region.

This arrangement flexibility was lost over evolutionary time: Anc.c' lost the ability to participate in interface P on its clockwise side, while the ability of Anc.c to participate in interface R has been eroded (Figure 10C,D).

The pairwise loss of participation in interface R (in Anc.c) and P (in Anc.c') is sufficient to explain the specific arrangement of proteolipid subunits. The loss of R on the clockwise side of Anc.c prevented Anc.c from occupying the 6:00 ring position adjacent to Anc.c", while the loss of P on the clockwise side of Anc.c' prevented Anc.c'

from occupying any position *except* at 6:00. These complementary losses created a structural sitution in which both subunits c and c' are necessary for proteolipid assembly and function. In addition to losing P participation, Anc.c' also lost the ability to participate in Q (on its counterclockwise side). The most parsimonious hypothesis is that Anc.c' lost Q as a neutral consequence of its forced confinement to the 6:00 ring position. A less parsimonious hypothesis is that Q was lost prior to the complementary losses of P and R, but this alternative explanation raises the question of why Anc.c' was conserved rather than psuedogenized.

The results of our diagnostic single-state mutation experiments are congruent with our model of subfunctionalization (Table 3). Two of the mutations with strongest effect, V15F and M22I, occurred within transmembrane domain 1 (TM1) of Anc.c and Anc.c'; this is consistent with our hypothesis that loss of participation in interfaces P and R primarily resulted from amino acid substitutions to the TM1/TM2 side of the duplicated subunits. However, correlations between functional effect and transmembrane location can be meretricious because the precise order of evolutionary appearance and epistatic interactions of the single amino acid mutations is unknown.

Our results also suggest a strong correlation between the evolution of subunit identity and assembly of the V_0 complex. Previous work has shown that assembly defects in the V-ATPase V_0 subdomain cause the stator subunit Vph1 to be rapidly degraded[42,43]. However, overexpression of the dedicated V-ATPase assembly factor Vma21 is able to suppress particular V_0 assembly defects[44]. Consistent with these findings, we observed that steady-state levels of Vph1 were reduced in *3*Δ or *11*Δ yeast expressing Anc.c-c', and that overexpression of Vma21 improved the growth of Anc.c-c'

in *3*Δ yeast (Figure 12). Furthermore, assembly defects were overcome by expression of either Anc.c or Anc.c' in place of Anc.c-c' (Figure 12). Lacking a crystal structure of the V-ATPase, the precise contribution of the residues present within Anc.c and Anc.c' will require further study.

It is also unknown if the incorporation of subunit c' conferred a fitness advantage within Fungi, or if the increased subunit complexity was preserved via neutral processes. The subfunctionalization model of duplication-degeneration-complementation suggests that multi-subunit complexity can evolve neutrally[45]. On the other hand, previous work suggests two possible molecular mechanisms by which proteolipid ring complexity could confer a fitness advantage. First, the V-ATPase does not form a passive channel for protons when the V_1 subdomain is removed[46,47] and hence proteolipid rings with two subunits are more efficient than rings with a single subunit. Extending this logic, a compelling hypothesis is that three subunits are more efficient than two. Second, ring asymmetry conferred by additional subunits could have allowed the V-ATPase to more efficiently avoid thermodynamic equilibrium (termed "proton slippage") and continue pumping protons under varying environmental conditions[48,49].

We presume that our subfunctionalization model applies to all fungal V_0 proteolipid rings because the subunit c/c' gene duplication event took place very early in the evolutionary trajectory of Eurkaryotes. The entire V-ATPase complex has a history of repeated gene duplications, and it is possible that other subunits---such as A and B[50]---have an evolutionary history involving ancestral subfunctionalization of subunit identity, similar to subunits c and c'.

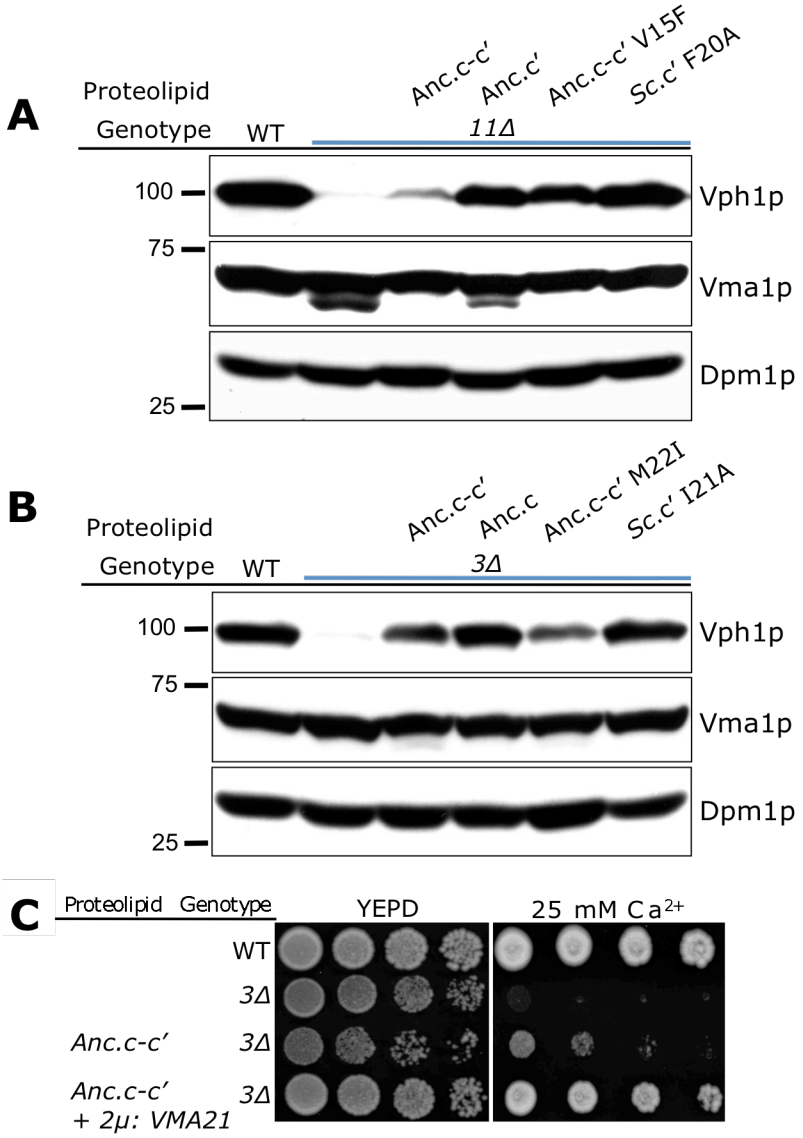

Figure 12. V-ATPase complexes containing ancestral proteolipids display V_0 assembly defects. (A) Whole cell extracts were prepared from yeast lacking Vma11 (*11*Δ) expressing either Anc.c-c', Anc.c', Anc.c-c' V15F, or *S. cerevisiae* subunit c' F20A and compared to controls. Equal amounts of protein were loaded, separated by SDS-PAGE, transferred to nitrocellulose membrane, and probed with anti-Vph1 and anti-Vma1 antibodies. Levels of Vma1 did not change in any of the tested strains. Dpm1 was used as loading control. The molecular mass (kilodaltons) of the nearest marker is shown on the left. (B) Extracts were also probed by Western blot from strains lacking Vma3 (*3*Δ) expressing either Anc.c-c', Anc.c, Anc.c-c' M22I, or *S. cerevisiae* subunit c I21A including controls and were treated in a similar manner. (C) Yeast lacking Vma3 and containing either Anc.c-c' or Anc.c-c' and a high-copy vector overexpressing *VMA21* were plated onto media containing 25 mM Ca^{2+} with controls strains.

Thinking beyond the V-ATPase, our results empirically demonstrate a general evolutionary and molecular process by which physiological phenotypes can be buffered against underlying increases in multiprotein complexity.

CHAPTER V

DISCUSSION AND SUMMARY

1. *Genetic screens and the V-ATPase*

Study of the V-ATPase enzyme complex will allow for a more complete understanding of how this critical molecular machine functions in all eukaryotes. Aside from its highly conserved role in organelle acidification, the V-ATPase has been implicated in a wide range of other biological processes (FORGAC 2007). Additionally, the recent discoveries of V-ATPase involvement in human diseases (including cancer) prompts additional research and makes the V-ATPase enzyme an attractive target for drug development (FORGAC 2007).

Over the past two decades, genetic screens have played important roles in providing critical components and pathways that involve the V-ATPase enzyme (OHYA *et al.* 1991; HO *et al.* 1993; SAMBADE *et al.* 2005). However, recent work has provided evidence that additional factors, pathways, and regulators might exist that have eluded detection in prior work (RYAN *et al*. 2008). As mentioned in Chapter II, the overwhelming levels of V-ATPase activity within the yeast cell are thought to mask subtle contributors to enzyme function. Therefore, reducing the total V-ATPase enzyme content of the cell by using specific alleles of assembly factors creates a sensitized genetic background that allows for a new screening strategy.

Not surprisingly, a large number of genes emerged from the SGA screens presented in Chapter II. Some of the pathways identified from these screens merit further investigation. Of particular interest would involve genes whose protein products localize to the ER, Golgi/endosomal network, as well as genes that are uncharacterized and have

no known molecular function. Components of ER-localized protein degradation pathways provide an interesting tangent to the life history of the V-ATPase complex. It is possible that there may be regulated interplay between components of the V_0 assembly machinery and ER quality control systems. Prior work has shown that upon disruption of V_0 assembly, subunit a (Vph1p or Stv1p), is targeted for degradation (GRAHAM *et al.* 1998; HILL and COOPER 2000). Additionally, other isoforms of subunit a that are not inherent to budding yeast (such as the ancestral Anc.a, or subunit a from *N. crassa* or *S. pombe*) are also still targeted for degradation if there is a V_0 assembly defect (unpublished results).

Secondly, these SGA screens have provided a large number of trafficking-related genes that are important for full V-ATPase function (Table 3, Chapter II and Table S1, Appendix A). While many of these belong to the well-characterized components of vesicular trafficking pathways that transit through the Golgi and endosome (such as the ESCRT machinery), some are involved in other trafficking functions. These provide interesting genetic interactions with the V-ATPase that have otherwise been unappreciated. Some of these might provide future insight into (i) V_0 exit from the ER to the early Golgi and (ii) differential trafficking of the two isoforms of the V-ATPase.

One of the many open questions regarding V-ATPase assembly and trafficking involves the specific factor(s) that govern recognition of the completed, assembled V_0 subcomplex in conjunction with Vma21p by vesicular budding machinery and subsequent exit from the ER. One of the difficulties in searching for factors that might serve as "cargo recognition" adaptor proteins is that redundancy can exist between cargo adaptors such as those belonging to the p24 family (MARZIOCH *et al.* 1999;

SPRINGER *et al*. 2000). Also, loss of the adaptor molecule might not cause a complete shift in the steady-state levels of the cargo. Rather, it may cause slowed, anterograde vesicular transit (BUE *et al.* 2006). Finally, many of the components required for vesicular transport from the ER to the Golgi are essential and are not included within the non-essential haploid deletion collection (GAYNOR *et al.* 1998).

However, current progress is being made to address these different technical problems. For one, future work will attempt to create a reporter protein out of one of the subunits of the V-ATPase that will allow for a kinetic, pulse-chase analysis. Many of the cargo proteins for which adaptor proteins (such as alkaline phosphatase) have been characterized can be detected by a pulse-chase assay because they undergo proteolytic cleavage within particular cellular compartments (COWLES *et al.* 1997; PIPER *et al.* 1997; STEPP *et al.* 1997). Supplementing the V-ATPase enzyme with a reporter protein that will allow for a kinetic assay of transit through the endo-membrane system will be invaluable for the investigation of V_0 ER exit.

Also, future genetic screens are being developed that will aid in specifically assaying whether Vph1p has been degraded rather than assaying survival on zinc or buffered calcium. Previous genetic screens have demonstrated that many genes are involved in zinc and/or calcium sequestration and homeostasis (SAMBADE *et al.* 2005; PAGANI *et al.* 2007). Separating genes that have no impact on V-ATPase function (such as *HPH1/HPH2*) from genes that may have an effect on V_0 assembly is crucial. Current work has shown that creating a triple gene fusion between Vph1p, GFP, and His3p will allow for a targeted genetic screen (either enhancer or suppressor) that will directly address the degradation of subunit a at steady-state (unpublished results).

Finally, trafficking genes that have been uncovered by the work in Chapter II will aid in projects targeted at characterizing the differential trafficking between Vph1p and Stv1p (also see Chapter III). While these SGA screens have not been designed with this purpose in mind, it is interesting to note that a number of genes that have emerged out of these screens also overlap with screens searching for *trans* effectors of Stv1p[1]. However, it is unclear how these genes interact with the V-ATPase. For example, components of the AP-3 complex, HOPS complex, and others (including Arl1), show strong genetic links to the V-ATPase (unpublished data; COSTANZO *et al.* 2010). It is important to mention that the SGA screens from Chapter II are designed with *both* Stv1p and Vph1p present in the cell. Therefore, comparison of these interaction networks to those generated by the Stv1p *trans* SGA screens might provide insight into which genes do not differentiate between subunit a isoforms and represent more generalized, genetic links to the V-ATPase.

Another prominent category of genes uncovered by the SGA screens in Chapter II involves lipids and membrane biology. Our work on *ORM1* and *ORM2* demonstrate that sphingolipid composition has a subtle effect on V-ATPase activity. However, additional genes involved in lipid composition are listed in Table 3 (Chapter II) such as those for ergosterol biogenesis (*erg3*Δ and *erg6*Δ) and others involved with sphingolipids (*sur4*Δ). Other reports have studied how alterations in the lipidome can affect cargo assembly, transport, and function (CHUNG *et al.* 2003; ZHANG *et al.* 2010). It appears that the V-ATPase is also sensitive to the lipid environment. Future work would likely include

[1] These SGA screens for *trans* effectors of the Stv1p-containing complex are performed in a *vph1*Δ genetic background and crossed to the haploid deletion collection as described in Chapter II. The purpose is to search for effectors that, when deleted, will cause Stv1p to be mislocalized to the vacuolar membrane in the absense of the Vph1p subunit.

understanding how the local lipid states (within particular subcellular organelles) can affect the V-ATPase. Prior to these genetic screens, others have provided evidence that membrane-bound compartments can have differential effects on V-ATPase function. Reversible dissociation of V_1 and V_0 only occurs when the V-ATPase enzyme (including either isoform of subunit a) is present on the vacuolar membrane and not on the Golgi (KAWASAKI-NISHI *et al.* 2001a). It seems likely that the local lipid environment is affecting the V-ATPase. Other future work might investigate whether other constituents of the lipidome (aside from sphingolipids) have similar effects on enzyme function and/or trafficking of cargo proteins.

The work from Chapter II is of great importance to understanding the evolution of the V-ATPase. Many of the different genetic pathways identified from these SGA screens are highly conserved in other eukaryotes. Of particular interest is the Orm1p/Orm2p duplicate protein pair. These proteins have been implicated in early childhood asthma in humans (FERREIRA *et al.* 2010). Many of the components of sphingolipid biogenesis are highly conserved (BRESLOW *et al.* 2010). Similarly, trafficking pathways are well conserved across different lineages and yeast has served as a useful model system for characterizing vesicular trafficking. Future work should involve separating yeast-specific phenomenon from processes that are well conserved in other creatures. While species-specific mechanisms are still of interest, a more global view of the V-ATPase and especially work in mammalian systems will require the separation of components that might not exist outside a small group of budding yeast species. (For example, it is likely that assembly factors Voa1p and Pkr1p evolved

recently within the budding yeasts and that these proteins are not found within other eukaryotes or distant fungi).

The use of genetic screens within yeast and other model organisms (such as flies, worms, and even mammalian cell culture) has the potential to provide a clear evolutionary picture of the cellular processes that affect the V-ATPase. Comparison of this genetic data will be critical in categorizing general versus species-specific V-ATPase mechanisms.

2. *The evolutionary history of the two subunit a isoforms in budding yeast*

The 100 kDa subunit a "stator" subunit of the V-ATPase is a critical component of the enzyme complex. Recent studies have focused on this subunit because of its proposed involvement in other cellular processes (such as pH sensing, membrane fusion, and enzyme transport) (FORGAC 2007). A thorough investigation of subunit a is critical because in many organisms, differential targeting of the V-ATPase is central to proper acidification of different organelle systems (TOEI *et al.* 2010). Mammals have four distinct isoforms of the V-ATPase including one that resides on the plasma membrane (OKA *et al.* 2001; TOYOMURA *et al.* 2003). This particular isoform has been implicated in a number of human diseases including cancer metastasis (FORGAC 2007). Understanding the mechanism(s) governing transport of the different isoforms of the V-ATPase will be critical in utilizing this enzyme as a pharmaceutical target.

However, subunit a presents a number of challenges that have impeded progress in evaluating its role in differential trafficking. For one, there is no high-resolution

crystal structure of subunit a (nor the V-ATPase in its entirety[2]). Secondly, the V-ATPase as a protein cargo is substantially more complex and larger in size and structure than other well characterized cargo proteins. Finally, horizontal evolutionary approaches (expressing V-ATPase subunits from one species into budding yeast) have not been successful for subunit a (unpublished data; AVIEZER-HAGAI *et al.* 2000); lineage-specific mutations and potential epistatic intramolecular interactions are not appreciated in this type of analysis. Even attempts to create chimeras between Vph1p and Stv1p have had very limited success (unpublished data, Bowers and Stevens). Thus, even different subunit a genes within the same species might also be constrained by isoform-specific changes that have evolved following gene duplication events.

Within budding yeast, Stv1p and Vph1p are proposed to have arisen from a gene duplication event within the fungal lineage (Figure 1, Chapter III). It is interesting to note that this does not include all fungal species; organisms such as *N. crassa* and *S. pombe* are basal to this duplication event and are proposed to have only a single isoform of subunit a (Figure 1, Chapter III). Understanding how to characterize the evolutionary history of Stv1p and Vph1p has been difficult with current molecular techniques. However, the use of ancestral reconstruction had the potential to provide a unique experimental system to study the evolution of Stv1p and Vph1p.

Given the results from Chapter III, it is likely that the ancestral isoform of budding yeast of subunit a functioned on both the Golgi/endosomal network and the vacuolar membrane. This seems to fit current observations that the V-ATPase in many organisms is found throughout the endo-membrane system and not exclusively on the

[2] There are crystal structures for individual subunits of the V-ATPase and several models that provide gross structural information of the yeast V-ATPase complex (ZHANG *et al.* 2008). This model is at 25 angstrom resolution.

vacuole (FORGAC 2007). Comparison of the localization of Anc.a to other organisms that have evolved with only a single isoform of the V-ATPase would provide support for these observations. However, work in *N. crassa* has shown that selectively marking the Golgi/endosome has been challenging (BOWMAN *et al.* 2009). While the V-ATPase complex is clearly found on vacuoles in *N. crassa*, it is unclear if it also localizes to the Golgi (although it clearly localizes to other vesicular structures that are not labeled by vacuolar markers).

To supplement our analysis of Anc.a, preliminary work was performed on the *N. crassa* subunit a isoform expressed in budding yeast. Surprisingly, the *N. crassa* isoform was able to provide a low level of complementation and localization data (unpublished results). While the majority of the *N. crassa* protein was present in the ER (indicative of a severe assembly defect), there was also fluorescent signal (for a GFP fusion protein) present on both the vacuole as well as punctate structures (unpublished results). Further study will be required to determine whether these puncta colocalize with Golgi and endosomal markers (like Anc.a) and whether these puncta will be transported to the vacuole upon treatment with cycloheximde. Creatures such as *N. crassa*, *S. pombe*, and *D. discoideum* are likely to localize the V-ATPase to not only the vacuole/lysosome, but other vesicular structures such as the Golgi and endosome. Work in the slime mold *D. discoideum* has shown that the V-ATPase localizes throughout the endo-membrane system (NOLTA *et al.* 1993; TEMESVARI *et al.* 1996; LIU and CLARKE 1996).

The proposed model of the evolution of Vph1p and Stv1p also proposes that a number of other regulatory elements have played a crucial role in the development of the current two-isoform system in budding yeast. It is interesting that the shift in Stv1p

localization had to be tightly coupled with changes in the (i) assembly and (ii) expression levels. Future work could investigate the evolution of the DNA regulatory regions driving Stv1p and Vph1p expression. While challenging, a similar process of ancestral reconstruction could be applied to these DNA regulatory elements. However, this type of approach would make the assumption that the extant transcriptional machinery would still recognize an ancient promoter sequence. However, if possible, this experiment would help confirm the evolutionary shift in *STV1* expression following the gene duplication event.

It has been speculated that Stv1p and Vph1p undergo differential assembly within the ER and that there is a connection between these two isoforms at the level of V_0 assembly (PERZOV *et al.* 2002; unpublished results). As mentioned in Chapter III, the observation that has prompted this model is that steady-state levels of Stv1p increase upon a loss of Vph1p. One possibility is that there is merely competition for assembly machinery within the ER and that Vph1p is more efficient at binding and sequestering factors such as Vma21p compared with Stv1p. It might be possible to assay levels of assembly factors that associate with either yeast subunit a isoform. However, one of the technical difficulties with such an approach has been the extremely low levels of Stv1p. Also, there is no current (promoter) system to drive Vph1p and Stv1p at identical expression levels. Therefore, the tight interplay between Vph1p and Stv1p levels might suggest a type of regulatory role of Vph1p in assembly of Stv1p (rather than competition).

A more thorough investigation of "intermediate" ancestors (see Figure 1, Chapter III) that exist along the Stv1p and/or Vph1p trajectories will provide a more complete

understanding of subunit a assembly, expression, and localization. It will be interesting to determine where along the Vph1p and Stv1p lineage did (i) the evolving Vph1p isoform stop localizing to the Golgi/endosome and when (ii) Stv1 became restricted to the Golgi/endosome. Further analysis could then characterize the sets of residues responsible for these gross phenotypic changes.

An analysis of the Stv1p sorting signal(s) that causes retention and/or retrieval within the Golgi/endosome network could also be possible using the Anc.a protein as a template to introduce potential targeting signals to determine if they are sufficient to cause a shift in localization of the V-ATPase. Given the complexity of the structure of subunit a (ZHANG *et al.* 2008), the sorting signal(s) within modern Stv1p may require the correct structural context in order to be fully recognized by the corresponding sorting machinery. The ancestral approach would help provide the more recent reconstructed subunit along the Stv1p trajectory that would allow for this gain of function experiment.

This work on Anc.a serves as a proof of principle for future reconstructions of other ancestral V-ATPase subunits including subunit a. Distinguishing between the different mammalian and human isoforms would greatly benefit from this type of evolutionary approach. Finally, coupling future biochemical studies of the V-ATPase complex (including a high-resolution structure of subunit a as part of the assembled enzyme) will greatly assist in translating information from sets of residues responsible for assembly, trafficking, or enzyme function to specific mechanisms that depict binding surfaces and protein-protein interactions.

3. *The evolution of complexity*

The work presented in Chapter III describes the subfunctionalization of the two fungal subunit a isoforms. While these reconstructed ancestral proteins still assembled and functioned with the other thirteen subunits of the V-ATPase, only a single isoform of the stator is incorporated into each complex. These findings describe the separate evolution of the two V-ATPase complexes. As previously described, there may be an intricate level of regulation and genetic interactions between the Stv1p and Vph1p-containing complexes. However, it is unknown whether the subunit isoforms directly interact.

Within the V-ATPase complex, a number of additional subunits also show some degree of homology (such as the V_1 subunits A and B). We chose one of the most challenging and intriguing portions of the V-ATPase complex, the proteolipid ring for further evolutionary study. This basic unit of ATPase function remains highly conserved across the tree of life; V, A, and F-type ATPase enzymes all contain an analogous structure that serves to translocate protons (either up or down an electrochemical gradient) (GRÜBER *et al* 2001). However, the size and composition of the ring has shifted dramatically within specific domains of life.

While the F-type ATP synthase complex has twelve identical subunits (each with two transmembrane passes) that make up the ring, other rings differ in both the size of the individual subunits (ie, number of transmembrane domains randing from two up to six) and the number of separate subunits that are incorporated into the ring (GRÜBER *et al* 2001). Some explanations for the diverse architectural shifts in ring membership include (i) regulation of the coupling efficiency and (ii) reversible proton flow (or its prevention

in the case of the V-ATPase ring) (ZHANG *et al.* 1992; GRABE *et al.* 2000; KAWASAKI-NISHI *et al.* 2001b; SAROUSSI and NELSON 2009). While these factors might be subject to selection, they are not sufficient to explain ring composition in several different scenarios. Comparison of the V-ATPase ring between the fungal and animal lineages is one example.

Therefore, we chose to use the proteolipid ring as a model system to test the hypothesis that increasing (protein) complexity can arise through neutral processes following gene duplication. It is important to note that this type of ancestral reconstruction is challenging for several reasons. While the ancestral subunit(s) have to also function in the context of the extant V-ATPase components, they also have to maintain ring integrity and function. As demonstrated in Chapter IV, the ancestral c-c' subunit has to compensate for a loss of two different yeast ring subunits.

The findings that the ancestral c-c' functioned within the extant V-ATPase are very surprising. The ring interacts with a number of other V_0 subunits as well as the primary assembly factors in yeast. The Anc.c-c' protein did not result in a large amount of functional complementation yet we were able to leverage this to perform our evolutionary analysis of the ring. Subsequent ancestral reconstructions of the "intermediate" c and c' ancestors along the subunit lineages provided critical information about (i) the relative timing[3] by which subfunctionalization of the two fungal subunits took place and (ii) the set of residues responsible for this molecular shift.

The work presented in Chapter IV leads us to propose a model by which the neutral inclusion of an additional subunit (ie, an increase in protein complexity) can occur

[3] The term "timing" here is not based on a temporal analysis, but rather to comment on the fact that these changes occurred basal to all fungal species that were sampled and would therefore be predicted to account for ring evolution within this entire clade.

through degenerataion of subunit-subunit interfaces. This applies to a unique scenario where all parts of this system (the proteolipid ring) are required for full enzymatic activity. Thus, the shift in ring architecture occurred while maintaining V-ATPase function. This work is significant because it presents a model of molecular evolution that might be present within other biochemical systems. There is an overwhelming amount of data supporting the notion that biological systems have increased in complexity through evolutionary time (ADAMI *et al.* 2000). Prior work has described how proteins can (i) acquire new functions following gene duplication events or (ii) partition the ancestral function of a protein into two (or more) new proteins (INNAN and KONDRASHOV 2010).

However, proteins that are part of multisubunit complexes present additional challenges; these peptides are often restricted in their ability to acquire new function(s) because their original role in the enzyme function and/or structure of the complex to which they belong to must be maintained. Clearly, complexes that have numerous subunits have evolved new subunits with new functions (WOLLENBERG and SWAFFIELD 2001; GABALDÓN *et al.* 2005). However, for some enzyme domains such as the V-ATPase proteolipid ring, it is unclear whether the difference in subunit number or composition causes a significant increase in enzyme function and therefore organism fitness.

The idea that complexity (in the context of a large, multisubunit protein complex) can also evolve via neutral processes is an interesting model for several reasons (ARCHIBALD *et al.* 1999; RUANO-RUBIO *et al.* 2007). Firstly, increasing the complexity of a protein complex also increases the amount of energy input required to

assemble and/or regulate the incorporation of the new subunit(s). The opportunity for mistakes in expressing and assembling more protein components also increases. It is also possible that additional factors will need to be recruited to aid in the more complex assembly process.

The model we describe in Chapter IV supports the idea that additional subunits might have been included within the proteolipid ring through asymmetric degeneration of the subunit interfaces and that the V_0 became "ratcheted" into this new conformation. We show that once the two new subunits c and c' have begun to acquire their "c-like" and "c'-like" identities (in terms of their structural interfaces within the ring), they are unable to substitute for the c' and c position, respectively. The ring has increased in subunit number by locking the new subunits into a specific position and they are unable to reverse this structural specificity. Others have shown that evolution is directional; mutational changes that have given rise to a new enzymatic function only work when introduced in a unidirectional fashion (BRIDGHAM *et al.* 2009).

Finally, our results provide an interesting tangent to V_0 assembly (see Chapter II) and the co-evolution of the V-ATPase and its supporting factors. One explanation for the large number of dedicated V_0 assembly factors in budding yeast is that there are three proteolipid subunits present within the ring rather than two. A ring that is composed of only two subunits will only have a single structural conformation (assuming that one subunit, in this case, c", is restricted to one copy per complex) (see Figure 10, Chapter IV). A ring that has three subunits (assuming two of the subunits are restricted to one per complex and the third is present at multiple copies as in the case of the yeast ring) has many different structural conformations possible. While our results suggest that the

inclusion of the third subunit occurred through degeneration of subunit interfaces, this does not explain the placement of the c' subunit adjacent to the c" subunit and why the c' subunit evolved to only be present at a single copy within the ring.

One area of study that might address these questions includes the interplay with dedicated assembly factors. Recent unpublished work suggests that yeast Vma21p associates with subunit c' in yeast and does not interface with subunit c very strongly. Also, Voa1p associates with subunit c (unpublished results, Ryan and Stevens). Since humans (and metazoans) only contain a c subunit (and lack c'), it is likely that human Vma21p interfaces with the c subunit. While the role of Vma21p as an assembly factor has not changed, its association with the proteolipid ring has undergone a dramatic structural shift given the change in ring composition. Future experiments should determine whether Vma21p is found in multiple copies per complex. The current model suggests that yeast Vma21p binds to yeast c'. Compared to the mammalian ring, it is possible that Vma21p in these species associates with the numerous copies of c. Future experiments on expressing both the human proteolipid ring (subunit c) as well as the human Vma21p in yeast cells lacking c and c' will add to this model. Since Voa1p is not conserved at all outside of budding yeasts (unpublished results), it is possible that *S. cerevisiae* has recruited a new factor to assist in V_0 assembly in this species. However, it is unknown how other fungi (that also have three proteolipid subunits) have responded to the addition of a new subunit.

The sets of residues identified within Chapter IV that are responsible for c or c' "identity" will require future investigation to determine the precise molecular contacts that are necessary for these interactions. Others (such as J. W. Thornton and colleagues)

have been working on a similar type of question that involves sorting through groups of residues to describe their order and function through evolutionary time to bring about a mechanistic shift in enzyme function. This type of analysis is extremely powerful yet challenging for several reasons. While our work has reduced the set of residues to approximately 25-30 total residues (out of a protein containing 160 residues), there are many, many combinations of how these sets of residues could have evolved. Unfortunately, our phylogeny will require additional species that are more basal than the intermediate nodes yet occurred after the c-c' duplication event to separate these groupings into smaller sets.

Additionally, modeling of these residues within the predicted structure of the proteolipids might allow for a rudimentary classification of residues based on their approximate positioning within the membrane-bound portion of the ring. Sites on lumenal or cytosolic faces of the membrane might help to eliminate residues that are unlikely to interface with adjacent subunits (although little has been described for how the cytosolic and/or lumenal portions of the proteolipids are required for function). Since the lumenal portions face away from the V-ATPase complex there is far less sequence conservation across species. Cytosolic regions of the proteolipids are highly conserved (and restricted in the lengths connecting adjacent transmembrane domains) and may interface with (i) other ring subunits, (ii) the N or C-terminal portion of subunit a, (iii) subunit d, and/or (iv) other V_1 subunits.

Ultimately, a future goal for this work would be to be able to describe the precise molecular events that took place after the duplication of c-c' into c and c' and which residues are responsible for shifting the subunit interactions to accommodate the new ring

member. Additional ancestral reconstructions of the V-ATPase subunits (and perhaps a full reconstruction of the entire V-ATPase enzyme) and its assembly factors will help provide a complete evolutionary history and allow for a more rigorous molecular analysis of this critical molecular machine.

APPENDIX A

SUPPLEMENTAL INFORMATION FOR CHAPTER II

Table S1. Genes identified by genome-wide SGA screens for V-ATPase effectors. The standard gene name and systematic names of all the genes identified from the 3 SGA enhancer screens are listed. X's indicate which of the three different SGA screens genes were identified from. The three different query strains used are labeled above each column. These data include scoring of double mutants on media containing either Ca^{2+} or Zn^{2+}.

Gene	ORF	*vma21QQ::Nat^R*	*vma21QQ voa1::Hyg^R*	*vma21QQ voa1Δ::Nat^R*
AAT2	YLR027C	X		X
ACO1	YLR304C	X		
ACO2	YJL200C	X		
ADA2	YDR448W	X		
ADI1	YMR009W		X	
ADO1	YJR105W			X
AGE2	YIL044C		X	
AIM14	YGL160W			X
ALG6	YOR002W	X		X
ALG8	YOR067C	X		X
ANP1	YEL036C	X		
APE3	YBR286W			X
API2	YDR525W		X	
APL5	YPL195W	X	X	
APL6	YGR261C		X	X
APM1	YPL259C		X	
APM3	YBR288C	X	X	
APS3	YJL024C	X	X	
ARF1	YDL192W		X	
ARG2	YJL071W		X	
ARG82	YDR173C	X		
ARL1	YBR164C	X	X	X
ARL3	YPL051W		X	X
ARO1	YDR127W	X	X	
ARO2	YGL148W	X	X	X
ARO7	YPR060C	X	X	X
ARP6	YLR085C		X	X
ARR4	YDL100C		X	
ASC1	YMR116C		X	X
ASF1	YJL115W		X	
ATG15	YCR068W			X
ATG21	YPL100W			X
ATG27	YJL178C		X	

Table S1. (continued).

Gene	ORF	*vma21QQ::Nat^R*	*vma21QQ voa1::Hyg^R*	*vma21QQ voa1Δ::Nat^R*
ATG8	YBL078C		X	
ATS1	YAL020C		X	X
AVT7	YIL088C		X	
BAP2	YBR068C		X	
BCK1	YJL095W			X
BCK2	YER167W	X	X	X
BDF1	YLR399C			X
BEM1	YBR200W	X		
BEM2	YER155C	X	X	X
BEM4	YPL161C	X	X	X
BMH1	YER177W		X	
BRE1	YDL074C	X	X	X
BRE2	YLR015W		X	
BSD2	YBR290W		X	X
BST1	YFL025C		X	
BTS1	YPL069C	X		
BUD14	YAR014C		X	
BUD30	YDL151C	X		
CAJ1	YER048C		X	
CAT5	YOR125C			X
CBF1	YJR060W	X	X	X
CCC2	YDR270W		X	
CCR4	YAL021C	X		X
CCW12	YLR110C		X	
CCZ1	YBR131W	X	X	
CDC50	YCR094W	X		
CEX1	YOR112W		X	
CHD1	YER164W			X
CHS5	YLR330W		X	X
CHS6	YJL099W			X
CKA1	YIL035C		X	
CKB1	YGL019W	X	X	X
CKB2	YOR039W	X	X	X
CLA4	YNL298W		X	X
CNB1	YKL190W			X
CNE1	YAL058W		X	
COG5	YNL051W		X	X
COG6	YNL041C		X	
COG7	YGL005C		X	X
COG8	YML071C		X	X
COY1	YKL179C		X	
CPR2	YHR057C			X

Table S1. (continued).

Gene	ORF	*vma21QQ::Nat^R*	*vma21QQ voa1::Hyg^R*	*vma21QQ voa1Δ::Nat^R*
CPR7	YJR032W		X	
CRZ1	YNL027W	X	X	X
CSF1	YLR087C	X	X	X
CSG2	YBR036C	X	X	X
CTF18	YMR078C		X	
CTF4	YPR135W			X
CTK1	YKL139W	X	X	X
CUE1	YMR264W		X	
CWH41	YGL027C		X	
CYK3	YDL117W		X	
CYS3	YAL012W	X		
DAL81	YIR023W			X
DBF2	YGR092W		X	
DBP7	YKR024C	X		X
DFG16	YOR030W			X
DFG5	YMR238W	X		
DIA2	YOR080W		X	
DLT1	YMR126C	X	X	X
DOA1	YKL213C		X	
DOM34	YNL001W		X	
DPH1	YIL103W		X	
DPH2	YKL191W		X	
DPH5	YLR172C		X	
DRS2	YAL026C	X	X	X
DST1	YGL043W		X	
DUF1	YOL087C			X
EAF3	YPR023C			X
EAF7	YNL136W			X
ECM38	YLR299W		X	
ECM40	YMR062C			X
EFT2	YDR385W		X	
ELF1	YKL160W			X
ELM1	YKL048C		X	X
ELP2	YGR200C		X	
ELP3	YPL086C		X	
ELP4	YPL101W		X	
ELP6	YMR312W		X	X
EMC1	YCL045C		X	
ERD1	YDR414C			X
ERG3	YLR056W	X	X	X
ERG6	YML008C	X	X	X
ERP3	YDL018C	X		

Table S1. (continued).

Gene	ORF	*vma21QQ::Nat^R*	*vma21QQ voa1::Hyg^R*	*vma21QQ voa1Δ::Nat^R*
ERV46	YAL042W		X	
FET3	YMR058W	X	X	
FET4	YMR319C			X
FIG4	YNL325C		X	
FKS1	YLR342W		X	
FLC2	YAL053W	X		
FMC1	YIL098C			X
FMP21	YBR269C			X
FPS1	YLL043W			X
FRA1	YLL029W			X
FRT1	YOR324C			X
FTR1	YER145C		X	
FUI1	YBL042C		X	
FUM1	YPL262W	X		
FYV10	YIL097W			X
GAL11	YOL051W			X
GAS1	YMR307W		X	
GCN1	YGL195W		X	
GCR2	YNL199C		X	
GCS1	YDL226C		X	
GEF1	YJR040W		X	
GET1	YGL020C	X	X	
GET2	YER083C	X	X	X
GIM4	YEL003W	X		
GIS4	YML006C		X	
GLY1	YEL046C	X		
GOS1	YHL031C	X	X	
GPA2	YER020W		X	
GSF2	YML048W			X
GSG1	YDR108W	X	X	X
GSH1	YJL101C	X	X	
GSH2	YOL049W		X	
GUP1	YGL084C		X	X
GVP36	YIL041W		X	
GYP1	YOR070C	X	X	X
HAC1	YFL031W	X		
HAL5	YJL165C		X	X
HCR1	YLR192C	X	X	
HEX3	YDL013W		X	
HGH1	YGR187C		X	
HMT1	YBR034C		X	
HOC1	YJR075W	X		

Table S1. (continued).

Gene	ORF	*vma21QQ::Nat^R*	*vma21QQ voa1::Hyg^R*	*vma21QQ voa1Δ::Nat^R*
HSC82	YMR186W		X	
HTZ1	YOL012C		X	X
ICE2	YIL090W	X	X	
IDH2	YOR136W	X	X	
IKI3	YLR384C		X	
ILM1	YJR118C		X	
ILV1	YER086W			X
IMG2	YCR071C	X		
INO2	YDR123C		X	
INP53	YOR109W		X	
IOC2	YLR095C		X	
IRA2	YOL081W	X		
IRC13	YOR235W		X	
IRC14	YOR135C	X	X	
IRC21	YMR073C			X
IRC25	YLR021W		X	
ISW1	YBR245C		X	
JJJ3	YJR097W		X	
KAR3	YPR141C		X	
KCS1	YDR017C	X		
KEM1	YGL173C	X	X	X
KES1	YPL145C		X	
KEX1	YGL203C			X
KEX2	YNL238W	X	X	
KRE1	YNL322C			X
KRE28	YDR532C	X	X	
KTI12	YKL110C		X	
LCL1	YPL056C	X		
LEO1	YOR123C		X	X
LGE1	YPL055C	X	X	X
LIP2	YLR239C	X	X	
LIP5	YOR196C	X		
LPD1	YFL018C			X
LSB3	YFR024C-A		X	
LSM1	YJL124C	X	X	
LSM6	YDR378C	X		
LST4	YKL176C		X	
LYS14	YDR034C	X	X	X
MAC1	YMR021C	X	X	
MAF1	YDR005C		X	
MBF1	YOR298C-A		X	
MCK1	YNL307C			X

Table S1. (continued).

Gene	ORF	*vma21QQ::Nat^R*	*vma21QQ voa1::Hyg^R*	*vma21QQ voa1Δ::Nat^R*
MDM10	YAL010C		X	
MDM20	YOL076W			X
MDM34	YGL219C			X
MDY2	YOL111C	X		
MET18	YIL128W		X	
MET22	YOL064C		X	
MGA2	YIR033W		X	
MGM101	YJR144W			X
MKS1	YNL076W		X	X
MMS1	YPR164W		X	
MMS22	YLR320W		X	
MNN10	YDR245W	X	X	
MNN2	YBR015C		X	
MOG1	YJR074W		X	
MON1	YGL124C	X	X	X
MPD2	YOL088C	X		
MRC1	YCL061C		X	
MRPL35	YDR322W			X
MSC1	YML128C		X	
MSN5	YDR335W	X	X	X
MTC2	YKL098W	X	X	X
MTC4	YBR255W		X	X
MTC6	YHR151C		X	
NAM7	YMR080C			X
NBP2	YDR162C	X	X	X
NCS2	YNL119W		X	
NCS6	YGL211W		X	
NHX1	YDR456W	X		
NMD2	YHR077C		X	
NPL3	YDR432W			X
NPT1	YOR209C			X
NST1	YNL091W		X	
NUP133	YKR082W		X	
OCA5	YHL029C		X	
OCT1	YKL134C			X
OPI1	YHL020C		X	X
OPI8	YKR035C	X	X	X
ORM2	YLR350W	X	X	X
OST3	YOR085W	X	X	
OST4	YDL232W		X	X
PAR32	YDL173W			X
PBS2	YJL128C			X

Table S1. (continued).

Gene	ORF	*vma21QQ::Nat^R*	*vma21QQ voa1::Hyg^R*	*vma21QQ voa1Δ::Nat^R*
PCL6	YER059W			X
PCT1	YGR202C			X
PDA1	YER178W		X	
PDB1	YBR221C	X		
PER1	YCR044C		X	X
PET191	YJR034W			X
PEX31	YGR004W	X		X
PFK1	YGR240C			X
PGD1	YGL025C			X
PHO2	YDL106C		X	
PHO4	YFR034C	X	X	X
PHO80	YOL001W	X	X	X
PHO81	YGR233C	X	X	
PHO85	YPL031C	X		X
PHO86	YJL117W	X	X	X
PIL1	YGR086C			X
PIN4	YBL051C		X	
PKR1	YMR123W		X	
PMC1	YGL006W	X	X	X
PMP3	YDR276C		X	
POC4	YPL144W		X	
POP2	YNR052C	X		X
PPM1	YDR435C			X
PPR1	YLR014C		X	
PSD2	YGR170W		X	
PSP2	YML017W		X	
PTK2	YJR059W			X
QRI8	YMR022W		X	
RAV1	YJR033C		X	X
RAV2	YDR202C	X	X	X
RBG2	YGR173W			X
RCY1	YJL204C		X	
RIF1	YBR275C		X	
RIM101	YHL027W		X	X
RIM20	YOR275C		X	X
RIM21	YNL294C		X	
RIM8	YGL045W		X	X
RIM9	YMR063W		X	X
RKR1	YMR247C		X	
RMD8	YFR048W		X	
RNR4	YGR180C			X
ROT2	YBR229C		X	

Table S1. (continued).

Gene	ORF	*vma21QQ::Nat^R*	*vma21QQ voa1::Hyg^R*	*vma21QQ voa1Δ::Nat^R*
RPA34	YJL148W		X	
RPL13A	YDL082W		X	
RPL13B	YMR142C			X
RPL17B	YJL177W			X
RPL22B	YFL035C-B			X
RPL29	YFR032C-A		X	
RPL2A	YFR031C-A		X	
RPL41B	YDL133C-A		X	
RPL9A	YGL147C		X	
RPN4	YDL020C		X	
RPO41	YFL036W		X	
RPP1A	YDL081C	X		
RPS11A	YDR025W			X
RPS11B	YBR048W		X	
RPS16B	YDL083C		X	
RPS19A	YOL121C			X
RPS21B	YJL136C	X	X	X
RPS24A	YER074W			X
RPS27B	YHR021C		X	
RPS28B	YLR264W		X	
RPS29B	YDL061C		X	
RPS4A	YJR145C	X		
RPS4B	YHR203C		X	
RPS6B	YBR181C		X	
RRF1	YHR038W			X
RRT2	YBR246W		X	
RSM28	YDR494W			X
RTG1	YOL067C		X	X
RTG2	YGL252C	X	X	X
RTG3	YBL103C		X	X
RTS1	YOR014W	X	X	X
RTT103	YDR289C		X	X
RTT109	YLL002W		X	
RUD3	YOR216C		X	
RVS161	YCR009C		X	
SAC1	YKL212W		X	X
SAC3	YDR159W		X	X
SAC7	YDR389W	X	X	X
SAP155	YFR040W		X	X
SAT4	YCR008W		X	
SBP1	YHL034C		X	
SCJ1	YMR214W		X	

Table S1. (continued).

Gene	ORF	*vma21QQ::Nat^R*	*vma21QQ voa1::Hyg^R*	*vma21QQ voa1Δ::Nat^R*
SCS2	YER120W		X	
SCW10	YMR305C			X
SDC1	YDR469W	X		
SEC22	YLR268W	X	X	
SEC28	YIL076W		X	
SEC66	YBR171W	X	X	X
SER2	YGR208W	X	X	
SET2	YJL168C		X	X
SHE1	YBL031W		X	
SHE4	YOR035C		X	X
SHP1	YBL058W			X
SIM1	YIL123W		X	
SIN4	YNL236W		X	
SIS2	YKR072C	X	X	X
SIT1	YEL065W		X	
SKG1	YKR100C		X	
SKN7	YHR206W		X	X
SLA1	YBL007C			X
SMF1	YOL122C			X
SMF3	YLR034C			X
SMI1	YGR229C	X	X	
SMP2	YMR165C	X	X	
SNA2	YDR525W-A		X	
SNF1	YDR477W		X	
SNF11	YDR073W			X
SNF2	YOR290C	X		X
SNF4	YGL115W			X
SNF5	YBR289W	X		
SNF6	YHL025W		X	
SNX4	YJL036W			X
SOD2	YHR008C			X
SOH1	YGL127C		X	
SOK2	YMR016C	X		
SOY1	YBR194W	X		
SPE1	YKL184W		X	
SPE3	YPR069C		X	
SPF1	YEL031W		X	X
SPT3	YDR392W		X	
SPT4	YGR063C			X
SQS1	YNL224C		X	
SRB2	YHR041C		X	X
SRB8	YCR081W		X	

Table S1. (continued).

Gene	ORF	*vma21QQ::Nat^R*	*vma21QQ voa1::Hyg^R*	*vma21QQ voa1Δ::Nat^R*
SRN2	YLR119W			X
SRO7	YPR032W		X	
SSE1	YPL106C		X	
STO1	YMR125W			X
STP1	YDR463W	X		X
STV1	YMR054W	X		
SUR1	YPL057C		X	X
SUR4	YLR372W			X
SWC3	YAL011W		X	
SWC5	YBR231C		X	X
SWD1	YAR003W	X		
SWD3	YBR175W	X		
SWF1	YDR126W		X	X
SWI4	YER111C	X	X	X
SWI6	YLR182W			X
SWP82	YFL049W			X
SWR1	YDR334W		X	
SYS1	YJL004C	X	X	X
TAE1	YBR261C		X	
TCO89	YPL180W			X
TDA4	YJR116W			X
TEF4	YKL081W		X	X
THR1	YHR025W	X	X	X
THR4	YCR053W	X	X	X
TLG2	YOL018C	X		
TMA17	YDL110C		X	
TMA23	YMR269W		X	
TOP1	YOL006C		X	
TOS2	YGR221C		X	
TOS9	YEL007W			X
TPD3	YAL016W	X		
TPM1	YNL079C		X	
TPS1	YBR126C		X	X
TRK1	YJL129C			X
TRP1	YDR007W		X	
TRP2	YER090W		X	
TRP4	YDR354W		X	
TSR2	YLR435W		X	
TUF1	YOR187W	X		
UBA3	YPR066W	X		
UBA4	YHR111W		X	
UBP13	YBL067C	X	X	

Table S1. (continued).

Gene	ORF	*vma21QQ::Nat^R*	*vma21QQ voa1::Hyg^R*	*vma21QQ voa1Δ::Nat^R*
UBP14	YBR058C		X	
UBP15	YMR304W	X	X	
UBP3	YER151C			X
UBP6	YFR010W		X	
UBX4	YMR067C		X	
UFD2	YDL190C		X	
UME6	YDR207C	X	X	X
UPF3	YGR072W		X	
URA4	YLR420W			X
URE2	YNL229C		X	
URM1	YIL008W		X	
VAC14	YLR386W		X	X
VAC8	YEL013W	X	X	X
VAM10	YOR068C	X	X	X
VAM6	YDL077C	X	X	
VAM7	YGL212W		X	
VHS2	YIL135C			X
VID21	YDR359C		X	
VID22	YLR373C		X	
VPH1	YOR270C	X	X	X
VPS1	YKR001C	X		
VPS13	YLL040C		X	
VPS17	YOR132W	X	X	
VPS19	YDR323C	X		
VPS2	YKL002W	X		
VPS21	YOR089C		X	X
VPS22	YPL002C	X		
VPS23	YCL008C	X		
VPS24	YKL041W	X	X	X
VPS25	YJR102C	X		
VPS26	YJL053W	X	X	X
VPS27	YNR006W	X	X	
VPS29	YHR012W	X	X	X
VPS3	YDR495C	X		
VPS33	YLR396C	X		X
VPS35	YJL154C	X	X	X
VPS36	YLR417W	X		
VPS4	YPR173C	X	X	X
VPS41	YDR080W		X	
VPS46	YKR035W-A	X	X	X
VPS5	YOR069W	X	X	X
VPS52	YDR484W	X		

Table S1. (continued).

Gene	ORF	*vma21QQ::Nat^R*	*vma21QQ voa1::Hyg^R*	*vma21QQ voa1Δ::Nat^R*
VPS53	YJL029C	X		
VPS55	YJR044C		X	X
VPS6	YOR036W	X		
VPS60	YDR486C		X	X
VPS62	YGR141W		X	
VPS71	YML041C			X
VPS72	YDR485C			X
VPS73	YGL104C		X	
VPS9	YML097C		X	
VTA1	YLR181C		X	X
VTC1	YER072W	X	X	X
VTC4	YJL012C	X	X	X
VTS1	YOR359W		X	X
XRS2	YDR369C		X	
YAK1	YJL141C			X
YAL058C-A	YAL058C-A		X	
YAP1801	YHR161C		X	
YAR029W	YAR029W		X	
YBL071C	YBL071C			X
YBL094C	YBL094C	X		
YBR174C	YBR174C	X		
YBR226C	YBR226C		X	
YBR284W	YBR284W			X
YCK3	YER123W	X	X	X
YCL046W	YCL046W		X	
YCR007C	YCR007C		X	
YCR061W	YCR061W			X
YDJ1	YNL064C		X	
YDL172C	YDL172C			X
YDL218W	YDL218W	X		
YDR048C	YDR048C		X	
YDR049W	YDR049W		X	
YDR089W	YDR089W	X		
YDR203W	YDR203W	X		X
YDR269C	YDR269C		X	
YDR271C	YDR271C	X	X	
YDR336W	YDR336W	X		
YDR433W	YDR433W			X
YDR455C	YDR455C	X	X	
YDR537C	YDR537C			X
YEH1	YLL012W			X
YEL045C	YEL045C	X		

Table S1. (continued).

Gene	ORF	*vma21QQ::Nat^R*	*vma21QQ voa1::Hyg^R*	*vma21QQ voa1Δ::Nat^R*
YER119C-A	YER119C-A		X	
YER156C	YER156C	X		
YFR024C	YFR024C		X	
YGL024W	YGL024W		X	X
YGL218W	YGL218W		X	X
YGR064W	YGR064W			X
YGR122W	YGR122W		X	
YGR237C	YGR237C		X	
YJL169W	YJL169W		X	X
YJL175W	YJL175W		X	X
YJR087W	YJR087W			X
YKE2	YLR200W	X		
YKG9	YKL069W		X	
YKL023W	YKL023W			X
YKL061W	YKL061W			X
YKL118W	YKL118W			X
YKR051W	YKR051W			X
YLR111W	YLR111W		X	
YLR143W	YLR143W		X	
YLR402W	YLR402W		X	
YML013C-A	YML013C-A		X	
YML020W	YML020W	X		
YND1	YER005W			X
YNL120C	YNL120C		X	X
YNL140C	YNL140C			X
YNL171C	YNL171C		X	
YNL198C	YNL198C		X	
YNL228W	YNL228W		X	
YNL296W	YNL296W		X	
YNR005C	YNR005C			X
YOL050C	YOL050C			X
YOR300W	YOR300W			X
YPL102C	YPL102C		X	
YPL168W	YPL168W			X
YPL205C	YPL205C	X		
YPR090W	YPR090W		X	
YPR123C	YPR123C	X	X	
YPR153W	YPR153W	X	X	X
YPT7	YML001W	X	X	X
YTA7	YGR270W		X	X
YUR1	YJL139C		X	
ZRC1	YMR243C		X	X

Table S1. (continued).

Gene	ORF	*vma21QQ::Nat^R*	*vma21QQ voa1::Hyg^R*	*vma21QQ voa1Δ::Nat^R*
ZUO1	YGR285C			X

Table S2. Gene Ontology (GO) analysis was performed using the Saccharomyces Genome Database (SGD) "Gene Ontology Term Finder" (v. 0.83). Of the 538 genes identified from our three SGA screens, 492 were included within the GO analysis (overlapping ORFs were excluded). The GO term ID# and GO categories are listed. The cluster and background frequency are shown for each GO term and hits with p-values of less than 0.01 were included. Results are listed beginning with GO categories with the lowest p-values.

GO ID#	GO Term	Cluster frequency	Background frequency	P-value
7034	vacuolar transport	47 out of 492 genes, 9.6%	124 out of 5797 background genes, 2.1%	4.94E-17
7034	vacuolar transport	47 out of 492 genes, 9.6%	124 out of 5797 background genes, 2.1%	4.94E-17
9987	cellular process	443 out of 492 genes, 90.0%	4336 out of 5797 background genes, 74.8%	2.56E-16
16192	vesicle-mediated transport	82 out of 492 genes, 16.7%	357 out of 5797 background genes, 6.2%	3.48E-15
65007	biological regulation	174 out of 492 genes, 35.4%	1199 out of 5797 background genes, 20.7%	1.56E-12
46907	intracellular transport	101 out of 492 genes, 20.5%	596 out of 5797 background genes, 10.3%	9.46E-10
65008	regulation of biological quality	75 out of 492 genes, 15.2%	389 out of 5797 background genes, 6.7%	2.28E-09
51649	establishment of localization in cell	105 out of 492 genes, 21.3%	648 out of 5797 background genes, 11.2%	5.71E-09
48193	Golgi vesicle transport	45 out of 492 genes, 9.1%	181 out of 5797 background genes, 3.1%	1.49E-08
51641	cellular localization	114 out of 492 genes, 23.2%	747 out of 5797 background genes, 12.9%	3.20E-08

Table S2. (continued).

GO ID#	GO Term	Cluster frequency	Background frequency	P-value
6623	protein targeting to vacuole	26 out of 492 genes, 5.3%	71 out of 5797 background genes, 1.2%	3.57E-08
6355	regulation of transcription, DNA-dependent	74 out of 492 genes, 15.0%	406 out of 5797 background genes, 7.0%	5.71E-08
6892	post-Golgi vesicle-mediated transport	25 out of 492 genes, 5.1%	70 out of 5797 background genes, 1.2%	1.61E-07
45449	regulation of transcription	76 out of 492 genes, 15.4%	433 out of 5797 background genes, 7.5%	1.99E-07
51252	regulation of RNA metabolic process	74 out of 492 genes, 15.0%	419 out of 5797 genes, 7.2%	2.67E-07
31326	regulation of cellular biosynthetic process	89 out of 492 genes, 18.1%	549 out of 5797 background genes, 9.5%	3.46E-07
9889	regulation of biosynthetic process	89 out of 492 genes, 18.1%	551 out of 5797 background genes, 9.5%	4.21E-07
10468	regulation of gene expression	85 out of 492 genes, 17.3%	518 out of 5797 background genes, 8.9%	5.04E-07
44249	cellular biosynthetic process	201 out of 492 genes, 40.9%	1666 out of 5797 background genes, 28.7%	9.93E-07
16197	endosome transport	23 out of 492 genes, 4.7%	65 out of 5797 background genes, 1.1%	1.10E-06
51179	localization	152 out of 492 genes, 30.9%	1162 out of 5797 background genes, 20.0%	1.35E-06
10556	regulation of macromolecule biosynthetic process	85 out of 492 genes, 17.3%	530 out of 5797 background genes, 9.1%	1.64E-06
2000112	regulation of cellular macromolecule biosynthetic process	85 out of 492 genes, 17.3%	530 out of 5797 background genes, 9.1%	1.64E-06
9058	biosynthetic process	202 out of 492 genes, 41.1%	1690 out of 5797 genes, 29.2%	2.09E-06

Table S2. (continued).

GO ID#	GO Term	Cluster frequency	Background frequency	P-value
19538	protein metabolic process	153 out of 492 genes, 31.1%	1180 out of 5797 background genes, 20.4%	2.26E-06
51234	establishment of localization	140 out of 492 genes, 28.5%	1057 out of 5797 background genes, 18.2%	3.62E-06
6810	transport	137 out of 492 genes, 27.8%	1030 out of 5797 background genes, 17.8%	4.35E-06
70727	cellular macromolecule localization	61 out of 492 genes, 12.4%	340 out of 5797 background genes, 5.9%	6.64E-06
19219	regulation of nucleobase, nucleoside, nucleotide and nucleic acid metabolic process	80 out of 492 genes, 16.3%	502 out of 5797 background genes, 8.7%	7.43E-06
51171	regulation of nitrogen compound metabolic process	80 out of 492 genes, 16.3%	504 out of 5797 background genes, 8.7%	8.97E-06
8104	protein localization	66 out of 492 genes, 13.4%	384 out of 5797 background genes, 6.6%	9.07E-06
45053	protein retention in Golgi apparatus	9 out of 492 genes, 1.8%	11 out of 5797 background genes, 0.2%	1.05E-05
60255	regulation of macromolecule metabolic process	89 out of 492 genes, 18.1%	588 out of 5797 background genes, 10.1%	1.24E-05
6351	transcription, DNA-dependent	87 out of 492 genes, 17.7%	571 out of 5797 background genes, 9.8%	1.36E-05
32774	RNA biosynthetic process	87 out of 492 genes, 17.7%	573 out of 5797 background genes, 9.9%	1.62E-05
34613	cellular protein localization	58 out of 492 genes, 11.8%	324 out of 5797 background genes, 5.6%	1.78E-05
31323	regulation of cellular metabolic process	95 out of 492 genes, 19.3%	648 out of 5797 background genes, 11.2%	1.91E-05

Table S2. (continued).

GO ID#	GO Term	Cluster frequency	Background frequency	P-value
19222	regulation of metabolic process	98 out of 492 genes, 19.9%	677 out of 5797 background genes, 11.7%	2.10E-05
80090	regulation of primary metabolic process	92 out of 492 genes, 18.7%	622 out of 5797 background genes, 10.7%	2.17E-05
6350	transcription	90 out of 492 genes, 18.3%	607 out of 5797 background genes, 10.5%	2.85E-05
34067	protein localization in Golgi apparatus	9 out of 492 genes, 1.8%	12 out of 5797 background genes, 0.2%	3.91E-05
6896	Golgi to vacuole transport	13 out of 492 genes, 2.6%	26 out of 5797 background genes, 0.4%	3.94E-05
44267	cellular protein metabolic process	144 out of 492 genes, 29.3%	1136 out of 5797 background genes, 19.6%	4.17E-05
33036	macromolecule localization	77 out of 492 genes, 15.7%	499 out of 5797 background genes, 8.6%	6.36E-05
55082	cellular chemical homeostasis	30 out of 492 genes, 6.1%	123 out of 5797 background genes, 2.1%	6.94E-05
6873	cellular ion homeostasis	30 out of 492 genes, 6.1%	123 out of 5797 background genes, 2.1%	6.94E-05
7033	vacuole organization	20 out of 492 genes, 4.1%	62 out of 5797 background genes, 1.1%	8.36E-05
34645	cellular macromolecule biosynthetic process	152 out of 492 genes, 30.9%	1231 out of 5797 background genes, 21.2%	8.90E-05
9059	macromolecule biosynthetic process	152 out of 492 genes, 30.9%	1233 out of 5797 background genes, 21.3%	9.95E-05
50801	ion homeostasis	30 out of 492 genes, 6.1%	127 out of 5797 background genes, 2.2%	0.00015
48878	chemical homeostasis	30 out of 492 genes, 6.1%	128 out of 5797 background genes, 2.2%	0.00018

Table S2. (continued).

GO ID#	GO Term	Cluster frequency	Background frequency	P-value
6357	regulation of transcription from RNA polymerase II promoter	48 out of 492 genes, 9.8%	269 out of 5797 background genes, 4.6%	0.00038
9892	negative regulation of metabolic process	46 out of 492 genes, 9.3%	253 out of 5797 background genes, 4.4%	0.00038
32447	protein urmylation	6 out of 492 genes, 1.2%	6 out of 5797 background genes, 0.1%	0.00038
31327	neg reg. of cellular biosynthetic process	43 out of 492 genes, 8.7%	230 out of 5797 background, 4.0%	0.00042
9890	negative regulation of biosynthetic process	43 out of 492 genes, 8.7%	230 out of 5797 background genes, 4.0%	0.00042
31324	negative regulation of cellular metabolic process	45 out of 492 genes, 9.1%	249 out of 5797 background genes, 4.3%	0.00062
50789	regulation of biological process	124 out of 492 genes, 25.2%	985 out of 5797 background genes, 17.0%	0.00083
10605	negative regulation of macromolecule metabolic process	43 out of 492 genes, 8.7%	236 out of 5797 background genes, 4.1%	0.00089
6325	chromatin organization	40 out of 492 genes, 8.1%	214 out of 5797 background genes, 3.7%	0.00111
30003	cellular cation homeostasis	26 out of 492 genes, 5.3%	111 out of 5797 background genes, 1.9%	0.00124
16568	chromatin modification	35 out of 492 genes, 7.1%	177 out of 5797 background genes, 3.1%	0.00139
50794	regulation of cellular process	118 out of 492 genes, 24.0%	935 out of 5797 background genes, 16.1%	0.0015
6366	transcription from RNA polymerase II promoter	61 out of 492 genes, 12.4%	395 out of 5797 background genes, 6.8%	0.00177
10558	negative regulation of macromolecule biosynthetic process	40 out of 492 genes, 8.1%	218 out of 5797 background genes, 3.8%	0.00181

Table S2. (continued).

GO ID#	GO Term	Cluster frequency	Background frequency	P-value
2000113	negative regulation of cellular macromolecule biosynthetic process	40 out of 492 genes, 8.1%	218 out of 5797 background genes, 3.8%	0.00181
19725	cellular homeostasis	30 out of 492 genes, 6.1%	142 out of 5797 background genes, 2.4%	0.00194
10629	negative regulation of gene expression	37 out of 492 genes, 7.5%	197 out of 5797 background genes, 3.4%	0.00253
55080	cation homeostasis	26 out of 492 genes, 5.3%	115 out of 5797 background, 2.0%	0.00253
40007	growth	30 out of 492 genes, 6.1%	144 out of 5797 background genes, 2.5%	0.00264
48519	negative regulation of biological process	56 out of 492 genes, 11.4%	356 out of 5797 background genes, 6.1%	0.00275
43486	histone exchange	7 out of 492 genes, 1.4%	10 out of 5797 background genes, 0.2%	0.00308
45934	negative regulation of nucleobase, nucleoside, nucleotide and nucleic acid metabolic process	39 out of 492 genes, 7.9%	215 out of 5797 background genes, 3.7%	0.00329
51172	negative regulation of nitrogen compound metabolic process	39 out of 492 genes, 7.9%	215 out of 5797 background genes, 3.7%	0.00329
48523	negative regulation of cellular process	55 out of 492 genes, 11.2%	350 out of 5797 background genes, 6.0%	0.00352
2097	tRNA wobble base modification	11 out of 492 genes, 2.2%	26 out of 5797 background genes, 0.4%	0.00368
2098	tRNA wobble uridine modification	11 out of 492 genes, 2.2%	26 out of 5797 background genes, 0.4%	0.00368
16043	cellular component organization	187 out of 492 genes, 38.0%	1680 out of 5797 genes, 29.0%	0.00373

Table S2. (continued).

GO ID#	GO Term	Cluster frequency	Background frequency	P-value
32507	maintenance of protein location in cell	13 out of 492 genes, 2.6%	36 out of 5797 background genes, 0.6%	0.00396
16481	negative regulation of transcription	36 out of 492 genes, 7.3%	194 out of 5797 background genes, 3.3%	0.00466
42592	homeostatic process	38 out of 492 genes, 7.7%	210 out of 5797 background genes, 3.6%	0.00471
45892	negative regulation of transcription,	35 out of 492 genes, 7.1%	187 out of 5797 background, 3.2%	0.00519
11	vacuole inheritance	9 out of 492 genes, 1.8%	18 out of 5797 background genes, 0.3%	0.00543
6914	autophagy	21 out of 492 genes, 4.3%	85 out of 5797 background genes, 1.5%	0.00545
51253	negative regulation of RNA metabolic process	35 out of 492 genes, 7.1%	188 out of 5797 background genes, 3.2%	0.00589
6464	protein modification process	76 out of 492 genes, 15.4%	549 out of 5797 background genes, 9.5%	0.0065
6886	intracellular protein transport	45 out of 492 genes, 9.1%	271 out of 5797 background genes, 4.7%	0.00678
45185	maintenance of protein location	13 out of 492 genes, 2.6%	38 out of 5797 background genes, 0.7%	0.00791

APPENDIX B

SUPPLEMENTAL INFORMATION FOR CHAPTER III

Table S1. Protein sequences used to generate the maximum likelihood phylogeny of Anc.a. Sequences are labeled with the first letter of their genus and the full name of their species followed by their GenBank accession ID number.

GenBank protein sequences used to generate phylogeny of Anc.a
A.capsulatus_EEH08148
A.capsulatus_EER39772
A.capsulatus_XP_001544538
A.clavatus_XP_001271993
A.dermatitidis_EEQ85687
A.fumigatus_XP_751699
A.nidulans_predicted_XP_663210
A.niger_NP_984223
A.oryzae_predicted_XP_001820188
A.terreus_XP_001213128
A.thaliana_NP_179736 -
B.fuckeliana_predicted_XP_001559630
C.albicans_EEQ44988
C.albicans_predicted_XP_712251
C.albicans_predicted_XP_712308
C.cinerea.okayama_predicted_XP_001839899
C.globosum_XP_001225834
C.immitis_XP_001247773
C.neoformans_XP_570271
D.discoideum_Q54E04 -
D.hansenii_CAG86124
E.bieneusi_XP_001827782
F.neoformans_AAK81705
G.zeae_predicted_XP_380994
M.globosa_predicted_XP_001732767
M_grisea_predicted_XP_361473
N.crassa_predicted_XP_956054
N.fischeri_predicted_XP_001266930
P.anserina_XP_001909914
P.brasiliensis_EEH20928
P.brasiliensis_EEH40703
P.brasiliensis_EEH45553
P.chrysogenum_CAP97862
P.marneffei_predicted_XP_002151272
P.nodorum_predicted_XP_001796790
P.tritici-repentis_XP_001931738

Table S1. (continued).

GenBank protein sequences used to generate phylogeny of Anc.a
S.japonicus_XP_002171793
S.pombe_NP_594219
S.sclerotiorum_predicted_XP_001587166
T.stipitatus_XP_002341761

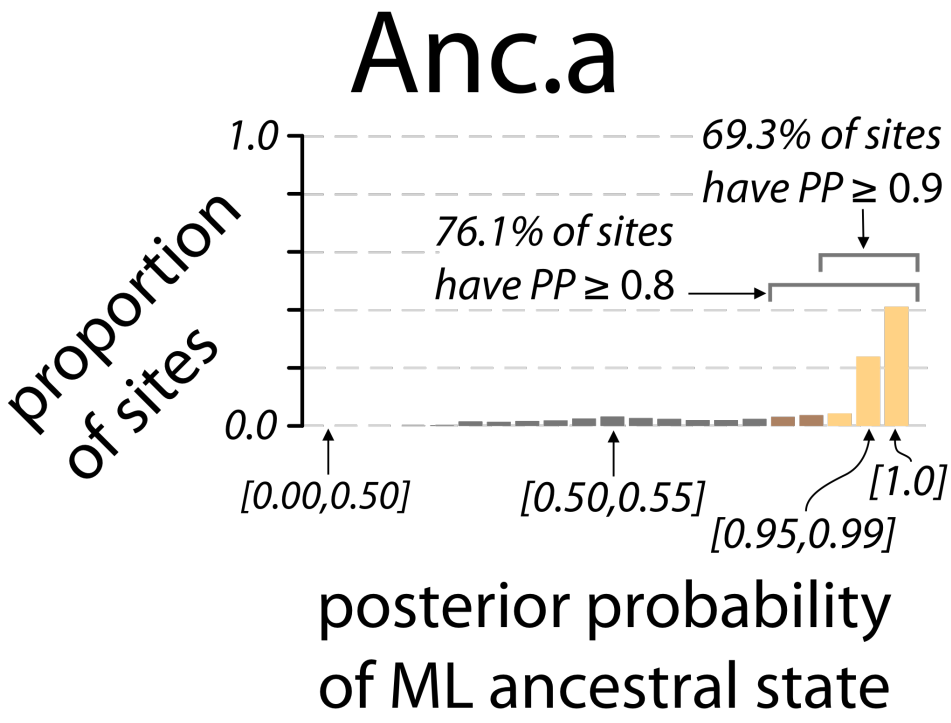

Figure S1. Support for the Anc.a reconstruction was characterized by binning 5%-sized bins and counting the proportion of total amino acid sites within each bin.

Table S2. Testing the robustness to uncertainty for the Anc.a sequence. 50 residues from the entire Anc.a sequence were chosen at random to represent the 134 independent sites with posterior probabilities of less than 80%. Single amino acid substitutions to Anc.a were introduced using a modified Quikchange protocol (Zheng *et al*., 2004). Vectors were transformed into *vph1*Δ *stv1*Δ yeast and tested on rich media containing 100 mM Ca^{2+} or rich media containing 3.5 mM Zn^{2+}. Alternative Anc.a genes were under control of the *STV1* promoter.

	100 mM Ca^{2+}	3.5 mM Zn^{2+}		100 mM Ca^{2+}	3.5 mM Zn^{2+}
WT	+++++	+++++	WT	+++++	+++++
*vph1*Δ			*vph1*Δ		
*stv1*Δ	-	-	*stv1*Δ	-	-
Anc.a	++++	+++	Anc.a	++++	+++
G25S	++++	+++	S268T	++++	+++
N46K	++++	+++	D274N	++++	+++
E76D	++++	+++	E278D	++++	+++
I82L	++++	+++	S279T	++++	+++
E83D	++++	+++	V302I	++++	+++
A90S	++++	+++	T337A	++++	+++
K99Q	++++	+++	E347D	++++	+++
D111N	++++	+++	E352D	++++	+++
E119Q	++++	+++	E361K	++++	+++
R120K	++++	+++	K364R	++++	+++
A134T	++++	+++	Q392R	++++	+++
G144A	++++	+++	S449T	++++	+++
T148S	++++	+++	I459V	++++	+++
E150D	++++	+++	K484E	++++	+++
Q160A	++++	+++	Q496E	++++	+++
E165D	++++	+++	I562V	++++	+++
S171A	++++	+++	V611I	++++	+++
D183E	++++	+++	V632I	++++	+++
E218D	++++	+++	H649N	++++	+++
E233Q	++++	+++	H650R	++++	+++
A236S	++++	+++	Q653E	++++	+++
K240R	++++	+++	S666A	++++	+++
D252N	++++	+++	D678E	++++	+++
F256Y	++++	+++	V747A	++++	+++
D261E	++++	+++	I750F	++++	+++

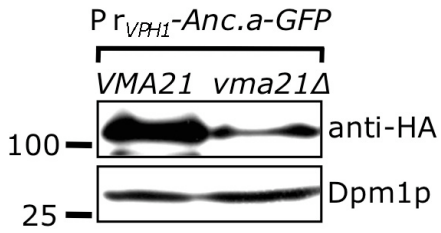

Figure S2. Stability of Anc.a protein is dependent on the presence of the V-ATPase assembly factor, Vma21p. Whole cell extracts were prepared from yeast expressing Anc.a-GFP under control of the *VPH1* promoter (Pr$_{VPH1}$::*Anc.a-GFP*; GFY256), and a strain expressing Anc.a-GFP deleted for *VMA21* (Pr$_{VPH1}$::*Anc.a-GFP vma21*Δ; GFY300). Western blot analysis was performed using anti-HA and anti-Dpm1p (loading control) antibodies. The size of the nearest molecular marker (kDa) is shown.

REFERENCES CITED

1. *References cited for Chapter I*

AVIEZER-HAGAI, K., H. NELSON, and N. NELSON, 2000 Cloning and expression of cDNAs encoding plant V-ATPase subunits in the corresponding yeast null mutants. Biochim. Biophys. Acta. **1459**: 489-498.

BAARS, T. L., S. PETRI, C. PETERS, and A. MAYER, 2007 Role of the V-ATPase in regulation of the vacuolar fission-fusion equilibrium. Mol. Bio. Cell **18**: 3873- 3882.

CHAVEZ, C., E. J. BOWMAN, J. C. REIDLING, K. H. HAW, and B. J. BOWMAN, 2006 Analysis of strains with mutations in six genes encoding subunits of the V ATPase: eukaryotes differ in the composition of the V_0 sector of the enzyme. J. Biol. Chem. **281**: 27052-27062.

DAVIS-KAPLAN, S. R., M. A. COMPTON, A. R. FLANNERY, D. M. WARD, J. KAPLAN *et al.*, 2006 *PRK1* encodes an assembly factor for the yeast V-type ATPase. J. Biol. Chem. **281**: 32025-32035.

FINBOW, M. E., S. F. GOODWIN, L. MEAGHER, N. J. LANE, J. KEEN, *et al*., 1994 Evidence that the 16 kDa proteolipid (subunit c) of the vacuolar H(+)-ATPase and dunctin from gap junctions are the same polypeptide in Drosophila and Manduca: molecular cloning of the Vha16k gene from Drosophila. J. Cell. Sci. **107**: 1817-1824.

FORGAC, M., 2007 Vacuolar ATPases: rotary proton pumps in physiology and pathophysiology. Nat. Rev. Mol. Cell Biol. **8**: 917-102.

FRATTINI, A., P. J. ORCHARD, C. SOBACCHI, S. GILIANI, M. ABINUN *et al.*, 2000 Defects in TCIRG1 subunit of the vacuolar proton pump are responsible for a subset of human autosomal recessive osteopetrosis. Nat. Genet. **25**: 343-346.

GAIGG, B., A. TOULMAY, and R. SCHNEITER, 2006 Very long-chain fatty acid-containing lipids rather than sphingolipids *per se* are required for raft association and stable surface transport of newly synthesized plasma membrane ATPase in yeast. J. Biol. Chem. **281**: 34135-34145.

GRAHAM, L. A., A. R. FLANNERY, and T.H. STEVENS, 2003 Structure and assembly of the yeast V-ATPase. J. Bioenerg. Biomembr. **35**: 301-312.

GRÜBER, G., H. WIECZOREK, W. R. HARVEY, and V. MÜLLER, 2001 Structure-function relationships of A-, F- and V-ATPases. J. Exp. Biol. **204**: 2597-2605.

GRUENBERG, J., and F. G. VAN DER GOOT, 2006 Mechanisms of pathogen entry through the endosomal compartments. Nat. Rev. Mol. Cell Biol. **7**: 495-504.

HARMS, M. J., and J. W. THORNTON, 2010 Analyzing protein structure and function using ancestral gene reconstruction. Curr. Opin. Struct. Biol. **20**: 360-366.

HARRISON, M. A., P. C. JONES, Y. I. KIM, M. E. FINBOW, and J. B. FINDLAY, 1994 Functional properties of a hybrid vacuolar H(+)-ATPase in *Saccharomyces* cells expressing the Nephrops 16-kDa proteolipid. Eur. J. Biochem. **221**: 111-120.

HIESINGER, P. R., A. FAYYAZUDDIN, S. Q. MEHTA, T. ROSENMUND, K. L. SCHULZE *et al.*, 2005 The v-ATPase V_0 subunit a1 is required for a late step in synaptic vesicle exocytosis in Drosophila. Cell **121**: 607-620.

HILL, K. J., and T. H. STEVENS, 1995 Vma22p is a novel endoplasmic reticulum associated protein required for assembly of the yeast vacuolar H^+-ATPase complex. J. Biol. Chem. **270**: 22329-22336.

HIRATA, R., N. UMEMOTO, M. N. HO, Y. OHYA, T. H. STEVENS *et al.*, 1993 *VMA12* is essential for assembly of the vacuolar H(+)-ATPase subunits onto the vacuolar membrane in *Saccharomyces cerevisiae.* J. Biol. Chem. **268**: 961-967.

HURTADO-LORENZO, A., M. SKINNER, E. I. ANNAN, M. FUTAI, G. H. SUN-WADA *et al.,* 2006 V-ATPase interacts with ARNO and Arf6 in early endosomes and regulates the protein degradative pathway. Nat. Cell Biol. **8**: 124-136.

IKEDA, M., M. HINOHARA, K. UMAMI, Y. TAGURO, Y. OKADA *et al.*, 2001 Expression of V-ATPase proteolipid subunit of Acetabularia acetabulum in a VMA3-deficient strain of *Saccharomyces cerevisiae* and its complementation study. Eur. J. Biochem. **268**: 6097-6104.

KANE, P. M., 2006 The where, when, and how of organelle acidification by the yeast vacuolar H^+-V-ATPase. Microbiol. Mol. Biol. Rev. **70**: 177-191.

KARET, F. E., K. E. FINBERG, R. D. NELSON, A. NAYIR, H. MOCAN *et al.*, 1999 Mutations in the gene encoding B1 subunit of H^+-ATPase cause renal tubular acidosis with sensorineural deafness. Nat. Genet. **21**: 84-90.

KAWASAKI-NISHI, S., K. BOWERS, T. NISHI, M. FORGAC, and T. H. STEVENS, 2001a The amino-terminal domain of the vacuolar proton-translocating ATPase a subunit controls targeting and *in vivo* dissociation, and the carboxyl-terminal domain affects coupling of protein transport and ATP hydrolysis. J. Biol. Chem. **276**: 47411-47420.

KAWASAKI-NISHI, S., T. NISHI, and M. FORGAC, 2001b Yeast V-ATPase complexes containing different isoforms of the 100 kDa a-subunit differ in coupling efficiency and *in vivo* dissociation. J. Biol. Chem. **276**: 17941-17948.

LAUWERS, E. G. GROSSMAN, and B. ANDRÉ, 2007 Evidence for coupled biogenesis of yeast Gap1 permease and sphingolipids: essential role in transport activity and normal control by ubquitination. Mol. Biol. Cell **18**: 3068-3080.

MALKUS, P., L. A. GRAHAM, T. H. STEVENS, and R. SCHEKMAN, 2004 Role of Vma21p in assembly and transport of the yeast vacuolar ATPase. Mol. Biol. Cell **15**: 5075-5091.

MANOLSON, M. F., D. PROTEAU, R. A. PRESTON, A. STENBIT, B. T. ROBERTS *et al.*, 1992 The *VPH1* gene encodes a 95-kDa integral membrane polypeptide required for *in vivo* assembly and activity of the yeast vacuolar H^+-ATPase. J. Biol. Chem. **267**: 14294-14303.

MANOLSON, M. F., B. WU, D. PROTEAU, B. E. TAILLON, B. T. ROBERTS *et al.*,1994 *STV1* gene encodes functional homologue of the 95-kDa yeast vacuolar H^+-ATPase subunit Vph1p. J. Biol. Chem. **269**: 14064-14074.

MARTÍNEZ-ZAGUILÁN, R., N. RAGHUNAND, R. M. LYNCH, W. BELLAMY, G. M. MARTINEZ *et al.*, 1999 pH and drug resistance. I. Functional expression of plasmalemmal V-type H^+-ATPase in drug-resistant human breast carcinoma cell lines. Biochem. Pharmacol. **57**: 1037-1046.

NEUBERT, C., L. A. GRAHAM, E. W. BLACK-MAIER, E. M. COONROD, T. Y. LIU, *et al*., 2008 Arabidopsis has two functional orthologs of the yeast V-ATPase assembly factor Vma21p. Traffic **9**: 1618-1628.

NISHI, T., S. KAWASAKI-NISHI, and M. FORGAC, 2003 Expression and function of the mouse V-ATPase d subunit isoforms. J. Biol. Chem. **278**: 46396-46402.

OKA, T., Y. MURATA, M. NAMBA, T. YOSHIMIZU, T. TOYOMURA *et al*., 2001a a4, a unique kidney-specific isoform of mouse vacuolar H^+-ATPase subunit a. J. Biol. Chem. **276**: 40050-40054.

OKA, T., T. TOYOMURA, K. HONJO, Y. WADA, and M. FUTAI, 2001b Four subunit a isoforms of *Caenorhabditis elegans* vacuolar H^+-ATPase. Cell-specific expression during development. J. Biol. Chem. **276**: 33079-33085.

QI, J., and M. FORGAC, 2007 Cellular environment is important in controlling V-ATPase dissociation and its dependence on activity. J. Biol. Chem. **282**: 24742-24751.

QI, J., and M. FORGAC, 2008 Function and subunit interactions of the N-terminal domain of subunit a (Vph1p) of the yeast V-ATPase. J. Biol. Chem. **283**: 19274-19282.

RYAN, M., L. A. GRAHAM, and T. H. STEVENS, 2008 Voa1p functions in V-ATPase assembly in the yeast endoplasmic reticulum. Mol. Biol. Cell **19**: 5131-5142.

TONG, A. H., and C. BOONE, 2006 Synthetic genetic array analysis in *Saccharomyces cerevisiae.* Methods Mol. Biol. **313**: 171-192.

TOYOMURA, T., Y. MURATA, A. YAMAMOTO, T. OKA, G. H. SUN-WADA *et al.*, 2003 From lysosomes to the plasma membrane: localization of vacuolar type H+ ATPase with the a3 isoform during osteoclast differentiation. J. Biol. Chem. **278**: 22023-22030.

WANG, Q., and A. CHANG, 2002 Sphingoid base synthesis is required for oligomerization and cell surface stability of the yeast plasma membrane ATPase, Pma1. Proc. Natl. Acad. Sci USA **99**: 12853-12858.

WANG, Y., D. J. CIPRIANO, and M. FORGAC, 2007 Arrangement of subunits in the proteolipid ring of the V-ATPase. J. Biol. Chem. **282**: 34058–34065.

WASSMER, T., R. KISSMEHL, J. COHEN, and H. PLATTNER, 2006 Seventeen a-subunit isoforms of paramecium V-ATPase provide high specialization in localization and function. Mol. Biol. Cell **17**: 917-930.

ZHANG, J., M. MYERS, and M. FORGAC, 1992 Characterization of the V_0 domain of the coated vesicle (H+)-ATPase. J. Biol. Chem. **15**: 9773-9778.

2. *References cited for Chapter II*

BOWERS, K. and T. H. STEVENS, 2005 Protein transport from the late Golgi to the vacuole in the yeast *Saccharomyces cerevisiae*. Biochim. Biophys. Acta. **1744:** 438-454.

BRESLOW, D. K., S. R. COLLINS, B. BODENMILLER, R. AEBERSOLD, K. SIMONS *et al.,* 2010 Orm family proteins mediate sphingolipid homeostasis. Nature **463:** 1048-1053.

CHUNG, J. H., R. L. LESTER, and R. C. DICKSON, 2003 Sphingolipid requirement for generation of a functional V_1 component of the vacuolar ATPase. J. Biol. Chem. **278:** 28872-28881.

COMPTON, M. A., L. A. GRAHAM, and T. H. STEVENS, 2006 Vma9p (subunit e) is an integral membrane V_0 subunit of the yeast V-ATPase. J. Biol. Chem. **281:** 15312-15319.

CONIBEAR E., and T. H. STEVENS, 2002 Studying yeast vacuoles. Method Enzymol **351:** 408-432.

COWART, L. A., and L. M. OBEID, 2007 Yeast sphingolipids: recent developments in understanding biosynthesis, regulation, and function. Biochim. Biophys. Acta. **1771:** 421-431.

DAVIS-KAPLAN, S. R., M. A. COMPTON, A. R. FLANNERY, D. M. WARD, J. KAPLAN *et al.*, 2006 *PRK1* encodes an assembly factor for the yeast V-type ATPase. J. Biol. Chem. **281:** 32025-32035.

EIDE, D. J., S. CLARKE, T. M. NAIR, M. GEHL, M. GRIBSKOV *et al.*, 2005 Characterization of the yeast ionome: a genome-wide analysis of nutrient mineral and trace element homeostasis in *Saccharomyces cerevisiae.* Genome Biol. **6:** R77.

FLANNERY, A. R., L. A. GRAHAM, and T. H. STEVENS, 2004 Topological characterization of the c, c', and c" subunits of the vacuolar ATPase from the yeast *Saccharomyces cerevisiae*. J. Biol. Chem. **279:** 39856-39862.

FORGAC, M., 2007 Vacuolar ATPases: rotary proton pumps in physiology and pathophysiology. Nat. Rev. Mol. Cell Biol. **8:** 917-102.

FRATTINI, A., P. J. ORCHARD, C. SOBACCHI, S. GILIANI, M. ABINUN *et al.*, 2000 Defects in TCIRG1 subunit of the vacuolar proton pump are responsible for a subset of human autosomal recessive osteopetrosis. Nat. Genet. **25:** 343-346.

GABLE, K., H. SLIFE, D. BACIKOVA, E. MONAGHAN, and T. M. DUNN, 2000 Tsc3p is an 80-amino acid protein associated with serine palmitoyltransferase and required for optimal enzyme activity. J. Biol. Chem. **275:** 7597-7603.

GAIGG, B., A. TOULMAY, and R. SCHNEITER, 2006 Very long-chain fatty acid-containing lipids rather than sphingolipids *per se* are required for raft association and stable surface transport of newly synthesized plasma membrane ATPase in yeast. J. Biol. Chem. **281:** 34135-34145.

GERRARD, S. R., B. P. LEVI, and T. H. STEVENS, 2000 Pep12p is a multifunctional yeast syntaxin that controls entry of biosynthetic, endocytic and retrograde traffic into the prevacuolar compartment. Traffic **1:** 259-269.

GRAHAM, L. A., K. J. HILL, and T. H. STEVENS, 1998 Assembly of the yeast vacuolar H^+-ATPase occurs in the endoplasmic reticulum and requires a Vma12p/Vma22p assembly complex. J. Cell Biol. **142:** 39-49.

GRAHAM, L. A., A. R. FLANNERY, and T.H. STEVENS, 2003 Structure and assembly of the yeast V-ATPase. J. Bioenerg. Biomembr. **35:** 301-312.

GOLDSTEIN, A. L., and J. H. MCCUSTER, 1999 Three new dominant drug resistance cassettes for gene disruption in *Saccharomyces cerevisiae*. Yeast **15:** 1541-1553.

HAN, S., M. A. LONE, R. SCHNEITER, and A. CHANG, 2010 Orm1 and Orm2 are conserved endoplasmic reticulum membrane proteins regulating lipid homeostasis and protein quality control. Proc. Natl. Acad. Sci USA **107:** 5851-5856.

HANADA, K., 2003 Serine palmitoyltransferase, a key enzyme of sphingolipid metabolism. Biochim. Biophys. Acta. **1632:** 16-30.

HEARN, J. D., R. L. LESTER, and R. C. DICKSON, 2003 The uracil transporter Fur4p associates with lipid rafts. J. Biol. Chem. **278:** 3679-3686.

HEATH, V. L., S. L. SHAW, S. ROY, and M. S. CYERT, 2004 Hph1p and Hph2p, novel components of calcineurin-mediated stress responses in *Saccharomyces cerevisiae*. Eukaryot Cell **3:** 695-704.

HILL, J. E., A. M. MYERS, T. J. KOERNER, and A. TZAGOLOFF, 1986 Yeast/E. coli shuttle vectors with multiple unique restriction sites. Yeast **2:** 163-167.

HILL, K., and A. A. COOPER, 2000 Degradation of unassembled Vph1p reveals novel aspects of the yeast ER quality control system. EMBO J. **19:** 550-561.

HILL, K. J., and T. H. STEVENS, 1994 Vma21p is a yeast membrane protein retained in the endoplasmic reticulum by a di-lysine motif and is required for the assembly of the vacuolar H^+-ATPase complex. Mol. Biol. Cell **5:** 1039-1050.

HILL, K. J., and T. H. STEVENS, 1995 Vma22p is a novel endoplasmic reticulum associated protein required for assembly of the yeast vacuolar H^+-ATPase complex. J. Biol. Chem. **270:** 22329-22336.

HIRATA, R., N. UMEMOTO, M. N. HO, Y. OHYA, T. H. STEVENS *et al.*, 1993 *VMA12* is essential for assembly of the vacuolar H(+)-ATPase subunits onto the vacuolar membrane in *Saccharomyces cerevisiae.* J. Biol. Chem. **268:** 961-967.

HIRATA, T., A. IWAMOTO-KIHARA, G. H. SUN-WADA, T. OKAJIMA, Y. WADA *et al.*, 2003 Subunit rotation of vacuolar-type proton pumping ATPase: relative rotation of the G as to c subunit. J. Biol. Chem. **278:** 23714-23719.

HJELMQVIST, L., M. TUSON, G. MARFANY, E. HERRERO, S. BALCELLS *et al.*, 2002 ORMDL proteins are a conserved new family of endoplasmic reticulum membrane proteins. Genome Biol. **3:** RESEARCH0027.

HO, M. N., K. J. HILL, M. A. LINDORFER, and T. H. STEVENS, 1993 Isolation of vacuolar membrane H(+)-ATPase-deficient yeast mutants; the *VMA5* and *VMA4* genes are essential for assembly and activity of the vacuolar H(+)-ATPase. J. Biol. Chem. **268:** 221-227.

IMAMURA, H., M. TAKEDA, S. FUNAMOTO, K. SHIMABUKURO, M. YOSHIDA *et al.*, 2005 Rotation scheme of V_1-motor is different from that of F_1-motor. Proc. Natl. Acad. Sci USA **13:** 17929-17933.

JORGENSEN, E. M., and S. E. MANGO, 2002 The art and design of genetic screens: *Caenorhabditis elegans*. Nat. Rev. Genet. **3:** 356-369.

KANE, P. M., 2006 The where, when, and how of organelle acidification by the yeast vacuolar H^+-V-ATPase. Microbiol. Mol. Biol. Rev. **70:** 177-191.

KANE, P. M., 2007 The long physiological reach of the yeast vacuolar H^+-ATPase. J. Bioenerg. Biomembr. **39:** 415-421.

KARET, F. E., K. E. FINBERG, R. D. NELSON, A. NAYIR, H. MOCAN *et al.*, 1999 Mutations in the gene encoding B1 subunit of H^+-ATPase cause renal tubular acidosis with sensorineural deafness. Nat. Genet. **21:** 84-90.

KLIONSKY, D. J., P. K. HERMAN, and S. D EMR, 1990 The fungal vacuole: composition, function, and biogenesis. Microbiol. Rev. **54:** 266-292.

LAUWERS, E. G. GROSSMAN, and B. ANDRÉ, 2007 Evidence for coupled biogenesis of yeast Gap1 permease and sphingolipids: essential role in transport activity and normal control by ubquitination. Mol. Biol. Cell **18:** 3068-3080.

MACDIARMID, C. W., M. A. MILANICK, and D. J. EIDE, 2002 Biochemical properties of vacuolar zinc transport systems of *Saccharomyces cerevisiae.* J. Biol. Chem. **277:** 39187-39194.

MALKUS, P., L. A. GRAHAM, T. H. STEVENS, and R. SCHEKMAN, 2004 Role of Vma21p in assembly and transport of the yeast vacuolar ATPase. Mol. Biol. Cell **15:** 5075-5091.

MANOLSON, M. F., D. PROTEAU, R. A. PRESTON, A. STENBIT, B. T. ROBERTS *et al.*, 1992 The *VPH1* gene encodes a 95-kDa integral membrane polypeptide required for *in vivo* assembly and activity of the yeast vacuolar H^+-ATPase. J. Biol. Chem. **267:** 14294-14303.

MANOLSON, M. F., B. WU, D. PROTEAU, B. E. TAILLON, B. T. ROBERTS *et al.*,1994 *STV1* gene encodes functional homologue of the 95-kDa yeast vacuolar H^+-ATPase subunit Vph1p. J. Biol. Chem. **269:** 14064-14074.

MARKWELL, M. A., S. M. HAAS, L. L. BIEBER, and N. E. TOLBERT, 1978 A modification of the Lowry procedure to simplify protein determination in membrane and lipoprotein samples. Anal Biochem. **87:** 206-210.

MARSHANSKY, V., and M. FUTAI, 2008 The V-type H^+-ATPase in vacuolar trafficking: targeting, regulation and function. Curr. Opin. Cell Biol. **20:** 1-20.

MARTÍNEZ-ZAGUILÁN, R., N. RAGHUNAND, R. M. LYNCH, W. BELLAMY, G. M. MARTINEZ *et al.*, 1999 pH and drug resistance. I. Functional expression of plasmalemmal V-type H^+-ATPase in drug-resistant human breast carcinoma cell lines. Biochem. Pharmacol. **57:** 1037-1046.

MISETA, A., R. KELLERMAYER, D. P. AIELLO, L. Fu, and D. M. BEDWELL, 1999 The vacuolar Ca^{2+}/H^+ exchanger Vcx1p/Hum1p tightly controls cytosolic Ca^{2+} levels in S. cerevisiae. FEBS Lett. **451:** 132-136.

OHYA, Y., N. UMEMOTO, I. TANIDA, A. OHTA, H. IIDA *et al.*, 1991 Calcium-sensitive *cls* mutants of *Saccharomyces cerevisiae* showing a Pet- phenotype are ascribable to defects of vacuolar membrane H(+)-ATPase activity. J. Biol. Chem. **266:** 13971-13977.

PAGANI, M. A., A. CASAMAYOR, R. SERRANO, S. ATRIAN, and J. ARIÑO, 2007 Disruption of iron homeostasis in *Saccharomyces cerevisiae* by high zinc levels: a genome-wide study. Mol. Microbiol. **65:** 521-537.

RAYMOND, C. K., I. HOWALD-STEVENSON, C. A. VATER, and T. H. STEVENS, 1992 Morphological classification of the yeast vacuolar protein sorting mutants: evidence for a prevacuolar compartment in class E vps mutants. Mol. Biol. Cell **3:** 1389-1402.

ROTHMAN, J. H., and T. H. STEVENS, 1986 Protein sorting in yeast: mutants defective in vacuole biogenesis mislocalize vacuolar proteins into the late secretory pathway. Cell **47:** 1041-1051.

RYAN, M., L. A. GRAHAM, and T. H. STEVENS, 2008 Voa1p functions in V-ATPase assembly in the yeast endoplasmic reticulum. Mol. Biol. Cell **19:** 5131-5142.

SAMBADE, M., M. ALBA, A. M. SMARDON, R. W. WEST, and P. M. KANE, 2005 A genomic screen for yeast vacuolar membrane ATPase mutants. Genetics **170:** 1539-1551.

SAMBROOK, J., and D. W. RUSSEL, 2001 Molecular cloning: A laboratory manual, 3rd ed., Cold Spring Harbor, NY: Cold Spring Harbor Laboratory Press.

SERRANO, R., D. BERNAL, E. SIMÓN, and J. ARIÑO, 2004 Copper and Iron are the limiting factors for growth of the yeast *Saccharomyces cerevisiae* in an alkaline environment. J. Biol. Chem. **279:** 19698-19704.

SHANER, N. C., R. E. CAMPBELL, P. A. STEINBACH, B. N. G. GIEPMANS, A. E. PALMER *et al.*, 2004 Improved monomeric red, orange and yellow fluorescent proteins derived from *Discosoma* sp. red fluorescent protein. Nat Biotechnol **22:** 1567-1572.

SIKORSKI, R. S., and P. HIETER, 1989 A system of shuttle vectors and yeast host strains designed for efficient manipulation of DNA in *Saccharomyces cerevisiae*. Genetics **122:** 19-27.

SIMONS, R. W., F. HOUMAN, and N. KLECKNER, 1987 Improved single and multicopy lac-based cloning vectors for protein and operon fusions. Gene **53:** 85-96.

ST JOHNSTON, D., 2002 The art and design of genetic screens: *Drosophila melanogaster*. Nat. Rev. Genet. **3:** 176-188.

TANIDA, I., A. HASEGAWA, H. IIDA, Y. OHYA, and Y. ANRAKU, 1995 Cooperation of calcineurin and vacuolar H(+)-ATPase in intracellular Ca^{2+} homeostasis of yeast cells. J. Biol. Chem. **270:** 10113-10119.

TOMASHEK, J. J., L. A. GRAHAM, M. U. HUTCHINS, T. H. STEVENS, and D. J. KLIONSKY, 1997 V_1-situated stalk subunits of the yeast vacuolar proton-translocating ATPase. J. Biol. Chem. **272:** 26787-26793.

TONG, A. H., M. EVANGELISTA, A. B. PARSONS, H. XU, G. D. BADER *et al.*, 2001 Systematic genetic analysis with ordered arrays of yeast deletions mutants. Science **294:** 2364-2368.

TONG, A. H., and C. BOONE, 2006 Synthetic genetic array analysis in *Saccharomyces cerevisiae.* Methods Mol. Biol. **313:** 171-192.

UCHIDA, E., Y. OSHUMI, and Y. ANRAKU, 1985 Purification and properties of H^+-translocating, Mg^{+2}-adenosine triphosphatase from vacuolar membrane of *Saccharomyces cerevisiae.* J. Biol. Chem. **260:** 1090-1095.

WANG, Q., and A. CHANG, 2002 Sphingoid base synthesis is required for oligomerization and cell surface stability of the yeast plasma membrane ATPase, Pma1. Proc. Natl. Acad. Sci USA **99:** 12853-12858.

WEISMAN, L. S., R. BACALLAO, and W. WICKNER, 1987 Multiple methods of visualizing the yeast vacuole permit evaluation of its morphology and inheritance during the cell cycle. J. Cell Biol. **105:** 1539-1547.

YOKOYAMA, K., M. NAKANO, H. IMAMURA, M. YOSHIDA, and M. TAMAKOSHI, 2003 Rotation of the proteolipid ring in the V-ATPase. J. Biol. Chem. **278:** 24255-24258.

3. *References cited for Chapter III*

Abascal, F., Zardoya, R., and Posada, D. (2005). Prottest: selection of best-fit models of protein evolution. Bioinformatics *21*, 2104-2105.

Adams, D. S., Robinson, K. R., Fukumoto, T., Yuan, S., Albertson, R. C., Yelick, P., Kuo, L, McSweeney, M., and Levin, M. (2006). Early, H^+-V-ATPase-dependent proton flux is necessary for consistent left-right patterning of non-mammalian vertebrates. Development *133*, 1657-1671.

Anismova, M., and Gascuel, O. (2006). Approximate likelihood-ratio test for branches: A fast, accurate, and powerful alternative. Syst. Biol. *55*, 539-552.

Aviezer-Hagai, K., Nelson, H., and Nelson, N. (2000). Cloning and expression of cDNAs encoding plant V-ATPase subunits in the corresponding yeast null mutants. Biochim. Biophys. Acta. *1459*, 489-498.

Baars, T. L., Petri, S., Peters, C., and Mayer, A. (2007). Role of the V-ATPase in regulation of the vacuolar fission-fusion equilibrium. Mol. Bio. Cell *18*, 3873-3882.

Barrowman, J., Bhandari, D., Reinisch, K., and Ferro-Novick, S. (2010). TRAPP complexes in membrane traffic: convergence through a common Rab. Nat. Rev. Mol. Cell Biol. *11*, 759-763.

Binns, D., Januszewski, T., Chen, Y., Hill, J., Markin, V. S., Zhao, Y., Gilpin, C., Chapman, K. D., Anderson, R. G., and Goodman, J. M. (2006). An intimate collaboration between peroxisomes and lipid bodies. J. Cell Biol. *173*, 719-731.

Bonifacino, J. S., and Hierro, A. (2010). Transport according to GARP: receiving retrograde cargo at the trans-Golgi network. Trends Cell Biol. DOI: 10.1016/j.tcb.2010.11.003.

Bridgham, J. T., Ortlund, E. A., and Thornton, J. W. (2009). An epistatic ratchet constrains the direction of glucocorticoid receptor evolution. Nature *461*, 515-519.

Chavez, C., Bowman, E. J., Reidling, J. C., Haw, K. H., and Bowman, B. J. (2006). Analysis of strains with mutations in six genes encoding subunits of the V-ATPase: eukaryotes differ in the composition of the V_0 sector of the enzyme. J. Biol. Chem. *281*, 27052-27062.

Cooper, A. A., and Stevens, T. H. (1996). Vps10p cycles between the late-Golgi and prevacuolar compartments in its function as the sorting receptor for multiple yeast vacuolar hydrolases. J. Cell Biol. *133*, 529-541.

Cowles, C. R., Odorizzi, G., Payne, G. S., and Emr, S. D. (1997). The AP-3 adaptor complex is essential for cargo-selective transport to the yeast vacuole. Cell *91*, 109-118.

Cross, R. L., and Müller, V. (2004). The evolution of the A-, F-, and V-type ATP synthases and ATPases: reversals in function and changes in the H+/ATP coupling ratio. FEBS Lett. *576*, 1-4.

Davis-Kaplan, S. R., Compton, M. A., Flannery, A. R., Ward, D. M., Kaplan, J., Stevens, T. H., and Graham, L. A. (2006). *PKR1* encodes an assembly factor for the yeast V-type ATPase. J. Biol. Chem. *281*, 32025-32035.

Dean, A. M., and Thornton, J. W. (2007). Mechanistic approaches to the study of evolution: the functional synthesis. Nat. Rev. Genet. *8*, 675-688.

Ediger, B., Melman, S. D., Pappas, D. L., Finch, M., Applen, J., and Parra, K. J. (2009). The tether connecting cytosolic (N terminus) and membrane (C terminus) domains of yeast V-ATPase subunit a (Vph1) is required for assembly of V_0 subunit d. J. Biol. Chem. *284*, 19522-19532.

Field, M. C., and Dacks, J. B. (2009). First and last ancestors: reconstructing evolution of the endomembrane system with ESCRTs, vesicular coat proteins, and nuclear pore complexes. Curr. Opin. Cell Biol. *21*, 4-13.

Fitch, W.M. (1971). Toward defining the course of evolution: Minimum change for a specific tree topology. Syst. Zool. *20*, 406–416.

Flannery, A. R., Graham, L. A., and Stevens, T. H. (2004). Topological characterization of the c, c', and c" subunits of the vacuolar ATPase from the yeast *Saccharomyces cerevisiae*. J. Biol. Chem. *279*, 39856-39862.

Force, A., Lynch, M., Pickett, F. B., Amores, A., Yan, Y. L., and Postlethwait, J. (1999). Preservation of duplicate genes by complementary, degenerative mutations. Genetics *151*, 1531-1545.

Forgac, M. (2007). Vacuolar ATPases: rotary proton pumps in physiology and pathophysiology. Nat. Rev. Mol. Cell. Biol. *8*, 917-929.

Frattini, A. *et al*. (2000). Defects in TCIRG1 subunit of the vacuolar proton pump are responsible for a subset of human autosomal recessive osteopetrosis. Nat. Genet. *25*, 343-346.

Goldstein, A. L., and McCusker, J. H. (1999). Three new dominant drug resistance cassettes for gene disruption in *Saccharomyces cerevisiae*. Yeast *15*, 1541-1553.

Graham, L. A., Hill, K. J., and Stevens, T. H. (1998). Assembly of the yeast vacuolar H^+-ATPase occurs in the endoplasmic reticulum andrequiresaVma12p/Vma22p assembly complex. J. Cell Biol. *142*, 39-49.

Graham, L. A., Flannery, A. R., and Stevens, T. H. (2003). Structure and assembly of the yeast V-ATPase. J. Bioenerg. Biomembr. *35*, 301-312.

Gruenberg, J., and van der Goot, F. G. (2006). Mechanisms of pathogen entry through the endosomal compartments. Nat. Rev. Mol. Cell. Biol. *7*, 495-504.

Guindon, S., and Gascuel, O. (2003). A simple, fast, and accurate algorithm to estimate large phylogenies by maximum likelihood. Syst. Biol. *52*, 696-704.

Hanson-Smith, V., Kolaczkowski, B., and Thornton, J. W. (2010). Robustness of ancestral sequence reconstruction to phylogenetic uncertainty. Mol. Biol. Evol. *27*, 1988-1999.

Harms, M. J., and Thornton, J. W. (2010). Analyzing protein structure and function using ancestral gene reconstruction. Curr. Opin. Struct. Biol. *20*, 360-366.

Hill, K., and Cooper, A. A. (2000). Degradation of unassembled Vph1p reveals novel aspects of the yeast ER quality control system. EMBO J. *19*, 550-561.

Hill, K. J., and Stevens, T. H. (1995). Vma22p is a novel endoplasmic reticulum-associated protein required for assembly of the yeast vacuolar H(+)-ATPase complex. J. Biol. Chem. *270*, 22329-22336.

Hirata, R., Umemoto, N., Ho, M. N., Ohya, Y., Stevens, T. H., and Anraku, Y. (1993). *VMA12* is essential for assembly of the vacuolar H^+-ATPase subunits onto the vacuolar membrane in *Saccharomyces cerevisiae*. J. Biol. Chem. *268*, 961-967.

Innan,H., and Kondrashov, F. (2010). The evolution of gene duplications: classifying and distinguishing between models. Nat. Rev. Genet. *11*, 97-108.

Jo, W. J., Kim, J. H., Oh, E., Jaramillo, D., Holman, P., Loguinov, A. V., Arkin, A. P., Nislow, C., Giaever, G., Vulpe, C. D. (2009). Novel insights into iron metabolism by integrating deletome and transcriptome analysis in an iron deficiency model of the yeast *Saccharomyces cerevisiae*. BMC Genomics *10*.

Kane, P. M. (2006). The where, when, and how of organelle acidification by the yeast vacuolar H^+-ATPase. Microbiol. Mol. Biol. Rev. *70*, 177-191.

Karet, F. E. *et al*. (1999). Mutations in the gene encoding B1 subunit of the H^+-ATPase cause renal tubular acidosis with sensorineural deafness. Nat. Genet. *21*, 84-90.

Kawasaki-Nishi, S., Bowers, K., Nishi, T., Forgac, M., and Stevens, T. H. (2001a). The amino-terminal domain of the vacuolar proton-translocating ATPase a subunit controls targeting and *in vivo* dissociation, and the carboxyl-terminal domain affects coupling of protein transport and ATP hydrolysis. J. Biol. Chem. *276*, 47411-47420.

Kawasaki-Nishi, S., Nishi, T. and Forgac, M. (2001b). Yeast V-ATPase complexes containing different isoforms of the 100 kDa a-subunit differ in coupling efficiency and *in vivo* dissociation. J. Biol. Chem. *276*, 17941-17948.

Kawasaki-Nishi, S., Nishi, T., and Forgac, M. (2001c). Arg-735 of the 100-kDa subunit a of the yeast V-ATPase is essential for proton translocation. Proc. Natl. Acad. Sci. USA *98*, 12397-12402.

Klionsky, D. J., Herman, P. K., and Emr, S. D. (1990). The fungal vacuole: composition, function, and biogenesis. Microbiol. Rev. *54*, 266-292.

Landolt-Marticorena, C., Williams, K. M., Correa, J., Chen, W., and Manolson, M. F. (2000). Evidence that the NH_2 terminus of Vph1p, and integral subunit of the V_0 sector of the yeast V-ATPase, interacts directly with the Vma1p and Vma13p subunits of the V_1 sector. J. Biol. Chem. *275*, 15449-15457.

Liu, D. C., and Nocedal, J. (1989). On the limited memory BFGS method for large scale optimization. Math. Program. *45*, 503-528.

Loytynoja, A., and Goldman, N. (2005). An algorithm for progressive multiple alignment of sequences with insertions. Proc. Natl. Acad. Sci. USA *102*, 10557-10562.

Loytynoja, A., and Goldman, N. (2008). Phylogeny-aware gap placement prevents errors in sequence alignment and evolutionary analysis. Science *5885*, 1632-1635.

MacDiarmid, C. W., Gaither, L. A., and Eide, D. (2000). Zinc transporters that regulate vacuolar zinc storage in *Saccharomyces cerevisiae.* EMBO J. *19*, 2845-2855.

Malkus, P., Graham, L. A., Stevens, T. H., and Schekman, R. (2004). Role of Vma21p in assembly and transport of the yeast vacuolar ATPase. Mol. Biol. Cell *15*, 5075-5091.

Manolson, M. F., Proteau, D., Preston, R. A., Stenbit, A., Roberts, B. T., Hoyt, M. A., Preuss, D., Mulholland, J., Botstein, D., and Jones, E. W. (1992). The *VPH1* gene encodes a 95-kDa integral membrane polypeptide required for *in vivo* assembly and activity of the yeast vacuolar H -ATPase. J. Biol. Chem. *267*, 14294 -14303.

Manolson, M. F., Wu, B., Proteau, D., Taillon, B. E., Roberts, B. T., Hoyt, M. A., and Jones, E. W. (1994). *STV1* gene encodes functional homologue of the 95-kDa yeast vacuolar H^+-ATPase subunit Vph1p. J. Biol. Chem. *269*, 14064-14074.

Markwell, M. A., Haas, S. M., Beiber, L. L., and Tolbert, N. E. (1978). A modification of the Lowry procedure to simplify protein determination in membrane and lipoprotein samples. Anal. Biochem. *87*, 206-210.

Marshansky, V. (2007). The V-ATPase a2-subunit as a putative endosomal pH-sensor. Biochem. Soc. Trans. *35*, 1092-1099.

Marshansky V., and Futai, M. (2008). The V-type H^+-ATPase in vesicular trafficking: targeting, regulation and function. Curr. Opin. Cell. Biol. *20*, 415-426.

Martínez-Zaguilán, R., Raghumand, N., Lynch, R. M., Bellamy, W., Martinez, G. M., Rojas, B., Smith, D., Dalton, W. S., and Gillies, R. J. (1999). pH and drug resistance. I. Functional expression of plasmalemmal V-type H^+-ATPase in drug-resistant human breast carcinoma cell lines. Biochem. Pharmacol. *57*, 1037-1046.

Miesta, A., Kellermayer, R., Aiello, D. P., Fu, L., and Bedwell, D. M. (1999). The vacuolar Ca^{2+}/H^+ exchanger Vcx1p/Hum1p tightly controls cytosolic Ca^{2+} levels in *S. cerevisiae*. FEBS Lett. *451*, 132-136.

Müller, V., and Grüber, G. (2003). ATP synthases: structure, function and evolution of unique energy converters. Cell. Mol. Life Sci. *60*, 474-494.

Nothwehr, S. F., Bryant, N. J., and Stevens, T. H. (1996). The newly identified yeast GRD genes are required for retention of late-Golgi membrane proteins. Mol. Cell Biol. *16*, 2700-2707.

Oka, T., Toyomura, T., Honjo, K., Wada, Y., and Futai, M. (2001a). Four subunit a isoforms of *Caenorhabditis elegans* vacuolar H^+-ATPase. Cell-specific expression during development. J. Biol. Chem. *276*, 33079-33085.

Oka, T., Murata, Y., Namba, M. Yoshimizu, T., Toyomura, T., Yamamoto, A., Sun-Wada, G. H., Hamasaki, N., Wada, Y., and Futai, M. (2001b). a4, a unique kidney-specific isoform of mouse vacuolar H^+-ATPase subunit a. J. Biol. Chem. *276*, 40050-40054.

Ortlund, E. A., Bridgham, J. T., Redinbo, M. R. and Thornton, J. W. (2007). Crystal structure of an ancient protein: evolution by conformational epistasis. Science *317*, 1544-1548.

Perzov, N., Padler-Karavani, V., Nelson, H., and Nelson, N. (2002). Characterization of yeast V-ATPase mutants lacking Vph1p or Stv1p and the effect on endocytosis. J. Exp. Biol. *205*, 1209-1219.

Philpott, C. C., and Protchenko, O. (2008). Response to iron deprivation in *Saccharomyces cerevisiae*. Eukrayot. Cell *7*, 20-27.

Piper, R. C., Bryant, N. J., and Stevens, T. H. (1997). The membrane protein alkaline phosphatase is delivered to the vacuole by a route that is distinct from the VPS-dependent pathway. J. Cell Biol. *138*, 531-545.

Qi, J., and Forgac, M. (2007). Cellular environment is important in controlling V-ATPase dissociation and its dependence on activity. J. Biol. Chem. *282*, 24742-24751.

Qi, J., and Forgac, M. (2008). Function and subunit interactions of the N-terminal domain of subunit a (Vph1p) of the yeast V-ATPase. J. Biol. Chem. *283*, 19274-19282.

Raymond, C. K., Howald-Stevenson, I., Vater, C. A., and Stevens, T. H. (1992). Morphological classification of the yeast vacuolar protein sorting mutants: evidence for a prevacuolar compartment in class E vps mutants. Mol. Biol. Cell *3*, 1389-1402.

Reynders, E., Foulquier, F., Annaert, W., and Matthijs, G. (2010). How Golgi glycosylation meets and needs trafficking: the case of the COG complex. Glycobiology DOI: 10.1093/glycob/cwq179.

Rothman, J. H., and Stevens, T. H. (1986). Protein sorting in yeast: mutants defective in vacuole biogenesis mislocalize vacuolar proteins into the late secretory pathway. Cell *47*, 1041-1051.

Rudolph, H. K., Antebi, A., Fink, G. R., Buckley, C. M., Dorman, T. E., LeVitre, J., Davidow, L. S., Mao, J. I., and Moir, D. T. (1989). The yeast secretory pathway is perturbed by mutations in *PMR1*, a member of the Ca^{2+} ATPase family. Cell *58*, 133-145.

Ryan, M., Graham, L. A., and Stevens, T. H. (2008). Voa1p functions in V-ATPase assembly in the yeast endoplasmic reticulum. Mol. Biol. Cell *19*, 5131-5142.

Sambrook, J., and Russel, D. W. (2001). Molecular cloning: A laboratory manual, 3rd ed., Cold Spring Harbor, NY: Cold Spring Harbor Laboratory Press.

Shaner, N. C., Campbell, R. E., Steinbach, P. A., Giepmans, B. N. G., and Palmer, A. (2004). Improved monomeric red, orange and yellow fluorescent proteins derived from *Discosoma* sp. red fluorescent protein. Nat. Biotechnol *22*, 1567-1572.

Sikorski, R. S., and Hieter, P. (1989). A system of shuttle vectors and yeast host strains designed for efficient manipuplation of DNA in Saccharomyces cerevisiae. Genetics *122*, 19-27.

Simons, R. W., Houman, F., and Kleckner, N. (1987). Improved single and multicopy lac-based cloning vectors for protein and operon fusions. Gene *53*, 85-96.

Stepp, J. D., Huang, K., and Lemmon, S. K. (1997). The yeast adaptor protein complex, AP-3, is essential for the efficient delivery of alkaline phosphatase by the alternate pathway to the vacuole. J. Cell Biol. *139*, 1761-1774.

Thompson, J. D., Higgins, D. G., and Gibson, T. J. (1994). CLUSTAL W: improving the sensitivity of progressive multiple sequence alignment through sequence weighting, position-specific gap penalties and weight matrix choice. Nucleic Acids Res. *22*, 4673-4680.

Toei, M., Saum, R., and Forgac, M. (2010). Regulation and isoform function of the V-ATPases. Biochemistry *49*, 4715-4723.

Toyomura, T., Murata, Y., Yamamoto, A., Oka, T., Sun-Wada, G. H., Wada, Y., and Futai, M. (2003). From lysosomes to the plasma membrane: localization of vacuolar type H+-ATPase with the a3 isoform during osteoclast differentiation. J. Biol. Chem. *278*, 22023-22030.

Wang, Y., Toei, M., and Forgac, M. (2008). Analysis of the membrane topology of transmembrane segments in the C-terminal hydrophobic domain of the yeast vacuolar ATPase subunit a (Vph1p) by chemical modification. J. Biol. Chem. *283*, 20696-20702.

Wassmer, T., Kissmehl, R., Cohen, J., and Plattner, H. (2006). Seventeen a-subunit isoforms of paramecium V-ATPase provide high specialization in localization and function. Mol. Biol. Cell *17*, 917-930.

Whelan, S., and Goldman, N. (2001). A general empirical model of protein evolution derived from multiple protein families using a maximum-likelihood approach. Mol. Biol. Evol. *18*, 691-699.

Wilkens, S., Inoue, T., and Forgac, M. (2004). Three-dimensional structure of the vacuolar ATPase. Localization of subunit H by difference imaging and chemical cross-linking. J. Biol. Chem. *279*, 41942-41949.

Yang, Z. (2007). PAML 4: Phylogenetic analysis by maximum likelihood. Mol. Biol. Evol. *24*, 1586-1591.

Zhang, Z., Zheng, Y., Mazon, H., Milgrom, E., Kitagawa, N., Kish-Trier, E., Heck, A. J., Kane, P. M., and Wilkens, S. (2008). Structure of the yeast vacuolar ATPase. J. Biol. Chem. *283*, 35983-35995.

Zheng, L., Baumann, U., and Reymond, J. L. (2004). An efficient one-step site-directed and site-saturation mutagenesis protocol. Nucleic Acids Res. *32*, e115.

4. *References cited for Chapter IV*

1. Gabaldón, T., Rainey, D., & Huynen, M.A. Tracing the evolution of a large protein complex in the eukaryotes, NADH:ubiquinone oxidoreductase (complex i). *J. Mol. Biol.* **348**, 857–870 (2005).

2. Wollenberg, K., & Swaffield, J.C. Evolution of proteasomal ATPases. *Mol. Biol. and Evol.* **18**, 962–974 (2001).

3. Forgac, M. Vacuolar ATPases: rotary proton pumps in physiology and pathophysiology. *Nat. Rev. Mol. Cell Biol.* **11**, 917–929 (2007).

4. Dean, A.M. & Thornton, J.W. Mechanistic approaches to the study of evolution: the functional synthesis. *Nat. Rev. Genet.* **8**, 675–688 (2007).

5. Liberles, D. editor. *Ancestral Sequence Reconstruction.* Oxford University Press, (2007).

6. Wagner, G. P., Pavlicev, M., & Cheverud, J.M. The road to modularity. *Nat. Rev. Genet.* **12**, 921–931 (2007).

7. Hirata, T., *et al.* Subunit rotation of vacuolar-type proton pumping ATPase: relative rotation of the g and c subunits. *J. Biol. Chem.* **278**, 23714–23719 (2003).

8. Imamura, H., *et al.* Rotation scheme of V1-motor is different from that of F1-motor. *Proc. Natl. Acad. Sci. USA* **102**, 17929–17933 (2005).

9. Hirata, R., Graham, L.A., Takatsuki, A., Stevens, T.H., & Anraku, Y. Vma11 and vma16 encode second and third proteolipid subunits of the saccharomyces cerevisiae vacuolar membrane H+-ATPase. *J. Biol. Chem.* **272**, 4795–4803 (1997).

10. Umemoto, N., Yoshihisa, T., Hirata, R., & Anraku, Y. Roles of the vma3 gene product, subunit c of the vacuolar membrane H(+)-ATPase on vacuolar acidification and protein transport. a study with vma3-disrupted mutants of *Saccharomyces cerevisiae*. *J. Biol. Chem.* **265**, 18447–18453 (1990).

11. Umemoto, N., Ohya, Y., & Anraku, Y. Vma11, a novel gene that encodes a putative proteolipid, is indispensable for expression of yeast vacuolar membrane H(+)-ATPase activity. *J. Biol. Chem.* **266**, 24526–24532 (1991).

12. Frattini, A., *et al.* Defects in tcirg1 subunit of the vacuolar proton pump are responsible for a subset of human autosomal recessive osteopetrosis. *Nat. Genet.* **25**, 343–346 (2000).

13. Pérez-Sayáns, M., Somoza-Martìn, J.M., Barros-Angueira, F., Rey, J.M.G. and Garcìa-Garcìa, A. V-atpase inhibitors and implication in cancer treatment. *Cancer Treat. Rev.* **35**, 707–713 (2009).

14. Xu, L., *et al.* Inhibition of host vacuolar H+-ATPase activity by a *Legionella pneumophila* effector. *PLoS Pathog.* **6**, e1000822 (2010).

15. Thompson, J.D., Higgins, D.G., & Gibson, T..J. CLUSTALW: improving the sensitivity of progressive multiple sequence alignment through sequence weighting position-specific gap penalties and weight matrix choice. *Nucleic Acids Res.* **22**, 4673–4680 (1994).

16. Hirokawa, T., Boon-Chieng, S., and Mitaku, S. SOSUI: classification and secondary structure prediction for membrane proteins. *Bioinformatics* **14,** 378-379 (1998).

17. Ryan, M., Graham, L.A., & Stevens, T.H. Voa1p functions in V-ATPase assembly in the yeast endoplasmic reticulum. *Mol. Biol. Cell* **19**, 5131–5142 (2008).

18. Loytynoja, A. & Goldman, N.. An algorithm for progressive multiple alignment of sequences with insertions. *Proc. Natl. Acad. of Sci. USA* **102**, 10557–10562 (2005).

19. Loytynoja, A. & Goldman, N. Phylogeny-aware gap placement prevents errors in sequence alignment and evolutionary analysis. *Science* **5884**, 1632–1635 (2008).

20. Whelan, S. & Goldman, N. A general empirical model of protein evolution derived from multiple protein families using a maximum-likelihood approach. *Mol. Biol. Evol.* **18**, 691–699 (2001).

21. Abascal, F., Zardoya, R., & Posada, D. Prottest: selection of best-fit models of protein evolution. *Bioinformatics* **21**, 2104–2105 (2005).

22. Guindon, S. & Gascuel, O. A simple, fast, and accurate algorithm to estimate large phylogenies by maximum likelihood. *Syst. Biol.* **52**, 696–704 (2003).

23. Anisimova, M. & Gascuel, O. Approximate likelihood-ratio test for branches: A fast, accurate, and powerful alternative. *Syst. Biol.* **55**, 539–552 (2006).

24. Aguinaldo, A.M.A., *et al.* Evidence for a clade of nematodes, arthropods, and other moulting animals. *Nature* **387**, 489–493 (1997).

25. Yang, Z. PAML 4: Phylogenetic analysis by maximum likelihood. *Mol. Biol. Evol.* **24**, 1586–1591 (2007).

26. Fitch, W.M. Toward defining the course of evolution: Minimum change for a specific tree topology. *Syst. Zool.* **20**, 406–416 (1971).

27. Edgar, R. MUSCLE: multiple sequence alignment with high accuracy and high throughput. *Nucleic Acids Res.* **32**, 1792–1797 (2004).

28. Do, C.B., Mahabhashyam, M.S., Brudno, M. & Batzoglou, S. ProbCons: Probabilistic consistency-based multiple sequence alignment. *Genome Res.* **15**, 330–340 (2005).

29. Fletcher, W. & Yang, Z. Indelible: a flexible simulator of biological sequence evolution. *Mo.l Biol. Evol.* **26**, 1879–88 (2009).

30. Sambrook, J., & Russel, D.W. *Molecular cloning: A laboratory manual*, 3rd ed., Cold Spring Harbor, NY: Cold Spring Harbor Laboratory Press (2001).

31. Goldstein, A. L., & McCuster, J.H. Three new dominant drug resistance cassettes for gene disruption in *Saccharomyces cerevisiae*. *Yeast* **15,** 1541-1553 (1999).

32. Zheng, L., Baumann, U., & Reymond, J.L. An efficient one-step site-directed and site-saturation mutagenesis protocol. *Nucleic Acids Res.* **32,** e115 (2004).

33. Rothman, J.H., & Stevens, T.H. Protein sorting in yeast: mutants defective in vacuole biogenesis mislocalize vacuolar proteins into the late secretory pathway. *Cell* **47,** 1041-1051 (1986).

34. Simons, R. W., Houman, F., & Kleckner, N. Improved single and multicopy lac-based cloning vectors for protein and operon fusions. *Gene* **53,** 85-96 (1987).

35. Sikorski, R. S., & Hieter, P. A system of shuttle vectors and yeast host strains designed for efficient manipulation of DNA in *Saccharomyces cerevisiae*. *Genetics* **122,** 19-27 (1989).

36. Hill, J. E., Myers, A.M., Koerner, T.J., & Tzagoloff, A. Yeast/E. coli shuttle vectors with multiple unique restriction sites. *Yeast* **2,** 163-167 (1986).

37. Wang, Y., Cipriano, D.J., & Forgac, M. Arrangement of subunits in the proteolipid ring of the V-ATPase. *J. Biol. Chem.* **282**, 34058–34065 (2007).

38. Uchida, E., Oshumi, Y., & Anraku, Y. Purification and properties of H^+-translocating, Mg^{+2}-adenosine triphosphatase from vacuolar membrane of *Saccharomyces cerevisiae*. *J. Biol. Chem*. **260,** 1090-1095 (1985).

39. Flannery, A. R., Graham, L.A., & Stevens, T.H. Topological characterization of the **c**, **c'**, and **c"** subunits of the vacuolar ATPase from the yeast *Saccharomyces cerevisiae*. *J. Biol. Chem.* **279,** 39856-39862 (2004).

40. Noumi, T., Beltrán, C., Nelson, H., & Nelson, N. Mutational analysis of yeast vacuolar H+-atpase. *Proc. Natl. Acad. Sci. USA*, **88**, 1938–1942 (1991).

41. Bridgham, J. T., Ortlund, E. A., & Thornton, J. W. An epistatic ratchet constrains the direction of glucocorticoid receptor evolution. *Nature* **461**, 515–519 (2009).

42. Hill, K. & Cooper, A.A. Degradation of unassembled vph1p reveals novel aspects of the yeast ER quality control system. *EMBO J.* **19**, 550–561 (2000).

43. Graham, L.A., Flannery, A.R. & Stevens, T.H. Structure and assembly of the yeast V-ATPase. *J. Bioenerg. Biomembr.* **35**, 301–312 (2003).

44. Davis-Kaplan, S.R., *et al.* Pkr1 encodes an assembly factor for the yeast V-type ATPase. *J. Bioenerg. Biomembr.* **281**, 32025–32035 (2006).

45. Force, A. *et al*. Preservation of duplicate genes by complementary, degenerative mutations. *Genetics*, **151,** 1531–1545 (1999).

46. Kawasaki-Nishi, S., Bowers, K., Nishi, T., Forgac, M., & Stevens, T.H. The amino-terminal domain of the vauolar proton-translocating ATPase a subunit controls targeting and in vivo dissociations, and the carboxyl-terminal domain affects coupling of proton transport and ATP hydrolysis. *J. Biol. Chem.* **276**, 47411–47420 (2001).

47. Zhang, J., Myers, M., & Forgac, M. Characterization of the V_0 domain of the coated vesicle (H+)-ATPase. *J. Biol. Chem.* **15**, 9773-9778 (1992).

48. Saroussi, S. & Nelson, N. Vacuolar H(+)-ATPase-an enzyme for all seasons. *Pflug. Arch. Eur. J. Phy.* **457**, 581–587 (2009).

49. Grabe, M., Wang, H., & Oster, G. The mechanochemistry of V-ATPase proton pumps. *Biophys. J.* **78**, 2798–2813 (2000).

50. Finbow, M. E. & Harrison, M.A. The vacuolar H+-ATPase: a universal proton pump of eukaryotes. *Biochem. J.* **324**, 697–712 (1997).

5. *References cited for Chapter V*

ADAMI, C., C. OFRIA, and T. C. COLLIER, 2000 Evolution of biological complexity. Proc. Natl. Acad. Sci. USA **97**: 4463-4468.

ARCHIBALD, J. M., J. M. LOGSDON, and W. F. DOOLITTLE, 1999 Recurrent paralogy in the evolution of archaeal chaperonins. Curr. Biol. **9**: 1053-1056.

AVIEZER-HAGAI, K., H. NELSON, and N. NELSON, 2000 Cloning and expression of cDNAs encoding plant V-ATPase subunits in the corresponding yeast null mutants. Biochim. Biophys. Acta. **1459**: 489-498.

BOWMAN, B. J., M. DRASKOVIC, M. FREITAG, and E. J. BOWMAN, 2009 Structure and distribution of organelles and cellular location of calcium transporters in *Neurospora crassa*. Eukaryot. Cell **8**: 1845-1855.

BRESLOW, D. K., S. R. COLLINS, B. BODENMILLER, R. AEBERSOLD, K. SIMONS *et al.,* 2010 Orm family proteins mediate sphingolipid homeostasis. Nature **463**: 1048-1053.

BRIDGHAM, J. T., E. A. ORTLUND, and J. W. THORNTON, 2009 An epistatic ratchet constrains the direction of glucocorticoid receptor evolution. Nature **461**: 515-519.

BUE, C. A., C. M. BENTIVOGLIO, and C. BARLOWE, 2006 Erv26p directs pro-alkaline phospatase into endoplasmic reticulum-derived coat protein complex II transport vesicles. Mol. Biol. Cell **17**: 4780-4789.

CHUNG, J. H., R. L. LESTER, and R. C. DICKSON, 2003 Sphingolipid requirement for generation of a functional V_1 component of the vacuolar ATPase. J. Biol. Chem. **278:** 28872-28881.

COSTANZO, M., A. BARYSHNIKOVA, J. BELLAY, Y. KIM, E. D. SPEAR *et al.*, 2010 The genetic landscape of the cell. Science **327**: 425-431.

COWLES, C. R., G. ODORIZZI, G. S. PAYNE, and S. D. EMR, 1997 The AP-3 adaptor complex is essential for cargo-selective transport to the yeast vacuole. Cell **91**: 109-118.

FERREIRA, M. A., A. F. MCRAE, S. E. MEDLAND, D. R. NYHOLD, S. D. GORDON *et al.,* 2010 Association between ORMDL3, IL1RL1 and a deletion on chromosome 17q21 with asthma risk in Australia. Eur. J. Hum. Genet. DOI: 10.1038/ejhg.2010.191.

FORGAC, M., 2007 Vacuolar ATPases: rotary proton pumps in physiology and pathophysiology. Nat. Rev. Mol. Cell Biol. **8**: 917-102.

GABALDÓN, T., D. RAINEY, and M. A. HUYNEN, 2005 Tracing the evolution of a large protein complex in the eukaryotes, NADH:ubiquinone oxidoreductase (complex i). J. Mol. Biol. **348**: 857-70.

GAYNOR, E. C., T. R. GRAHAM, and S. D. EMR, 1998 COPI in ER/Golgi and intra-Golgi transport: do yeast COPI mutants point the way? Biochim. Biophys. Acta. **1404**: 33-51.

GRABE, M., H. WANG, and G. OSTER, 2000 The mechanochemistry of V-ATPase proton pumps. Biophys. J. **78**: 2798-813.

GRAHAM, L. A., K. J. HILL, and T. H. STEVENS, 1998 Assembly of the yeast vacuolar H^+-ATPase occurs in the endoplasmic reticulum and requires a Vma12p/Vma22p assembly complex. J. Cell Biol. **142**: 39-49.

GRÜBER, G., H. WIECZOREK, W. R. HARVEY, and V. MÜLLER, 2001 Structure-function relationships of A-, F- and V-ATPases. J. Exp. Biol. **204**: 2597-2605.

HILL, K., and A. A. COOPER, 2000 Degradation of unassembled Vph1p reveals novel aspects of the yeast ER quality control system. EMBO J. **19**: 550-561.

HO, M. N., K. J. HILL, M. A. LINDORFER, and T. H. STEVENS, 1993 Isolation of vacuolar membrane H(+)-ATPase-deficient yeast mutants; the *VMA5* and *VMA4* genes are essential for assembly and activity of the vacuolar H(+)-ATPase. J. Biol. Chem. **268**: 221-227.

INNAN, H., and F. KONDRASHOV, 2010 The evolution of gene duplications: classifying and distinguishing between models. Nat. Rev. Genet. **11**: 97-108.

KAWASAKI-NISHI, S., K. BOWERS, T. NISHI, M. FORGAC, and T. H. STEVENS, 2001a The amino-terminal domain of the vacuolar proton-translocating ATPase a subunit controls targeting and *in vivo* dissociation, and the carboxyl-terminal domain affects coupling of protein transport and ATP hydrolysis. J. Biol. Chem. **276**: 47411-47420.

KAWASAKI-NISHI, S., T. NISHI, and M. FORGAC, 2001b Yeast V-ATPase complexes containing different isoforms of the 100 kDa a-subunit differ in coupling efficiency and *in vivo* dissociation. J. Biol. Chem. **276**: 17941-17948.

LIU, T., and M. CLARKE, 1996 The vacuolar proton pump of *Dictyostelium discoideum*: molecular cloning and analysis of the 100 kDa subunit. J. Cell Sci. **106**: 1041-1051.

MARZIOCH, M., D. C. HENTHORN, J. M. HERRMANN, R. WILSON, D. Y. THOMAS *et al.,* 1999 Erp1p and Erp2p, partners for Emp24p and Erv25p in a yeast p24 complex. Mol. Bio. Cell **10**: 1923-1938.

NOLTA, K. V., H. PADH, and T. L. STECK, 1993 An immunocytochemical analysis of the vacuolar proton pump in *Dictyostelium discoideum*. J. Cell Sci. **105**: 849-859.

OHYA, Y., N. UMEMOTO, I. TANIDA, A. OHTA, H. IIDA *et al.*, 1991 Calcium-sensitive *cls* mutants of *Saccharomyces cerevisiae* showing a Pet- phenotype are ascribable to defects of vacuolar membrane H(+)-ATPase activity. J. Biol. Chem. **266**: 13971-13977.

OKA, T., Y. MURATA, M. NAMBA, T. YOSHIMIZU, T. TOYOMURA *et al*., 2001a a4, a unique kidney-specific isoform of mouse vacuolar H^+-ATPase subunit a. J. Biol. Chem. **276**: 40050-40054.

PAGANI, M. A., A. CASAMAYOR, R. SERRANO, S. ATRIAN, and J. ARIÑO, 2007 Disruption of iron homeostasis in *Saccharomyces cerevisiae* by high zinc levels: a genome-wide study. Mol. Microbiol. **65**: 521-537.

PERZOV, N., V. PADLER-KARAVANI, H. NELSON, and N. NELSON, 2002 Characterization of yeast V-ATPase mutants lacking Vph1p or Stv1p and the effect on endocytosis. J. Exp. Biol. **205**: 1209-1219.

PIPER, R., N. J. BRYANT, and T. H. STEVENS, 1997 The membrane protein alkaline phosphatase is delivered to the vacuole by a route that is distinct from the VPS-dependent pathway. J. Cell Biol. **138**: 531-545.

RUANO-RUBIO, V., and M. A. FARES, 2007 Testing the neutral fixation of hetero-oligomerism in the archaeal chaperonin cct. Mol. Biol. Evol. **24**: 1384–1396.

RYAN, M., L. A. GRAHAM, and T. H. STEVENS, 2008 Voa1p functions in V-ATPase assembly in the yeast endoplasmic reticulum. Mol. Biol. Cell **19**: 5131-5142.

SAMBADE, M., M. ALBA, A. M. SMARDON, R. W. WEST, and P. M. KANE, 2005 A genomic screen for yeast vacuolar membrane ATPase mutants. Genetics **170**: 1539-1551.

SAROUSSI, S. and N. NELSON, 2009 Vacuolar H(+)-ATPase-an enzyme for all seasons. Pflug. Arch. Eur. J. Phy. **457**: 581-587.

SPRINGER, S., E. CHEN, R. DUDEN, M. MARZIOCH, A. ROWLEY *et al.*, 2000 The p24 proteins are not essential for vesicular transport in Saccharomyces cerevisiae. Proc. Natl. Acad. Sci. USA **97**: 4034-4039.

STEPP, J. D., K. HUANG, and S. K. LEMMON, 1997 The yeast adaptor protein complex, AP-3, is essential for the efficient delivery of alkaline phosphatase by the alternate pathway to the vacuole. J. Cell Biol. **139**: 1761-1774.

TEMESVARI, L. A., J. M. RODRIGUEZ-PARIS, J. M. BUSH, L. ZHANG, J. A. CARDELLI *et al*., 1996 Involvement of the vacuolar proton-translocating ATPase in multiple steps of the endo-lysosomal system and in the contractile vacuole system of *Dictyostelium discoideum.* J. Cell Sci. **109**: 1479-1495.

TOEI, M., R. SAUM, and M. FORGAC, 2010 Regulation and isoform function of the V-ATPases. Biochemistry **49**: 4715-4723.

TOYOMURA, T., Y. MURATA, A. YAMAMOTO, T. OKA, G. H. SUN-WADA *et al.*, 2003 From lysosomes to the plasma membrane: localization of vacuolar type H+ ATPase with the a3 isoform during osteoclast differentiation. J. Biol. Chem. **278**: 22023-22030.

WOLLENBERG, K., and J. C. SWAFFIELD, 2001 Evolution of proteasomal ATPases. Mol. Biol. Evol. **18**: 962-974.

ZHANG, J., M. MYERS, and M. FORGAC, 1992 Characterization of the V_0 domain of the coated vesicle (H+)-ATPase. J. Biol. Chem. **15**: 9773-9778.

ZHANG, Z., Y. ZHENG, H. MAZON, E. MILGRAM, N. KITAGAWA *et al.,* 2008 Structure of the yeast vacuolar ATPase. J. Biol. Chem. **283**: 35983-35995.

ZHANG, Y. Q., S. GAMARRA, G. GARCIA-EFFRON, S. PARK, D. S. PERLIN *et al.,* 2010 Requirement for ergosterol in V-ATPase function underlies antifungal activity of azole drugs. PLoS Pathog. **6**: e1000939.